INTERACTIONS IN POLY(*N*-ISOPROPYLACRYLAMIDE) HYDROGELS

PhD thesis

Author: Enikő Rita Manek

Supervisor: Prof. Krisztina László

Department of Physical Chemistry and Materials Science

Budapest University of Technology and Economics

George Olah Doctoral School

Budapest

2018

CONTENTS

1. Introduction

1.1. Polymer hydrogels

Chemical polymer hydrogels are covalently bound three-dimensional, cross-linked networks of macromolecules that can absorb large quantities of water without dissolving in the liquid media. In hydrogels water is retained by the polymer network and prevents the collapse of the polymer chains providing that gels are deformable and able to keep their shape.[1,2] The swelling of gels is limited by the number of cross-link points in the macromolecular network.[3] Depending on the structure of the polymer network and the interactions between the polymer chains and water molecules the consistency of gels varies between viscous liquids and solid materials.

Smart stimuli-sensitive hydrogels change their physical properties in response to external physical (temperature, mechanical effect, electromagnetic radiation, electric or magnetic field) or chemical stimuli (solvent conditions: composition, dissolved species, pH, ionic strength) (Fig.1).[2,4] Since temperature is a highly important parameter in the mammalian body, temperature-sensitive hydrogels have become the most investigated responsive polymers.[5,6] Upon elevating temperature the polymer network expands in positively temperature sensitive (e.g. partially hydrolysed polyacrylamide), and contracts in negatively temperature sensitive systems (e.g. poly(*N*-isopropylacrylamide)).[2,3]

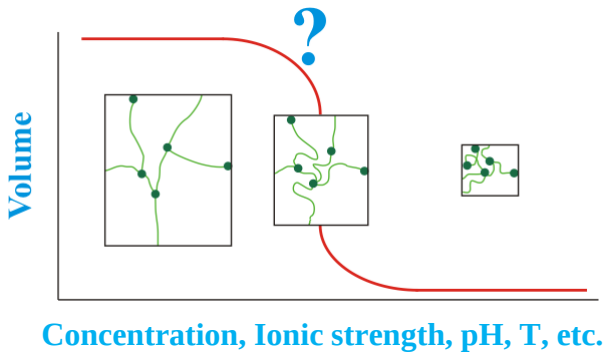

Figure 1. Volume phase transition of hydrogels induced by external stimuli.

Responsive gels that resemble biological tissues are intensively studied for biomedical applications. Soft polymers are hydrophilic;[1,7] their well-defined structure can be tailored to biocompatibility,[7] functionality or degradability;[1] can be synthetized in mild conditions; don't

denature encapsulated biomacromolecules (e.g. DNA, proteins) and their pores may accommodate living cells.[1,2,5,8] Their disadvantages are low mechanical strength and sterilization difficulties.[7] Potential application fields of smart hydrogels include vehicles for controlled drug delivery;[1,2,9,10] biosensors;[1,3] scaffolds in tissue growing and engineering;[1,7,9,10] immobilization of cells and enzymes;[2] bioseparation;[2] materials for contact lenses[3] and wound dressings,[11] from those targeted drug delivery is of major interest.

Conventional drug delivery results in a peak in drug concentration, followed by a plateau and a decline phase, thus may lead to toxic or ineffective concentrations (Fig.8a).[6] In case of existing side-effects, not required drug release is undesirable. Several diseases follow a rhythmic pattern requiring pulsatile release.[6] In hydrogels that are sensitive to physiological conditions drug release and targeting to specific tissues, organs or cells can be modulated by the adjustment of the gel structure by external stimuli (Fig.8b).[2] Upon stepwise temperature changes, pulsing drug release also can be obtained (Fig.8c).[2,6] Hydrogels can also protect drug molecules from unfavourable conditions, such as the presence of enzymes or low pH,[2] while reducing the toxicity or degradation of drugs during the delivery.[4]

1.1.1. The poly(*N*-isopropylacrylamide) hydrogel

The majority of thermosensitive hydrogels investigated in the past decades are synthetic polymers based on poly(*N*-isopropylacrylamide) (PNIPA).[1,2,3,5] The PNIPA hydrogel can be synthetized from *N*-isopropylacrylamide (NIPA) monomer and *N,N'*-methylenebisacrylamide (BA) crosslinker by chemical or gamma irradiation initiated free radical polymerization.

The crosslink density, i.e. the molar ratio [NIPA] / [BA] of the PNIPA gel determines the swelling degree of the gel: elevating the crosslink density results in a reduction of the swelling. The typical PNIPA gel crosslink densities for biomedical applications are between 100 and 150, resulting in the swelling degree of 35-40. The glass transition temperature (T_g) of PNIPA polymers varies between 126-141 °C, based on the molar mass and tacticity.[12]

The PNIPA gel exhibits a reversible non-linear volume phase transition (VPT) at its lower critical solution temperature (LCST) around 34 °C, i.e. close to the natural temperature of the human body.[3] Below the LCST the gel is hydrophilic, swollen and transparent. Upon increasing temperature, it becomes hydrophobic, expelling a great part of the liquid previously filling the space among the polymer chains (Fig.2a).[2,13,14] The phase transition derives from the entropic gain related to the discharge of water molecules from the isopropyl groups into the bulk aqueous phase, as the temperature rises.[15] In the initial stage of phase transition the gel

surface collapses first, resulting in the formation of a dense surface skin layer. During the presence of the skin layer shrinkage takes place only by cooperative diffusion. The increasing pressure in the gel eventually leads to the formation of bubbles on the polymer surface and thus water can be expelled again.[2,16,17]

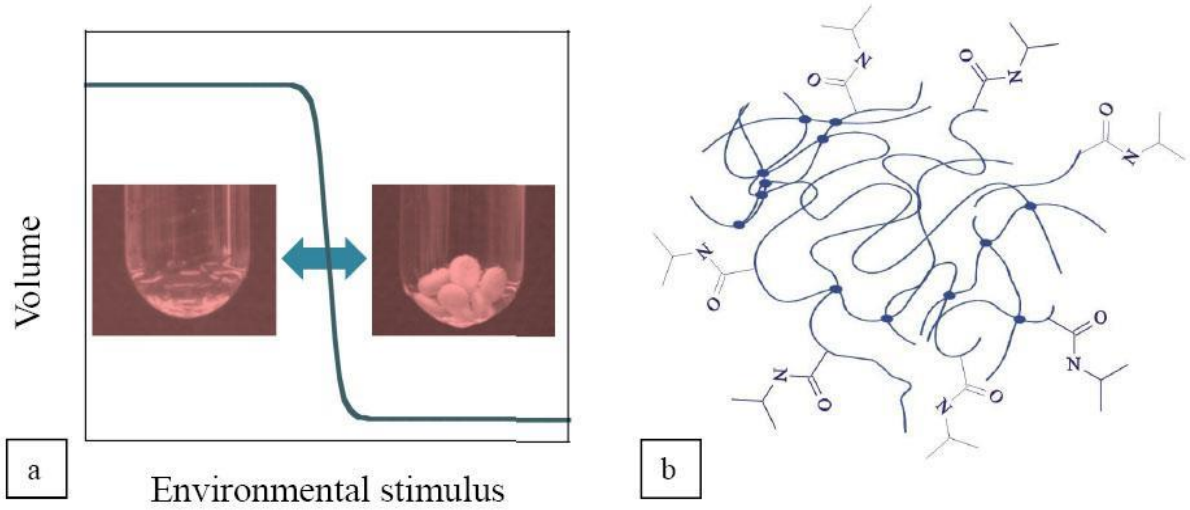

Figure 2. Temperature induced volume phase transition and structure of one of the most studied temperature-responsive polymers, the poly(*N*-isopropylacrylamide) (PNIPA).

The amphiphilic PNIPA gel consists of hydrophilic (carbonyl and amide groups) and hydrophobic (isopropyl group and the polymer carbon backbone) units (Fig.2b). In aqueous media its polar groups can interact with water molecules and other hydrophilic groups on the identical (intermolecular) or adjacent (intramolecular) polymer chains by forming hydrogen bonds. Hydrophobic interactions can develop between the hydrophobic polymer units and during their solvation by water molecules. The miscibility of the gel is determined by the balance between the competing forces of hydrogen bridge formation and hydrophobic interactions (Fig.3).

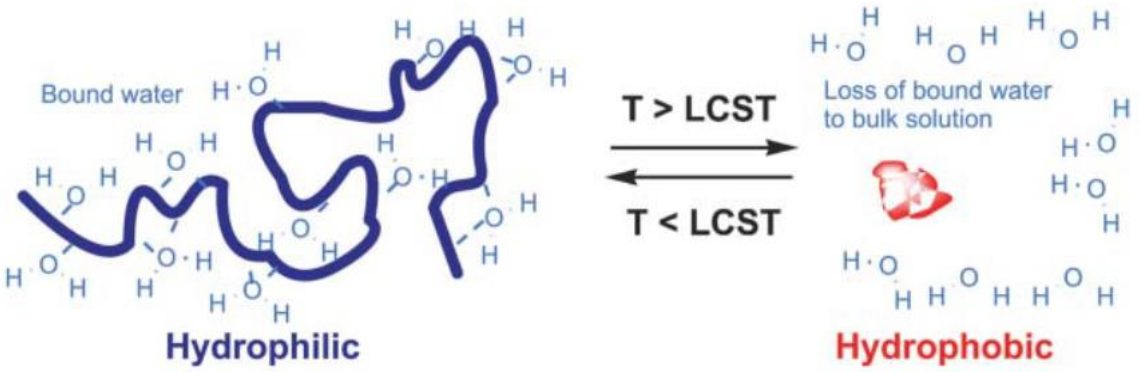

Figure 3. Schematic of PNIPA miscibility changes with temperature.[15]

As the LCST of PNIPA can be tuned under or above 34 °C by the incorporation of co-monomers,[1,15] it is especially suitable for biomedical applications, such as targeted drug delivery,[3] transportation of highly sensitive agents,[3] mediation of cell adhesion[15] or tissue-engineering.[15]

1.1.2. Intrinsic ionic behaviour in cross-linked PNIPA hydrogel

Major, still unelucidated, inconsistencies exist in the literature among measurements of the thermodynamic properties of PNIPA solutions and gels. It has recently been pointed out by Halperin et al.[18] that, among the immense body of experimental investigations into the phase diagram of aqueous solutions of PNIPA that have been conducted since the pioneering work of Heskins and Guillet,[19] agreement remains at best qualitative. By contrast, measurements of the osmotic pressure, a relevant thermodynamic parameter, are rare[20,21] and in this case also, agreement is merely qualitative, the numerical results being mutually incompatible. Such disorder, which should be a legitimate source of concern for the scientific discipline, suggests that the PNIPA system may be more complex than previously believed.

Part of the observed experimental variation may stem from the inherent difficulty of preparing monodisperse samples of thermosensitive polymers. Another „usual suspect" source of inconsistencies is chain branching, but in the polymerization of PNIPA this seems unlikely to play a significant role. Differences between measurements can also arise from variations of tacticity due to preparation at different temperatures or in solvents of different polarity.[22,23] It

is conceivable, for example, that the size of the statistical segment length depends on the extent of syndio-, iso- or atactic regions that develop during polymerization. A further, rarely discussed source of variation may be a frustrated thermal equilibrium or memory effect.

In the case of cross-linked PNIPA hydrogels, yet another possible cause arises if polymer chains acquire partial ionic character during free radical polymerisation in water. In the literature this eventuality is frequently cited, but only inferred.[24,25,26,27] Clear evidence, either for or against, is lacking. Schild, in an incisive review of the properties of PNIPA both in hydrogels and in aqueous solution, explicitly refers to this possibility, opining that „the amount of ionic groups introduced by the initiator and differences among the various experimental techniques employed for observing the transition account for the discrepancies among the various research groups".[28] While different experimental techniques may yield different types of average in a measurement, it is well established that ionic groups certainly do change the physical properties of the PNIPA homopolymer.[22, 23, 29, 30] (In this thesis, for the case of gels, the term homopolymer only used for referring exclusively to the network chains, ignoring the cross-linker.) The presence of intrinsic ionic groups, however, is difficult to ascertain. For example PNIPA in the uncross-linked state is reported to display electrophoretic mobility,[31] but since the polymer subunits are amphiphilic, this property could stem from associated rather than from intrinsic ions. The colloidal stability of PNIPA microgel suspensions in deionised water,[32] however, could constitute evidence for the presence of ionic groups formed during polymerisation, but is not conclusive.

Another indicator of intrinsic ionic content in PNIPA can be its pH sensitivity. While the literature contains an immense amount of information on the effects of pH on the transition properties of PNIPA under different conditions,[33,34,35,36,37, 38, 39] verdicts are controversial. While some papers noted that the PNIPA gel is insensitive to pH, in some investigations it displayed limited pH sensibility.

Jones found that varying the pH of the aqueous solution from 1 to 4 has no significant effect on T_{VPT}.[34] The research group of Cai also found that the swelling degree was pH independent in buffer solutions with pH 1-13.[35] Beltran and co-workers investigated the swelling degree of PNIPA gel in citrate – phosphate buffer solutions of ionic strength 0.01 M from pH 3 to 8, and in pH 6 buffers with ionic strength 0.005-0.5 M. They concluded that the swelling of PNIPA was influenced in neither case.[36] Brazel et al. examined the swelling degree of PNIPA at 37 °C in a series of Na_2HPO_4 – KH_2PO_4 based Sorensen buffers in the pH interval 4.86-9, where the ionic strength of the buffers varied between 0.700 and 0.289 M.[40] They found

that the swelling degree of the PNIPA gel above T_{VPT} was independent of the buffer employed, i.e., of the pH and the ionic strength.[37]

By contrast, in other studies moderate pH sensitivity of PNIPA has been confirmed. In aqueous media at pH 2.2 (0.0078 M HCl, 0.05 M KCl), at pH 4.5 (0.05 M KH_2PO_4) and at pH 6.8 (0.05 M KH_2PO_4, 0.0224 M NaOH) a slight decrease of the equilibrium swelling degree was observed at 25 °C with increasing pH.[38] In buffer solutions having different pH values, pH 1.2 (KCl), pH 4 ($C_8H_5O_4K$), pH 6.8 (KH_2PO_4) and pH 10 (KCl, KH_2PO_4), the shift in T_{VPT} followed the order pH 4 < pH 6.8 < pH 1.2 < pH 10 (Fig.4).

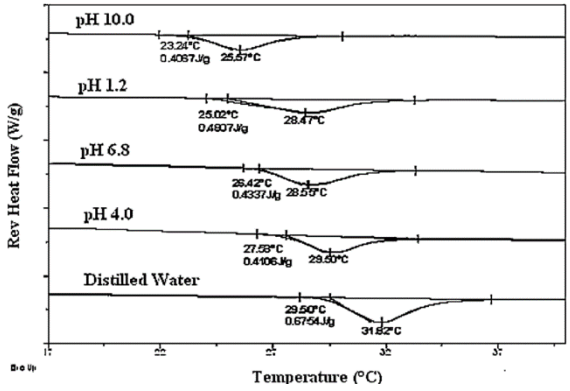

Figure 4. DSC thermograms of aqueous poly(*N*-isopropylacrylamide) homopolymer solutions in buffers of various pH values.[41]

It is important to note that in setting the pH it is often overlooked that adding ionic compounds also changes the ionic strength of the solvent. It is well known that PNIPA is sensitive to various ions and that the effect of ions on the hydrogel can be correlated to their position in the Hofmeister series (Fig.5).[42,43, 44,45,46,47]

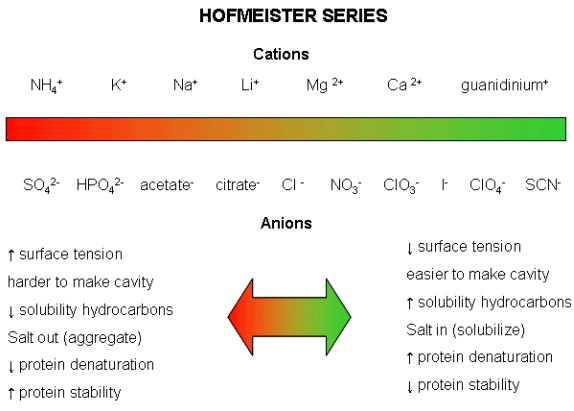

Figure 5. The Hofmeister series of ions.[42]

Albeit in some studies pH seemingly had a strong effect on the T_{VPT} of PNIPA, the influence of various salts, as well as HCl or NaOH used in buffer preparation, is not negligible. However, the T_{VPT} shift induced by buffers did not follow the order of effectiveness of the incorporated salts on the transition: the different concentrations of salts required for producing buffers and the addition of HCl and NaOH must also be taken into account. It was reported earlier that NaOH has a more pronounced influence on T_{VPT} than HCl. Thus, the greatest shift found for the pH 10 buffer may be attributed to the highest amount of NaOH in the solution.[41] These findings highlight that composition of the background electrolyte is of crucial importance in the investigation of the transition properties of PNIPA.

1.1.3. Interactions of PNIPA with dissolved molecules

The volume phase transition properties of PNIPA hydrogel may be significantly influenced by dissolved species of the aqueous media. Guest molecules can shift the T_{VPT} of PNIPA to lower (e.g. phenols, benzene derivatives), and in a few cases, to higher temperatures (e.g. surfactants, organic quaternary ammonium salts) by chemical interactions and/or disturbing its hydrophobic/hydrophilic balance.[48,49,50,51,52,53]

The effect of small aromatic molecules on the PNIPA hydrogel has been investigated by several research groups on benzene derivative – PNIPA gel systems. It was found that benzene derivatives reduce the phase transition temperature of PNIPA. According to Dhara, their T_{VPT} lowering effectiveness follows the order of 4-methylcathecol > 1,3-dihydroxybenzene > 1,4-dihydroxybenzene > 1,2-dihydroxybenzene > 1,2,3-trihydroxybenzene (Fig.6).[54]

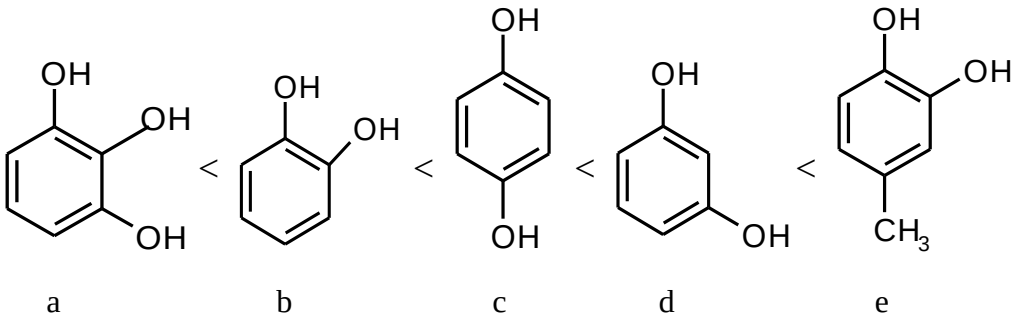

Figure 6. LCST reducing effect of benzene derivatives[54] (a) 1,2,3-trihydroxybenzene (b) 1,2-dihydroxybenzene (c) 1,4-dihydroxybenzene, (d) 1,3-dihydroxybenzene (e) 4-methyl-1,2-dihydroxybenzene.

In case of various benzoates (benzoic acid, sodium benzoate, methyl-4-hydroxybenzoate, propyl-4-hydroxybenzoate), it was observed that the length of the ester side chain determines the volume phase transition inducing guest molecule concentration at 25 °C. The concentration at which the volume phase transition occurs increases in the order of nonil-phenol < propyl-phenol < ethyl-phenol < methyl-phenol < phenol, i.e. the more hydrophobic the molecule is, the smaller is the phase transition inducing concentration. Comparing the effect of sodium benzoate and benzoic acid also demonstrates the importance of hydrophobicity: while sodium benzoate has a weaker effect on the LCST and does not alter the swelling degree of the gel at all, benzoic acid has a significant impact on swelling and T_{PVT} due to its hydrophobic interaction with PNIPA.[53,55] The hydrophobic interaction between PNIPA and benzenes is be regulated by the number and steric accessibility of the hydroxyl or aldehyde groups. In benzoic acids these groups are easily accessible, but as the hydroxyl group is getting closer to the aldehyde substituent on the ring, interactions become limited.[50,54]

Among benzene derivatives, phenol is of utmost importance as environmental pollutant and model drug molecule. Phenol has a strong T_{VPT} reducing effect and induces PNIPA phase transition at 25 °C from the concentration of 40 mM in aqueous solutions. Its significant influence can be explained by two phenomena: the hydrophobic interaction between the phenyl group of phenol and the isopropyl group of PNIPA; and the formation of hydrogen bonds between the OH group of the guest molecule and the gel's amide group.[51,52,53,56] In infrared spectroscopic measurements it was found that the hydrogen binding increases the chemical potential of water molecules hydrating the polymer chains.[51] The resulting phenol – amide group complex is not miscible with water so it segregates form it, that breaks the tetrahedral structure of water and thus induce a discontinuous volume change in PNIPA gel.[52,53,57]

Despite the findings demonstrated above, the interactions between the PNIPA gel and benzene derivatives – e.g. the effect of different phenols on the phase diagram of the polymer – are not fully explored, that has led our research group to study how phenols with hydroxyl groups in meta position (phenol; 1,2-dihydroxybenzene and 1,3,5-trihydroxybenze) interact with the hydrogel. It was observed that these guest molecules altered the swelling properties of PNIPA gel and induced rapid collapse of the gel at fixed temperature (20 °C) when the phenol content of the aqueous solution reached a "critical" concentration (c_{crit}) that was characteristic of the guest molecule. It was also found that with the increasing number of hydroxyl groups c_{crit} shifts to lower concentrations (Fig.7): c_{crit} equals to 52.6 mM, 49.8 mM and 35.5 mM in case of phenol, 1,2-dihydroxybenzene and 1,3,5-trihydroxybenze, respectively.[58,59,60,61] The increasing number of OH substitution also results in a reducing T_{VPT} and the broadening of the endotherm peak of PNIPA phase transition.

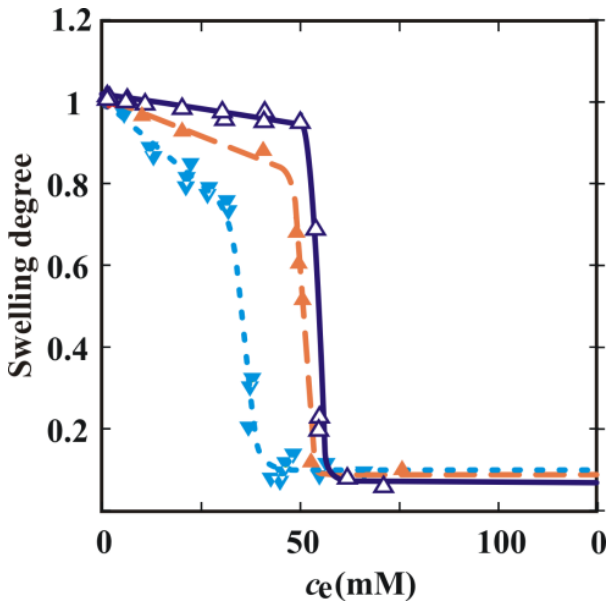

Figure 7. Swelling degree of PNIPA hydrogel in different phenolic molecule solutions at 20 °C as the function of equilibrium concentration in the free liquid phase:[58]
Δ phenol, ▲1,3-dihydroxybenzene, ▼ 1,3,5-trihydroxybenzene.

Despite that the potential guest – polymer interactions are crucial factors determining the swelling and drug release process of hydrogels, as well as the LCST shift inducing effect of small molecules, systematic studies of the additive properties (e.g. number and position of functional groups; ability to hydrophobic interaction) are infrequent.[50,55,56,62] In order to provide a deeper insight into the interactions between PNIPA and small aromatic molecules, my aim

was to continue the work of our research group and carry out studies on the effects of various substituted phenols on the PNIPA hydrogel.

1.1.4. Drug uptake and release in hydrogels

Drug molecules can be incorporated into hydrogel matrices by polymerization in the presence of drug molecules; or by soaking the gel into drug solutions. The benefits of the latter method are better control over drug loading amount and the elimination of release hindering side-reactions.[63]

Drug uptake as well as release is determined by several factors, such as the swelling rate and degree of the gel; guest – polymer interactions (e.g. hydrogen bonding, hydrophobic or electrostatic interaction); solubility, concentration, molecular size and logP value of the loading molecule; and the diffusion properties of drug inside the gel matrix.[55,63,64,65] Besides the above mentioned, discharge is also strongly influenced by drug loading (e.g. the release of poorly soluble molecules reduces with increasing loading), the geometry (aspect ratio and total volume) of hydrogel matrix, and the hydrophilic/hydrophobic balance of the drug molecule.[63,64]

By the application of hydrogel based drug delivery systems different release patterns can be obtained. The sudden shrinkage of temperature responsive gels upon temperature elevation results in a prompt drug release, i.e. the quick increase of the concentration of the drug that is discharged with the swelling liquid (Fig.8a). Parallel to the deswelling a dense skin layer develops on the gel surface, which eventually stops the release of drug molecules, thus allowing a quick on-off type drug discharge (Fig.8c).[66,67]

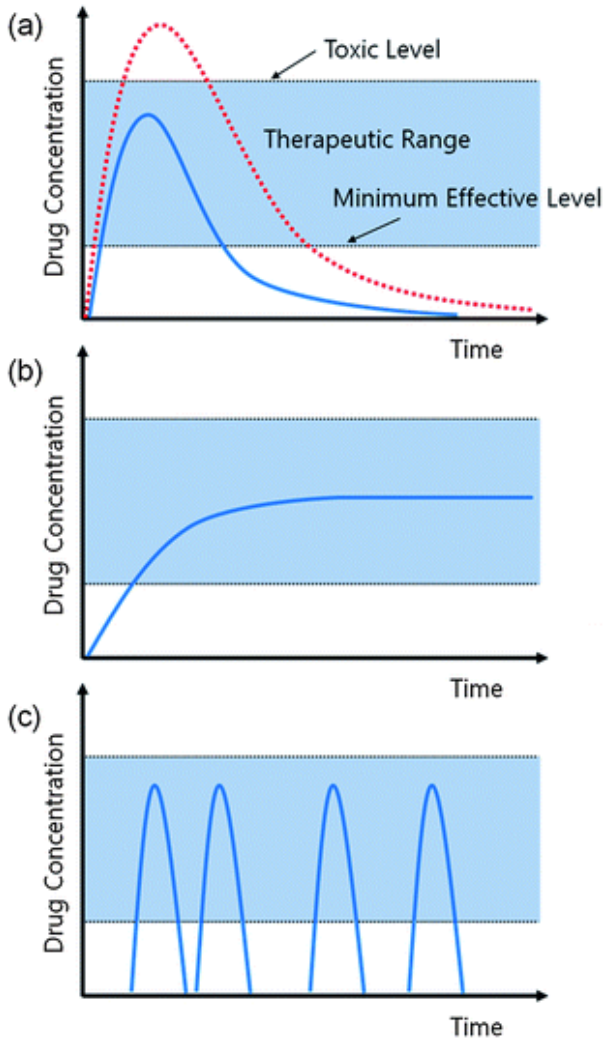

Figure 8. Dependence of the drug concentration profile in body fluids on the release mechanism: (a) prompt release from conventional dosage forms (injection or tablet) or from sudden shrinkage of polymer gels (b) controlled profile (prolonged release) (c) on-off type drug discharge.[68]

Another drug release mechanism is the retard type, which is based on the shape memory of the gel carrier: dry drug loaded gels may provide prolonged release (Fig.8b) by their slow reswelling.[69] Drug release from dry ("glassy") hydrogels includes simultaneous absorption of water and desorption of drug molecules, most commonly through a swelling-controlled mechanism,[70,71] and is influenced by the rate and ratio of reswelling (Fig.9); the interaction between drug, polymer and water molecules; the solubility of the guest molecule;[66] and local drug concentrations.[72,73]

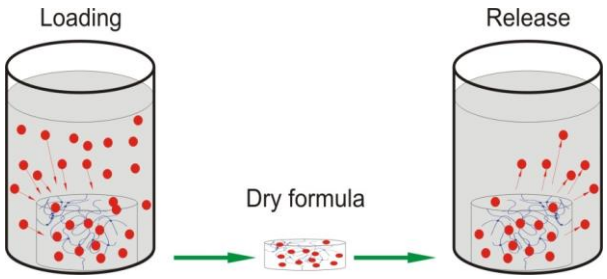

Figure 9. The gel carrier can be easily loaded with drug then stored in dry state. The release of drug molecules is determined by the rate of reswelling.

The final state of drug in a dry polymer matrix is determined by several factors, such as crosslink density, hydrophobic co-monomer content or storage humidity.[74] Embedding of a drug into a hydrogel matrix may stabilize its – otherwise metastable – amorphous state by hindering the development of the thermodynamically stable crystalline form.[75] Stabilizing poorly water soluble drugs in their amorphous state enables the enhancement of their dissolution and bioavailability.[74,75] Recrystallization inhibiting effect of hydrogel matrices was observed on sodium diclofenac, piroxicam and naproxem drug loaded 2-hydoxyethyl methacrylate (PHEMA) dry gel disks. For all three drugs, hydrogen bonding was observed between the PHEMA and the guest molecules by FTIR spectroscopy. It was concluded that the formation of hydrogen bonds resulted in a better compatibility between the drug and the gel, which decreased the mobility of guest molecules inside the polymer network, thus inhibiting nucleation and crystallization. The crystallization retarding effect was limited by the drug concentration within the polymer matrix. Above a loading threshold, the effective polymer concentration reduced thus the drugs formed fine crystalline particles.[74] In PNIPA gel – benzoate systems the crystallization hindering property of the hydrogel was proved by X-ray diffraction (XRD). The crystal formation inhibiting effect of PNIPA was higher for benzoic acid than for sodium benzoate, which is consistent with the finding that the benzoic acid – PNIPA interaction is stronger than the benzoate salt – PNIPA one. In case of the ionic form of benzoic acid no binding was found to the polymer, which enabled the development of crystalline peaks in the XRD spectra.[55] Incorporating drug molecules into hydrogels may also give the possibility of obtaining crystallites with reduced particle sizes and narrow size distribution, that is another way of facilitating dissolution.[74,76] Reducing crystallite sizes by loading the drugs into hydrogel matrices has several advantages over the widely used

micronizing techniques, e.g. better control of particle size distribution, or preventing contamination and degradation of the drug.[77,78,79]

Despite their crucial importance, the effect of drug – polymer interactions on gel swelling; drug loading and release; as well as crystallization and particle sizes of guest molecules are not widely investigated. Only a few studies examined and reported ionic or hydrophobic interactions between guest molecules and hydrogels.[55] As drug – polymer interactions may significantly hinder the release process by the binding of guest molecules to polymer chains and the inhibition of gel swelling, their examination is vital prior to the application of hydrogel drug delivery systems.[55]

1.1.5. PNIPA – carbon nanoparticle hybrid gels

Although hydrogels are frequently proposed vehicles of controlled drug delivery, their poor mechanical strength due to the high water content limits their application possibilities including repetitive loading.[80,81,82] The preparation of interpenetrating polymer networks through chemical cross-linking can offer improved mechanical properties, however, cross-linker residues may lead to toxic side effects.[81] Another solution is the reinforcement of hydrogels with various nanoparticles, such as nanocarbons, polymer-based nanomaterials, metal or ceramic nanoparticles.[83,81,82] Nanoparticles can either be physically trapped within the polymer gel or cross-linked into the network structure via surface functionalities.[83] In the latter case the resulting nanocomposite materials may not only possess improved mechanical strength, but also novel optical, thermal, electronic, magnetic, remote actuation or drug release properties.[83,84,85,81,82]

Their outstanding mechanical and conductive properties, combined with their unique structure and low density, place carbon nanoparticles (CNP) among the most commonly proposed and investigated additives.[81,82,83] Carbon nanoparticles – e.g. carbon nanotubes (CNT), graphene, nanodiamonds and fullerenes – are carbon allotropes with at least one dimension in the nanometre range (Fig.10).[81] Among CNPs, carbon nanotubes[85,86,87,88,89,90,91] together with graphene and its derivatives[92,93,94,95,96,82] – mainly graphene oxide (GO) – were of especially great interest in the last few years as additives to hydrogels.[83,81]

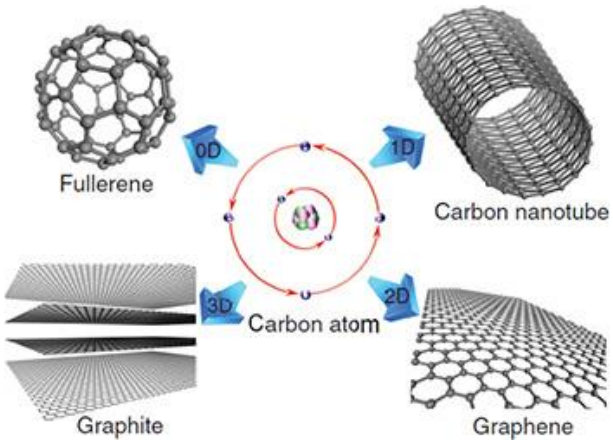

Figure 10. Carbon nanostructures of various dimensions.[97]

Notwithstanding the diverse functionality of nanocarbons, their potential toxic effects should also be mentioned. Uncertainty on the toxicity of carbon nanotubes may limit their usage as filler materials to hydrogels for biomedical applications.[85] In case of CNTs both positive and negative cytotoxic effects have been observed in vitro as well as in vivo, and the mechanisms governing their toxicity are still not well-explored.[81] Nanotubes may present high respiratory risk due to their pin-like shape combined with their light weight, that facilitates aerosolization and thus inhalation.[81] On the contrary, graphene was reported to be non-toxic and highly biocompatible.[85]

Carbon nanotubes as well as graphene are conjugated polycyclic structures composing solely of sp^2 hybridized carbon atoms.[81] CNTs can be classified as single wall carbon nanotubes (SWCNT) and multiwall carbon nanotubes (MWCNT).[81,83,85] SWCNTs comprise of one cylindrically rolled-up graphene sheet with the typical diameter of 1-2 nm.[81,98] MWCNTs are built up from individual concentric tubes of graphene sheets with the average interlayer separation of approximately 0.34 nm and an the outer diameter of 2 to 100 nm (Table 1).[81,99] Both single and multiwall CNTs are capped by hemispherical networks of carbon atoms at both ends of the tubes.[85] While SWCNTs are characterized by a well-defined wall, MWCNTs may present defects in their carbon structure resulting in lower stability and facilitating their chemical modification.[81] The chemistry of carbon nanostructures comprising of extensive conjugated cyclic systems is dominated by π-π dispersion type interactions.[81,7,8] Due to their extremely high aspect ratio, polarizable nature and smooth, hydrophobic graphene side walls, carbon nanotubes have a tendency to interact with each other by strong cohesive forces. As a result, the formation of insoluble bundled aggregates limits the dispersibility of pristine CNTs

in various solvents and matrices relevant in biomedical applications, including hydrophilic gel networks.[81,100,83] In order to solve this problem CNTs are frequently applied in chemically modified forms with polar – e.g. amine (NH_2), hydroxyl (OH) or carboxyl (COOH) – groups.[100]

Compared to carbon nanotubes, graphene exhibits several favourable properties, such as lower cost, facile fabrication and modification, higher surface area, absence of toxic metal particles, low toxicity and outstanding biocompatibility.[96] Graphene is a two dimensional nanostructure, which comprises of a honeycomb-arranged single layer of sp^2-hybridized carbon atoms, with epoxy and hydroxyl groups on the sides and carboxyl groups around the edges.[81,96] Owing to the pure sp^2 hybridization network, graphene derivatives are often characterized by record values of tensile strength, elastic modulus, thermal conductivity, intrinsic electrical conductivity, aspect ratio and flexibility (Table 1).[82,83] Due to its planar structure graphene is highly susceptible to the establishment of strong van der Waals as well as π-π interactions and less prone to form covalent bonds.[81] Similarly to nanotubes, pristine graphene is greatly hydrophobic and poorly dispersible in aqueous media.[96] The incorporation of graphene into polymer matrices is generally facilitated by inducing surface and edge functionalities onto the graphene sheets by thermal oxidative treatment.[83,82] The resulting graphene oxide (GO) can be considered as an amphiphilic material, that bears both hydrophobic and hydrophilic domains on its surface[83] and is able to form stable colloids in aqueous media.[96] The amphiphilic nature of GO promotes the establishment of both physical and covalent interactions with hydrophilic polymers, significantly contributing to the mechanical improvement of nanocomposites.[82,83] In case of very strong interactions, GO was reported to act as a gelation component by increasing the number of cross-links in the polymer matrix.[82]

Table 1. Comparison of the physical properties of carbon nanotubes and nanostructured graphene.

	Carbon nanotube	Nanostructured graphene
Number of layers	SWCNT: single MWCNT: multiple	multiple
Thickness	SWCNT: 1-2 nm[98] MWCNT: 2-100 nm[99]	0.3-100 nm[101,102]
Lateral size	SWCNT: up to mm[99] MWCNT: up to μm[103]	μm range[104]
Surface area	1200 m^2/g [105]	2630 m^2/g [105]
Young's modulus	SWCNT: 1 TPa MWCNT: 0.3-1 TPa [106]	1–42 GPa [101]
Tensile strength	SWCNT: 5-500 GPa MWCNT: 10-60 GPa [106]	15–193 MPa [101,107]
Density	1.3 g/cm^3 [99]	2.2 g/cm^3 [108]
Thermal conductivity	1100-7000 W/m K [109]	600-5000 W/m K [109]

Albeit carbon nanoparticles are usually applied as physical fillers without chemical bonding, in most studies clear synergy was observed between nanocarbons and polymer matrices resulting in enhanced mechanical properties of the hybrid systems.[83] Improved elastic modulus and compressive strength of CNT[110,111,112] and GO[113,114,115] incorporated PNIPA based composites were proved in several investigations. The durability of hybrid materials mostly depends on the effectiveness of load transfer from the polymer network to the filler material as well as the dispersion state of nanoparticles, and less determined by the mechanical strength of the additive itself.[82,98] Fine nanoparticle dispersion contributes to strong interfacial adhesion between the phases, which facilitates load transfer from the matrix to the nanoparticles resulting in stronger hydrogels.[98] On the contrary, nanofillers with poor adherence act as structural defects and weaken the hybrid network by inducing local stress concentrations and reducing the flexural strength of the composite system.[82,98] In case of laminar additives, the strength of the nanocomposite can be dramatically increased by the efficient exfoliation of the stacked sheets which enables the intercalation of the polymeric chains into the filler particles (Fig.11).[82]

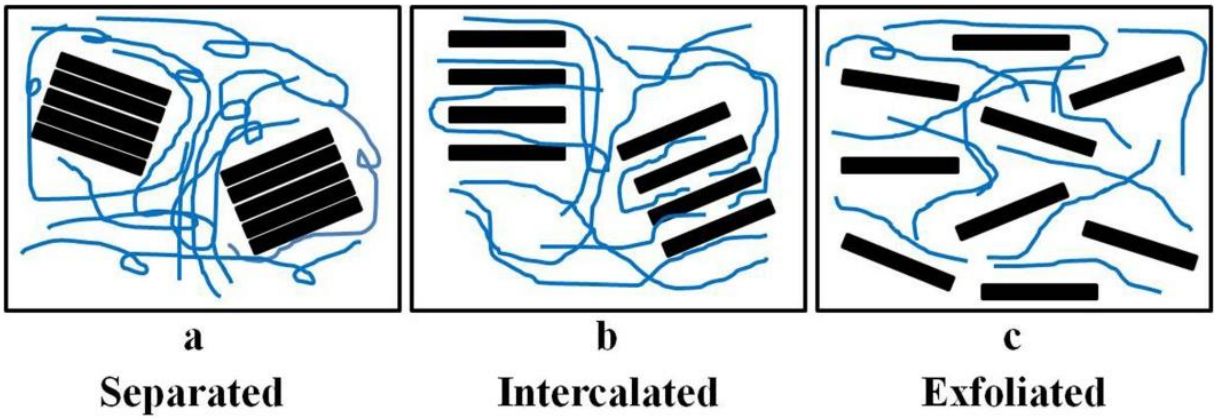

Figure 11. Dispersing scenarios of laminar nanoparticles in a polymer matrix[116]

It was observed that carbon nanotubes have a mechanical performance enhancing effect in polymer gels only at low concentrations.[117] This phenomenon can be explained by that in case of lower loadings a finer nanoparticle dispersion can be achieved, which facilitates the load transfer promoting tube – polymer adhesion over tube – tube interactions.[100] However, CNTs have a weakening effect on composite systems in case of poor dispersion state and/or aggregation within the polymer matrix.[118] Extremely smooth nanotube side walls may also worsen the durability of polymers by reducing the adhesion forces between the phases, which can even result in the pull-out of CNTs from the matrix during deformation.[118] The special advantage of nanotubes is that due to their pin-like shape they are particularly suitable for the improvement of the out-of-plane properties of hybrid systems by linking together individual laminar layers.[98] It has been proved that the expansion of fissures in composite structures are effectively hindered by the bridging effect of CNTs perpendicularly aligned to the crack faces.[98] At the same time – as a result of its superior stiffness and flexibility – GO has a greater strengthening effect on gel matrices compared to carbon nanotubes.[82] Graphene oxide was reported to significantly improve the elastic modulus, tensile strength, elongation and toughness of various polymer matrices.[82] Unlike in the case of CNTs, for GO the enhancement of the mechanical properties is proportional to the additive concentration.[119,120,121,122] The disadvantage of graphene derivatives is that due to the outstanding flexibility and high aspect ratio their layers can be easily folded and crumpled by even modest shearing forces during manufacturing.[82] Therefore for graphitic fillers, enhanced stiffness and additional functionalities of the composites can be achieved by establishing optimal contact between while applying. gentle processing conditions.[82]

Beside mechanical deficiencies, their poor heat transfer properties may also limit the applicability of polymer gels.[123] The thermal conductivity of insulating polymers is frequently enhanced by the incorporation of carbon derivatives, which have the highest inherent thermal conductivity (up to 7000 W/m K) among any known materials at room temperature.[82,98,102,124] Thermal conductivity of carbon composites is characterized by a percolation threshold, which can be attained even at very low additive concentrations due to the high aspect ratio of the nanofillers.[98] The conductivity of carbon nanoparticle composites varies between broad limits depending on the polymer matrix, the properties of nanofillers (e.g. geometry, orientation, volume fraction and dispersion) as well as on the interfacial thermal resistance between the phases.[102] The thermal conductivity of carbon nanoparticle composites can be characterized by a percolation-type threshold and elevates by increasing the nanofiller content.[98,102] The percolation threshold is mainly determined by the polymer matrix, as well as the type and the distribution of the nanocarbons.[98] For example, in case of randomly oriented CNTs extremely low percolation thresholds can be obtained, which is can be attributed to the formation of a tube-network.[98] However, despite their outstanding thermal properties and low percolation values, cylindrical nanocarbons do not enhance the thermal conductivity of polymeric systems significantly. On the contrary, graphene derivatives were reported to increase the thermal conductivity of nanocomposites by two to three times order of magnitude. This can be explained by their better dispersibility combined with the two-dimensional nature, which enables a more effective 2D transport of phonons compared to the 1D path provided by nanotubes.[102]

Another beneficial property of carbon nanoparticle additives is their light absorption capacity, which can provide additional functionality to PNIPA hydrogels.[125,126,127] Fast and reversible optical response of CNT[128,129,81,100] and GO[127] incorporated PNIPA gels has been observed under infrared (IR) laser excitation, which may stem from the strong warming effect of nanocarbons.[127] The non-invasive and remote control over the swelling of hydrogels by optical irradiation can open the route for the construction of responsive biocompatible devices, e.g. novel drug delivery systems and actuators.[125]. Furthermore, the light absorption of carbon nanoparticles in the ultraviolet (UV) to infrared (IR) regions may also enable the selective thermal ablation of malignant tissues in cancer therapies, without surgical resection or side-effects on healthy cells.[96]

In addition to improving the physical properties of polymers, carbon nanoparticles may also act as effective drug binding sites in composite materials.[81,119,120,130,131,132,96] CNTs can interact with therapeutic agents in various ways, including the physical trapping of the active ingredient within the nanotube bundle; the chemical bonding between therapeutic molecules

and functional groups on the tube surfaces; and the immobilization of drug molecules within the nanotube channels.[81] In case of several drugs (e.g. diclofenac, doxorubicin and gentamicin sulphate) carbon nanotubes were proved to be superior delivery systems over conventional formulations.[81,125,100,81,133] As graphene has the highest surface area among nanomaterials, its drug delivery potential is even more promising than that of nanotubes.[96] In the planar graphene monolayer each atom is exposed to the surface, which results in an exceptionally high drug loading potential.[96] Beside the high surface area, their amphiphilic nature, unsubstituted oxygenated domains and π–π stacking also contribute to the outstanding drug binding capacity of graphene derivatives. Electrostatic interactions and/or hydrogen bonding of several anionic and cationic drugs (e.g. doxorubicin and camptothecin) as well as dyes were observed to GO containing hydrogels, leading to enhanced loading levels of the guest molecules.[119,120,130,131,132,96]

As carbon nanoparticle – PNIPA composite gels were investigated with a variety of cross-link densities and/or with different co-monomers, as well as diverse conditions of synthesis, it is not possible to obtain a comparable evaluation of the effects of carbon nanotubes and graphene on the properties of the PNIPA gel. In my thesis work, my objective was to provide a detailed study of the structural and dynamical properties (e.g. swelling-, mechanical- and phase transition properties, pore structure and IR sensitivity) of carbon nanotube and graphene oxide incorporated hybrid PNIPA hydrogels.

2. Objectives of the PhD thesis

The objective of my PhD thesis is to explore the interactions of the thermosensitive poly(*N*-isopropylacrylamide) (PNIPA) hydrogel that may determine its potential for controlled drug delivery applications.

First of all, I investigated the effect of pH on the hydrogel. The purpose of my research was to look for evidence of intrinsic ionic behaviour in the PNIPA homopolymer gel by measurements over a wide pH and ionic strength range.

Thereafter I examined the response of the PNIPA gel to small aromatic molecules in the swelling medium. On one hand, I continued the previous investigations of our research group on phenols – that are environmental pollutants and model compounds for several drug molecules – by studying the effect of various phenol substitution arrangements on the hydrogel. I also extended my experiments to drug molecules that – due to their different functional groups – are expected to interact with PNIPA in a dissimilar way compared to phenols. I have chosen two drugs widely used in practice: dopamine (4-(2-aminoethyl)benzene-1,2-diol), that is a neurotransmitter present in the brain and peripheral nervous system; and the hydrophobic non-steroidal anti-inflammatory drug, ibuprofen (2-(4-isobutylphenyl)-propionic acid).

Subsequently I explored the possibilities for the preparation of different types of drug formulations utilizing the dissimilar interactions of the guest molecules with the polymer. In order to confirm the interactions in dry state, I examined the thermal behaviour of dry PNIPA matrices loaded with phenol, dopamine and ibuprofen. I also studied the effect of the drying process on the crystalline state of the probe molecules, which is a crucial factor in dosage and bioavailability.

Lastly, I investigated carbon nanoparticle – PNIPA composite hydrogels as potential advanced drug delivery systems with enhanced mechanical performance and novel functionalities. In order to obtain a comparable evaluation of the impact of different carbon nanoparticles, I studied the properties of carbon nanotube as well as graphene-oxide nanoparticle incorporated PNIPA hybrid gels on the macroscopic and microscopic scales. I also characterized the application related performance of these composites by their infrared sensitivity and the kinetic response of their volume after an external temperature jump.

3. Materials and methods

3.1. Materials

Materials used for gel synthesis and preparation of different swelling media are summarized in Appendix (Table A1-A3). All chemicals were applied as received except NIPA. Double distilled water was used in every experiment.

3.1.1. Aromatic guest molecules

Phenols were purchased from Merck. Dopamine hydrochloride and ibuprofen sodium were obtained from Sigma-Aldrich (Table A1). For the investigation of PNIPA gel interactions with guest molecules of environmental and biomedical relevance, aromatic solutions were prepared in the concentration range of 0-1 M in doubly distilled water, unless saturation limit was lower. Characteristic physical and chemical properties of the model guest molecules are summarized in Table 2.

Table 2. Properties of guest molecules.

Guest molecule	Structure	Molar mass (g/mol)	pK_a, 25 °C	Solubility in water, 20 °C (M)	TPSA* (Å^2)[134,135]	Polariza-bility** (Å^3)[135]	logP***
Phenol	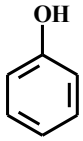	94.11	9.99[136]	0.892[137]	20.23	10.94	1.46[138]
Catechol	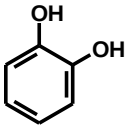	110.11	9.34; 12.6[136]	4.096[139]	40.46	11.54	0.88[140]
Hydroquinone		110.11	9.85; 11.4[136]	0.636[141]	40.46	11.54	0.59; 0.64[142]
Resorcinol	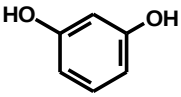	110.11	9.32; 11.1[136]	9.082[143]	40.46	11.54	0.80[144]
Pyrogallol	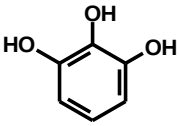	126.11	9.01[145]	4.956[146]	60.69	12.18	0.29[147]
Phloroglucinol	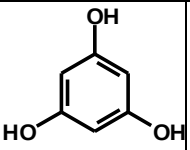	126.11	8.45[136]	0.079[148]	60.69	12.18	0.06[149]
Dopamine hydrochloride	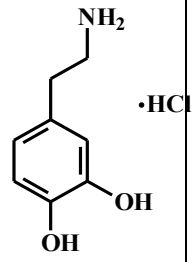	189.64	8.80[150]	Freely soluble[151]	68.10	16.61	-0.98[152]

Ibuprofen sodium	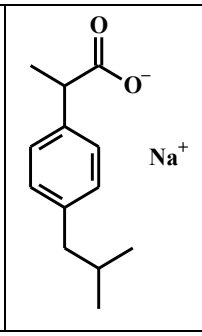	228.26	4.26[153]	Freely soluble[77]	40.13	23.58	3.72[154]

*topological polar surface area: the 2-dimensional estimate of the surface belonging to polar atoms, which correlates well with passive molecular transport through membranes[155]

**molecular polarizability[156]

***octanol/water partition coefficient[157]

3.1.2. Carbon nanoparticles

Multiwall nanotube was produced by Chengdu Organic Chemicals Co. Ltd. (China). The commercial nanotube was oxidized in cc. HNO_3 (65%) (3 hours, 80 °C) then washed with distilled water until pH neutrality. NaOH treatment was applied to remove fulvic acids. 1 M aqueous HCl was used to reprotonate the surface.

Graphene oxide (GO) was obtained by the improved Hummer's method[158] from natural graphite (from Madagascar). The graphene-oxide suspension was purified by centrifugation (6989 g) with 1 M HCl five times and with water two times, decanting away the supernatant after every cycle. The nanoparticle content of the suspension after 10-day dialysis was 0.2 w/w%. The main properties of the investigated carbon nanoparticles are summarized in Table 3.

Table 3. Properties of carbon nanoparticles.

Carbon nanoparticle	Geometry	Size	S_{BET} (m^2/g)	C/O ratio*
Carbon nanotube (CNT)	cylindrical	9-20 nm diameter	221	11.2
Graphene oxide (GO)	planar	2-50 μm lateral extension	22	1.7

*****from XPS measurements

3.1.3. Synthesis of PNIPA gel

Materials used of gel synthesis are summarized in Table A2. NIPA was recrystallized from toluene-hexane mixture prior to the synthesis. PNIPA gel films with the molar ratio of [NIPA] / [BA] = 150 were synthesised by mixing 1 M aqueous solution of NIPA (18.75 mL) and 0.1 M solution of BA (1.225 mL) with water (4.9 mL) and TEMED (0.25 μL). After addition of APS (125 μL) to the mixture, free radical polymerization took place at 20 °C within 24 hrs.[61] The 2 mm thick gel films and 1x1 cm isometric cylinders were dialyzed in double distilled water. For swelling experiments gel films were cut into disks with diameter of 7 mm, for X-ray powder diffraction (XRD) and nuclear magnetic resonance (NMR) measurements of 17 mm, then dried and stored in desiccator over concentrated sulphuric acid, if otherwise stated. For calorimetric measurements, dry gel disks were powdered (particle size 0.2-1 mm).

In order to avoid the effect of APS in potentiometric titrations, PNIPA hydrogel with the same molar ratio was synthetized by gamma initiated polymerization in CO_2 free aqueous solution of NIPA and BA (radiation dose 5 kGy, dose rate 2 kGy/h). Gels were purified as above.

3.1.4. Synthesis of PNIPA – carbon nanoparticle hybrid gels

To obtain composite gels aqueous carbon nanoparticle suspensions of the required concentration were mixed with the precursor solution of NIPA, BA and TEMED. In case of the CNT containing composites ultrasonication (Elmasonic X-tra 150H ultrasonic bath, 4 hours, 20 ± 2 °C, sweep mode, 45 kHz) was used to ensure homogeneity of the dispersion. The precursor suspensions were polymerised and purified in the same way as the nanoparticle-free PNIPA gel.[159] Gels with ≥20 mg GO/g_{NIPA} content were prepared by adding in succession solid NIPA, solid BA and TEMED to the GO suspension. The reaction medium was stirred in an ice-bath for 15 min after addition of each component then polymerised as described earlier.

3.2. Methods

3.2.1. Equilibrium swelling degree

Swelling measurements were carried out by equilibrating dry PNIPA gel disks with excess aqueous acid, base, salt, buffer and aromatic guest molecule solutions of different initial concentrations (c_0) for one week at 20.0 ± 0.2 °C. The mass/volume ratio of the dry gel and the liquid phase was 0.012. If otherwise stated, the equilibrium swelling ratio ($1/\varphi_e$) was calculated from the mass balance as:

$$1/\varphi_e = \frac{m_{\text{gel, dry}} /\rho_{\text{gel, dry}} + (m_{\text{gel, swollen}} - m_{\text{gel, dry}}) /\rho_{\text{solution}}}{m_{\text{gel, dry}} /\rho_{\text{gel,dry}}}, \qquad \text{(Eq. 1)}$$

where $m_{gel,dry}$ and $m_{gel,swollen}$ are the mass of the dry and the equilibrated gel disks, respectively. The density of dry PNIPA gel ($m_{gel,dry}$) is 1.115 g/cm^3.[60] The density of the free liquid phase ($\rho_{solution}$) was taken as 1 g/mL. The swelling degrees φ_0/φ_e displayed in the figures are relative values, defined by the ratio of the equilibrium polymer volume fraction of the gel in pure water φ_0 to that in the solvent φ_e. Reproducibility of the swelling degree is 0.25-1.75% and 1.5-3.5% for identical and different batches, respectively.

3.2.2. Mechanical properties

The mechanical properties of isometric (1x1 cm) fully swollen gel cylinders were investigated by using an INSTRON 5543 type mechanical testing equipment. Samples were compressed by 10% of their initial height in steps of 0.1 mm with the relaxation time of 4·4 s and force threshold 300 N. Nominal stress can be calculated as $\sigma_N = \frac{F_x}{A_0}$, where F_x is the x-direction force and A_0 is cross-section of the non-deformed sample. Deformation can be characterized by $\lambda_x = \frac{h_x}{h_0}$, where h_0 and h_x is the height of the gel cylinder before and after deformation, respectively. Introducing $D = \lambda_x - \lambda_x^{-2}$ gives the Mooney-Rivlin equation $\frac{\sigma_N}{D} = C_1 + C_2\lambda_x^{-1}$, where C_1 and C_2 are material constants. In gels of high swelling degree, where C_2 = 0, elastic modulus can be determined from the slope of σ_N – D neo-Hook representation.

3.2.3. Kinetics of temperature induced phase transition

Prior to the measurements disks of 13 mm diameter were cut from the swollen film and kept at 20 ± 0.2 °C for 2 days to allow them to reach equilibrium. The samples were then plunged into a water bath at 50 ± 1 °C. The shrinkage induced by the thermal shock was recorded photographically by monitoring the diameter *D* of the disks. *D* values are given as the average of five different measurements read from the images by JMicroVision software and compared to the initial diameter D_0 of the fully swollen gels.

3.2.4. Differential scanning microcalorimetry (DSC)

DSC measurements were performed on a MicroDSCIII apparatus (SETARAM). Powdered PNIPA gel was used in order to reduce the role of diffusion. The dry gel/liquid mass to volume ratio was 0.02. Samples were incubated for 2 hours in aqueous solutions, then heated from 10 to 40 °C with the scanning rate of dT/dt = 0.02 °C/min, unless otherwise stated. Enthalpy values (ΔH) were obtained from the peak integrals with the standard error of 5-10%. Entropy values (ΔS) were estimated as:

$$\Delta S = \frac{\Delta H}{T} \qquad \text{(Eq. 2).}$$

3.2.5. Calculation of aromatic uptake

Aromatic guest uptake n_a (mmol/$g_{dry\ gel}$), was determined from the initial (c_0) and equilibrium molar concentrations (c_e):

$$n_a = \frac{c_0 V_0 - c_e V_e}{m_0}, \qquad \text{(Eq. 3)}$$

where c_0 and V_0 are the concentration and volume of the aromatic molecule in the initial liquid phase, and c_e and V_e are the same in the free liquid in equilibrium.

3.2.6. Scanning electron microscopy (SEM)

Dialysed gel films in the equilibrium swelling state were frozen in liquid nitrogen and broken immediately (Fig.12) prior to lyophilisation (Scanvac Coolsafe freeze dryer, Lynge,

Denmark; T = 25 °C, p = 10^{-2} mbar, 24 hours). Broken surfaces were coated with metal alloy (atomic ratio Au : Pd = 1.5 : 1), and observed by using a Hitachi SU6600 type analytical variable pressure scanning electron microscope equipped with a ZrO/W Schottky field emission electron source and an environmental secondary electron detector (Hitachi Ltd., Tokyo, Japan). The size distribution of the pores was determined from 80-100 data for each sample.

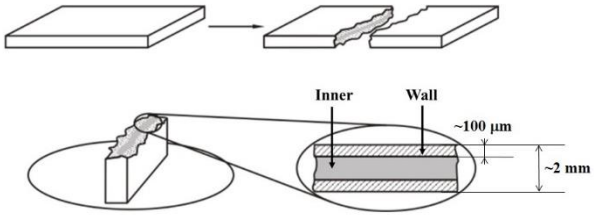

Figure 12. Preparation of gel films for SEM observation.

3.2.7. Simultaneous thermal analysis (STA)

STA investigations were performed on an STA6000 instrument (PerkinElmer) in high purity (99.9995%) nitrogen with the flow rate 20 mL/min. Dry PNIPA gel disks were equilibrated in excess aqueous aromatic solutions ($m_{\text{dry gel}}$: m_{solution} = 0.012) of c_0 = 500 mM for 1 week at 20 ± 0.2 °C, then dried until mass stability. Guest molecule uptake was calculated from Equation 2. Dry guest molecule loaded samples (stored over silica gel) were incubated at 30 °C for 5 minutes then heated from 30 to 650 °C with a scanning rate of 10 °C min^{-1}. The thermogravimetric (TG), differential thermogravimetric (DTG) curves and differential thermal analysis (DTA) curves were recorded. The position of the peaks of the DTG and DTA curves was characterized by the temperature at their maximum. All the heat effects deduced from DTA are endothermic.

3.2.8. X-ray powder diffraction (XRD)

For XRD measurements dry gel disks were equilibrated in phenol, dopamine hydrochloride and ibuprofen sodium solutions with the initial concentration of c_0 = 500 mM (1 week, 20.0 ± 0.2 °C). XRD spectra were obtained daily during the drying process of the samples on at room temperature by a PANanalytical X'pert Pro MPD XRD powder diffractometer (V = 40 kV, I = 30 mA, mask 20 mm).[160] Spectra of the loaded gels were corrected with the background of the gel equilibrated in pure water in the identical drying state. Pure model drugs

freshly recrystallized from water were used as comparison. Crystallite sizes (D_p) were estimated from the Debye-Scherrer equation:

$$D_p = \frac{0.94\lambda}{\beta_{1/2} cos\Theta}, \quad \text{(Eq. 4)}$$

where 0.94 is the Debye factor, λ is the wavelength of the Cu K_α source (1.5418 Å), β is the full width at half maximum (FWHM) value of the peak and Θ is the Bragg angle.

3.2.9. Infrared (IR) irradiation

The surface of 10x10 mm swollen gel films, placed on a glass plate, was exposed to a CO_2 laser beam (wavelength: 10.6 μm, power: 0.500 W, spot size: 15 mm). Thermal maps were recorded at ambient conditions as video files by a Testo 890 thermal imaging camera (Testo, Alton, UK) for 30 seconds prior to the irradiation, then during laser exposure for 2 minutes. After irradiation, the cooling of the gels was monitored for 2.5 minutes. The temperature of the irradiated gels was determined as the average temperature of 20 positions within the laser exposed zone.

4. Results and discussion

4.1. A search for evidence of intrinsic ionic behaviour in the response of the PNIPA hydrogel

The principal purpose of the present investigation is to circumscribe the causes of the observed diaspora of experimental results by examining one of the above possible sources, namely the ionic group hypothesis. The presence of ionic groups is in fact difficult to ascertain, as the task of distinguishing the effects of intrinsic ionic groups on the properties of a polymer from those of attendant ions that surround polar groups is not always clear-cut. For this reason the objective is to look for evidence of intrinsic ionic behaviour in the PNIPA hydrogel synthesized in water under normal conditions, according to standard recipes with ammonium persulphate as initiator,[41,46] but avoiding deliberate functionalization of the polymer,[161] with a variety of observational methods and in a wide range of pH (Table A4-A6) and ionic strength conditions. A sensitive indicator of intrinsic ionic content is the osmotic pressure of gels.

The amount by which a gel swells in a given solvent is determined by the balance between the osmotic pressure Π, which expands the network, and the volume elastic modulus G_V, which limits the chain expansion. The shear elastic moduli of the fully swollen PNIPA hydrogel samples obtained by chemical and gamma initiation were respectively $G = 0.83 \pm 0.04$ kPa ($1/\varphi = 37.1$) and $G = 0.87 \pm 0.04$ kPa ($1/\varphi = 35.7$). Within experimental error, these two results are indistinguishable. The analysis used in the following is based on the scheme of Horkay and Zrinyi,[162] according to which at swelling equilibrium with the free solvent

$$\Pi = G_V \qquad \text{(Eq. 5).}$$

In lightly cross-linked gels such as those described here the volume elastic modulus G_V is numerically equal to the shear elastic modulus G.[163] For a given gel composed of independent Gaussian chains,[164]

$$G = G_0 \varphi^{1/3}, \qquad \text{(Eq. 6)}$$

where φ is the polymer volume fraction and G_0 depends only on the cross-link density and on the absolute temperature T. The osmotic pressure Π can be expressed as follows:[165]

$$\Pi = A\varphi^n, \qquad \text{(Eq. 7)}$$

where n is close to 9/4. Thus, for a given gel at swelling equilibrium φ_e with the solvent,

$$A = G_0 \varphi_e^{-23/12} \qquad \text{(Eq. 8)}$$

For consistency, in what follows, the polymer volume fraction is replaced by the mass concentration $c = \rho\varphi$, where ρ=1.115 g/mL is the density of the dry polymer.[166] From Eqs. 5-8, this yields for the osmotic pressure in the gel

$$\Pi_{gel} = (2.2 \pm 0.1)\, c^{2.25} \text{ MPa}, \qquad \text{(Eq. 9)}$$

with c expressed in g/mL.

An independent estimation of osmotic pressure in the PNIPA hydrogel was derived from dynamic light scattering measurements[39] resulting

$$\Pi_{gel} = 1.85\, c^{2.25} \text{ MPa}. \qquad \text{(Eq. 10)}$$

The non-aqueous synthesis route and careful sample preparation employed by Nagahama et al. allowed these authors to minimize ionic impurities, thus establishing a benchmark for osmotic pressure data for aqueous solutions of PNIPA. The osmotic pressure measurements of Nagahama *et al.*[21] on solutions of uncross-linked PNIPA, interpolated to 20 ºC, yield for

$$\Pi = 3.73\, c^{2.25} \text{ MPa} \qquad \text{(Eq. 11)}$$

(with c in g/mL).

Comparison of the value of A of the cross-linked PNIPA hydrogel (Eq. 10) with that of a reference uncross-linked polymer solution (Eq. 11) is an important indicator of the presence of electrostatic interactions in the gel. In spite of the experimental uncertainties inherent in the two independent estimates of A in Eq. 10 and 11, it is clear that the osmotic pressure prefactor is appreciably lower in the gel than in the uncross-linked solution. Experimental observations on a variety of polymer gels have shown that the prefactor A of the osmotic pressure in the gel is invariably lower than in the uncross-linked solution.[167,168] Conversely, when incompletely screened ionic groups and thus electrostatic interactions are present, uncross-linked polymer solutions exhibit a significant increase in their osmotic prefactor A.[169,170] Comparison of the values found above for A in the PNIPA hydrogel with that of A in Eq. 11 for uncross-linked solutions implies that, if any ionic groups are present in the gels investigated here, their quantity is vanishingly small.

The acid-base properties of PNIPA hydrogel were studied by continuous potentiometric titration in the pH range of 3 to 10 in CO_2-free media (see Appendix A3). The potentiometric titration curve calculated from the H^+/OH^- balance in Figure 13 demonstrates that PNIPA is sensitive to pH. Starting from the immersion pH 5.5 up to pH 10, then down to pH 3 and

returning to pH 5.5, the titration cycle reveals irreversibility. This irreversibility stems from the limited mobility of ions within the swollen gel, especially of negatively charged OH^- ions from the base titrant above pH 6, where the gel matrix is polarized negatively (upgoing curves).[171] At pH < 5.5 surface proton excess occurs, probably due to protonation of the basic nitrogen on the polymer backbone. At higher pH, the negative values generally correspond to proton release or to binding of hydroxyl ions. In this case the pH response indicates that the acidic character is weak. The curve is asymmetric, base consumption being much larger than proton excess in the corresponding pH region. This asymmetry is also an indicator of preferential affinity of the PNIPA gel for anions. At the highest pH values, chemical degradation takes place. [172] These observations bear no hallmark of intrinsic ionic behaviour. They are, on the contrary, consistent with recent work that highlights the important role played in the transition by local interactions between anions and the amide groups in the PNIPA chain.[41,44,45,173]

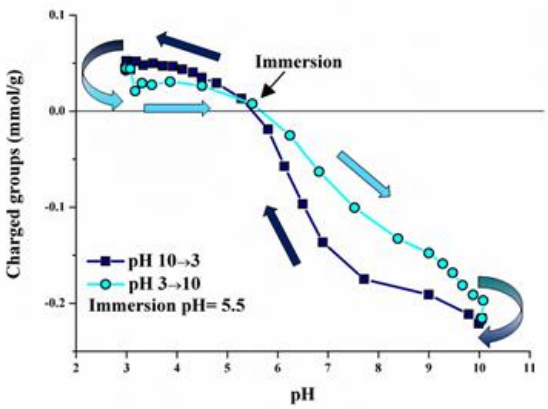

Figure 13. Potentiometric titration cycle of PNIPA hydrogel at 25 °C in 0.01 M NaCl background electrolyte concentration, starting from immersion pH 5

Up to these days, numerous studies have investigated the potential pH sensitivity of PNIPA hydrogels,[33,34,35,37,38,39] but these works refer mainly to co-polymer systems. Of particular interest is the investigation of Hirotsu et al.,[29] which showed that at neutral pH, NIPA-acrylic acid copolymer gels undergo a discontinuous transition as a function of temperature above a certain acrylic acid content. For the PNIPA gels described here, the transition is continuous.[174] This condition sets an upper limit for their intrinsic ionic content of about 0.1%. Figure 14 shows the equilibrium swelling degree φ_0/φ_e, as well as the onset temperature T_{onset}, as a function of pH under different solvent conditions. The maximum in φ_0/φ_e around pH 3 is the consequence of induced polyelectrolyte behaviour associated with protonation of the NIPAM polar group, as mentioned above. In the acidic region below pH 3, φ_0/φ_e decreases

almost linearly with decreasing pH in response to the increasing ionic strength (HCl, ionic strength range 0.001-1 M). Conversely, in the range pH 11– 13 (KOH, ionic strength range 0.001–1 M), φ_0/φ_e increases linearly with increasing pH. This behaviour is the signature of increasing hydrolysis at high pH. At pH 13.5 and 14 the ionic strength of the solution causes the gel to collapse. To the naked eye, however, the gels remain intact. The onset temperature, T_{onset}, is practically independent of pH in the range $3 \leq \text{pH} \leq 10$. Outside this range, T_{onset} decreases, almost certainly also due to the accompanying increase in ionic strength.

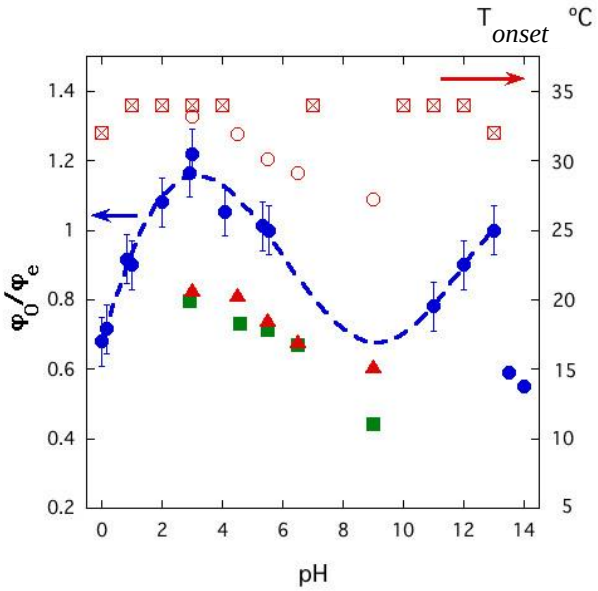

Figure 14**.** Dependence of equilibrium swelling degree φ_0/φ_e (left hand axis) and T_{onset} (right hand axis) at 20 °C on pH. ●: φ_0/φ_e with no added salt, pH being defined only by HCl or KOH (dashed line: polynomial fit to data, excluding points at pH>13), ▲: φ_0/φ_e with phosphate buffer, ■: φ_0/φ_e with Britton-Robinson buffer. ☒**:** T_{onset} with either HCl or KOH alone, ○: T_{onset} with phosphate buffer.

Figure 14 also illustrates how, when buffer solutions are used to modify the pH, the swelling ratio decreases markedly with respect to the salt free condition, and that T_{onset} decreases with increasing pH, highlighting the importance of the background electrolyte (see also Appendix A4).

The DSC response of PNIPA samples in acidic solutions for the range $0 \leq \text{pH} \leq 3$ and in basic solutions in the range $11 \leq \text{pH} \leq 14$, with no added salt is shown in Figure 15. At pH = 0, the shape of the transition broadens, indicating a change in the network chains. This change is reversible. At high pH, the shape and the position of the transition peak also vary, but more strongly. The hydrolysis of the polymer chains is irreversible. The enthalpy ΔH and the

corresponding entropy Δ*S* of the endothermic transition in aqueous solutions of HCl and KOH are practically independent of the pH (Table 4). For comparison, the values of Δ*H* and Δ*S* with pure water are also listed in Table 4.

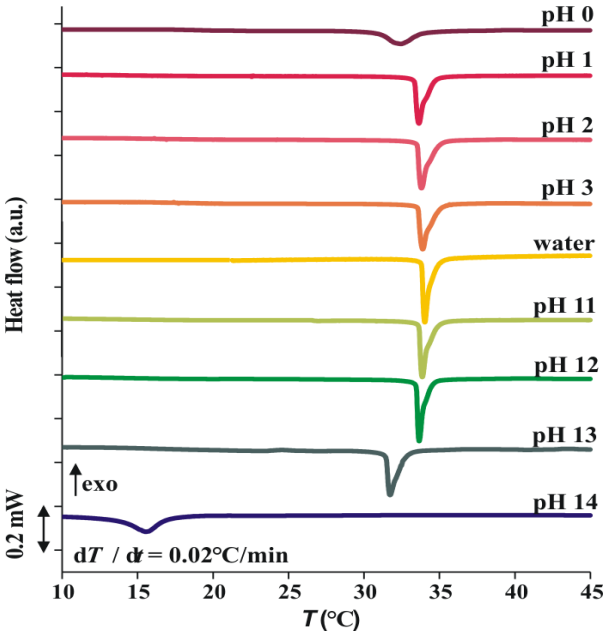

Figure 15. DSC response of PNIPA at various pH set by either HCl or KOH solutions.

Table 4. Enthalpy and entropy of the transition in aqueous solutions of HCl and KOH.

	Δ*H* (J/$g_{dry\ gel}$)	Δ*S* (J/g K)
H_2O	67 ± 5.9	0.22 ± 0.02
HCl	60.0 ± 4.9	0.21 ± 0.01
KOH	63.2 ± 2.7	0.20 ± 0.02

The effect of the ionic salts KCl and $CaCl_2$ on the swelling degree and the osmotic pressure of the gels is shown in Figure 16. On plotting φ_0/φ_e as a function of the ionic strength *I* of the solution surrounding the gel, with these two salts the VPT occurs at different values of *I* (Fig. 16a). In both cases φ_0/φ_e decreases exponentially with *I* in the region before the collapse. This response is inconsistent with that of polyelectrolytes, where the osmotic pressure obeys a power law function of ionic strength.[175] With the divalent salt $CaCl_2$, the deswelling exhibits a two-step process that implies partial chain folding, analogous to that observed by Zhang and Cremer with Na_2SO_4.[44] The gel remains transparent as far as $\varphi_0/\varphi_e \approx 0.4$.

The corresponding calculated variation of the osmotic pressure pre-factor *A*, defined at each salt concentration by the equilibrium condition, is plotted in Figure 16b as a function of concentration of Cl^- ions for both KCl and $CaCl_2$, rather than as a function of ionic strength *I*, as in Figure 16a. In this semi-logarithmic representation, the straight-line behaviour in the swollen state for KCl ($c_{Cl^-} < 1$ M) reproduces the exponential behaviour seen in Figure 16a. This response differs markedly from that of T_{onset} (Fig. A2), which decreases linearly with respect either to *I* or to c_{Cl^-}. Figure 16b provides confirmation that it is the anion concentration that determines the VPT, which at 20 ºC takes place at $c_{Cl^-} = 1$M. With $CaCl_2$ the initial decrease is indistinguishable from that with KCl, but at $c_{Cl^-} > 0.5$ M it diverges, decreasing in discontinuous steps. It is also remarkable that in the swollen state, neither response resembles that of a polyelectrolyte solution, where the osmotic pressure varies with ionic strength as $I^{-0.75}$ (broken lines in Fig. 16b).[169,170] A striking contrast to this behaviour is provided by polyelectrolyte gels in equilibrium with an infinite bath: the critical ion concentration in the surrounding solution at which the present gels collapse is about three orders of magnitude greater than for polyelectrolyte gels, and the ion exchange capacity is negligible.[176] This comparison again shows that the ionic content of the gel is very much smaller than 1%.

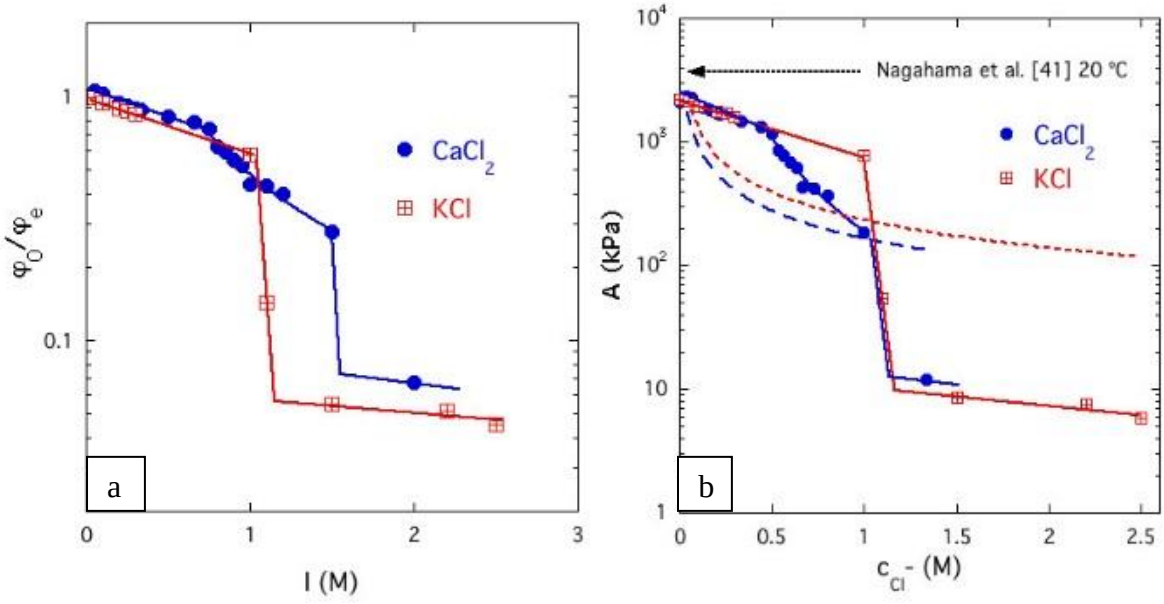

Figure 16. (a) Ionic strength dependence of the equilibrium swelling ratio φ_0/φ_e of PNIPA gels in solutions of KCl (squares) and $CaCl_2$ (circles) at 20 °C (b) Dependence of the osmotic pressure pre-factor *A* on the Cl^- anion concentration in aqueous solutions of KCl (squares) and $CaCl_2$ (circles) at 20ºC. Dashed curves: osmotic pressure of polyelectrolyte solutions as the ionic strength *I* is varied ($\propto I^{-0.75}$).[169,170] Horizontal arrow: osmotic pressure pre-factor *A* for solution of uncross-linked polymer at 20 ºC (Eq. A7).[177]

From measurements of the swelling and osmotic properties, as well as potentiometric titration and DSC response investigations of lightly cross-linked PNIPA hydrogels demonstrated that the intrinsic ionic content of the gel is vanishingly small. The osmotic response to added salt is also inconsistent with that of polyelectrolyte systems. Our investigation forecloses the idea that charged ionic groups acquired during free radical synthesis of PNIPA play a significant role in the saga of past experimental inconsistencies.

The equilibrium swelling degree of the hydrogel depends both on pH and on the nature of the buffer solution (Table A7, Fig. A1), but in the latter case the effect of the salt is stronger than that of pH. As expected, at high pH the network chains become increasingly hydrolysed, and ultimately collapse, in response to the elevated anion concentration in the solution. These findings highlight the importance of the background electrolyte.

Although ionic salts affect the osmotic pressure, the phase transition temperature appears to have no direct relationship to the value of the osmotic pressure at the transition threshold. The response of the swelling degree to the ionic salts KCl and $CaCl_2$ confirms that the VPT of the gel is governed not by the ionic strength, but by the anion concentration in the surrounding solution.

4.2. Interactions of small aromatic molecules with PNIPA hydrogel

Small aromatic molecules may influence the swelling behaviour of the PNIPA gel in various ways. While some molecules have only a slight effect or no effect at all, other guest molecules can change the transition temperature even at low additive concentrations, inducing the collapse of the hydrogel already at or below room temperature. The nature and strength of the interaction between drug molecules and the PNIPA polymer chains are of vital importance in terms of efficiency of controlled delivery. When a small molecule interacts with the polymer chains in a reversible or irreversible way, it may determine the rate of release, e.g. interactions between the guest molecule and the gel network can inhibit release by binding of the drug to the polymer chains and/or by altering the swelling properties of the gel. While chemical properties of the guest molecule and potential drug – polymer interactions are of crucial importance in the swelling and release process, these interactions are poorly understood at the molecular level.

4.2.1. Phenols

Phenols with –OH groups in meta position (phenol; 1,2-dihydroxybenzene; 1,3,5-trihydroxybenze) were investigated by our research group previously. At fixed temperature (20 °C) a significant collapse of PNIPA gel was observed when the phenol content of the aqueous solution reached a "critical" concentration (c_{crit}) that was characteristic of the guest molecule. It was also found that with the increasing number of hydroxyl groups c_{crit} shifts to lower concentrations[58] (Fig.17a). In order to reveal the correlation between the swelling and phase transition characteristics of PNIPA hydrogel and the substitution pattern of phenols in detail, studies were extended to additional bi- and tri-hydroxy phenols (1,3-dihydroxybenzene; 1,4-dihydroxybenzene; and 1,3,5-trihydroxybenzene).

The shape of the swelling curves was found to be affected by the structure of the small molecules dissolved in the swelling medium. All phenols slightly reduce the swelling degree at low concentrations that can be characterized by an "initial slope". Exceeding c_{crit} induces an abrupt volume change already at 20 °C that is characterized by the "slope of transition". Above the transition the swelling of PNIPA gel is very limited (Fig.17, Table 5). In case of meta phenols, the initial slope lessens as c_{crit} increases. On the contrary, for ortho phenols (phenol; 1,2-dihydroxybenzene; 1,2,3-trihydroxybenzene) the initial slope increases with elevating c_{crit}, also c_{crit} increases with the increasing number of –OH groups (Fig.17b). It can be concluded that relative to phenol, ortho –OH substitution increase, while meta positions decrease c_{crit} at 20 °C (Table 5). Comparing phenols with two –OH groups, the sequence is meta < para < ortho. Multiple –OH substituted phenols show a stronger influence below the critical concentration: for both meta and ortho phenols, the slope of the initial region increases with the number of –OH groups.

In the transition, increasing the number of hydroxyl groups results in the reduction and widening of the slope, both in case of meta and ortho substituted phenols. Generally speaking, if the effect of the concentration below VPT is more pronounced then the phase transition appears to be wider and less steep (Table 5).

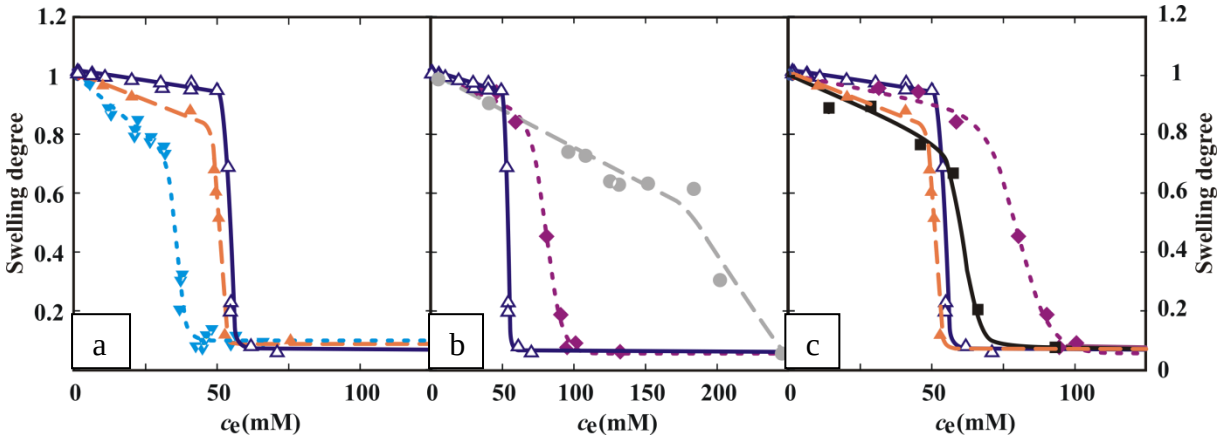

Figure 17. Swelling degree of PNIPA hydrogel in different phenolic molecule solutions at 20 °C as the function of equilibrium concentration in the free liquid phase: (a) Meta substituted phenols[58]: Δ phenol, ▲1,3-dihydroxybenzene (resorcinol), ▼ 1,3,5-trihydroxybenzene (phloroglucinol); (b) Ortho substituted phenols: Δ phenol, ◆ 1,2-dihydroxybenzene (catechol) ● 1,2,3-trihydroxybenzene (pyrogallol); (c) Δ phenol, ◆ 1,2-dihydroxybenzene (catechol), ▲1,3-dihydroxybenzene (resorcinol), ■1,4-dihydroxybenzene (hydroquinone).[178,179,180,181]

Table 5. c_{crit} of the phase transition and slope* of the swelling isotherms of PNIPA hydrogel in aqueous phenol solutions.[181]

	Phenol	Meta		Ortho		Para
		1,3-dihydroxy-benzene (resorcinol)	1,3,5-trihydroxy-benzene (phloroglucinol)	1,2-dihydroxy-benzene (catechol)	1,2,3-trihydroxy-benzene (pyrogallol)	1,4-dihydroxy-benzene (hydroquinone)
c_{crit} (mM)	53[58]	50[58]	36[58]	81	194	62
Initial slope (1/mM)	$-1.4\cdot10^{-3}$	$-4.7\cdot10^{-3}$	$-6.0\cdot10^{-3}$	$-2.7\cdot10^{-3}$	$-2.8\cdot10^{-3}$	$-5.5\cdot10^{-3}$
Slope in transition range (1/mM)	$-161*10^{-3}$	$-111*10^{-3}$	$-87*10^{-3}$	$-35*10^{-3}$	$-7.3*10^{-3}$	$-47*10^{-3}$

*the error of the linear fit is 8-20%

The phase transition of PNIPA gel swollen in aqueous guest molecule solutions was also investigated by high sensitivity DSC. Raising the concentration of phenols significantly lowers the transition temperature and broadens the response curve that becomes slightly more endothermic (Fig.18, Table 6). Broadening may indicate slower relaxation of the PNIPA

polymer chains during the transition as the concentration increases and/or reduced heat conductivity as water is expelled. Observations on the effect of phenols on the phase transition were confirmed by NMR measurements.

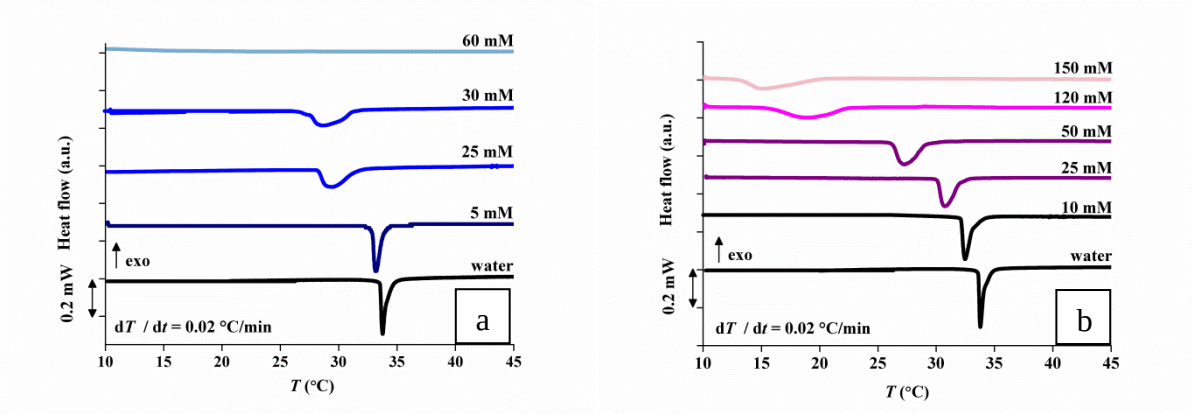

Figure 18. DSC response of powdered PNIPA gel in (a) phenol and (b) cathecol Successive curves are shifted vertically.[181]

Table 6. Δ*H* values of the phase transition of PNIPA hydrogel swollen in aqueous phenol and cathecol solutions.[181]

Phenol		Cathecol	
c (mM)	Δ*H* (J/g)	*c* (mM)	Δ*H* (J/g)
0	57 ± 5	0	57 ± 5
5	60 ± 5	10	59 ± 5
25	71 ± 6	25	60 ± 5
30	70 ± 6	50	68 ± 6
60	72 ± 6	100	68 ± 6
		150	62 ± 5

Interaction of phenols with PNIPA gel and their effect on polymer structure on the molecular level were investigated on phenol and cathecol loaded gels by solid state NMR techniques. In present thesis the main conclusions of the published NMR results[182,178] are highlighted.

^{1}H Magic Angle Spinning (MAS) spectra revealed that the pore structure of the guest molecule loaded gel is more complex in case of phenol than for cathecol. This observation is highly consistent with the DSC results. The broader DSC transition of phenol reflects a greater variety of polymer configurations compared to cathecol. Broad signal develops when the rearrangement of the aromatic molecules after deswelling is slower, which is due to the more complicated pore structure. According to the MAS NMR investigations no phenol or cathecol

molecules are present in the free water phase, suggesting a possible interaction between the phenolic compounds and PNIPA.

Direct information about these molecular associations was derived from Combined Rotation and Multiple-Pulse Spectroscopy (CRAMPS) spectra which map the connectivity between proton resonances (Appendix A5). When the proton-proton distance is less than 1 nm, intermolecular cross-peaks appear, demonstrating the existence of host-guest interactions. Phenol molecules were found to be connected by strong H-bonds to the carbonyl groups of the PNIPA acrylamide side chains (Fig.19). This observation was confirmed by Density Functional Theory (DFT) calculations: the most favourable structure is when phenols are attached by strong hydrogen bonds to the carbonyl groups of PNIPA gel, in which case they can freely rotate around the C=O axis.

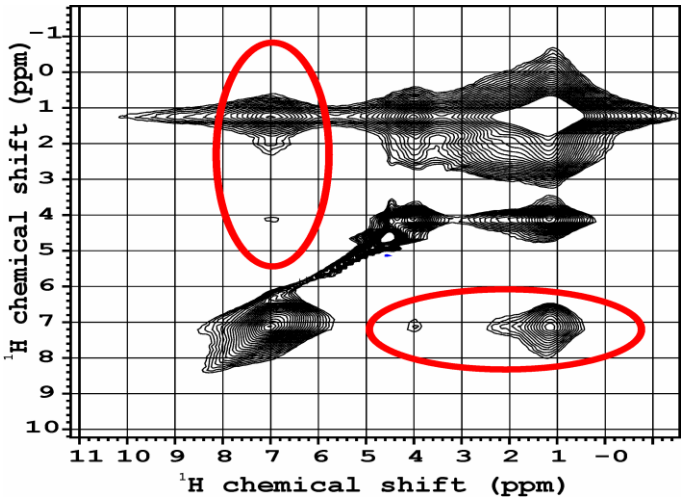

Figure 19. ^{1}H-^{1}H correlation CRAMPS spectra at 10 kHz spinning rate with 1000 μs of mixing time above VPT. Appearance of intermolecular cross-peaks demonstrates the close proximity in swollen PNIPA gel containing phenol above the VPT.[178]

4.2.2. Dopamine and ibuprofen

It was found that all phenols have a major influence on the PNIPA phase transition. Swelling, DSC and NMR measurements confirmed that the effect of these guest molecules strongly depend on their chemistry, i.e. both on the number and on the position of OH groups. In order to extent the investigations to further functional groups, two drug molecules that are applied in real practice and have different functional groups were chosen: dopamine and ibuprofen.

The effect of both drug molecules on the hydrogel is fundamentally different compared to phenols. Introducing an aminoethyl group into 1,2-dihydroxybenzene changed the interactions dramatically: contrary to phenols, no VPT occurs even in very concentrated (c_0 = 1 M) solutions of dopamine. Ibuprofen also does not induce phase transition, but causes a minor depletion in the swelling degree; that is proportional to its concentration (Fig.20).

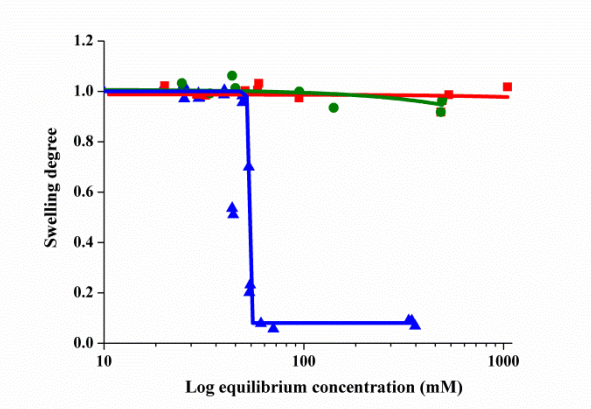

Figure 20. Swelling degree of the PNIPA hydrogel in model drug solutions at 20 °C, as the function of equilibrium concentration in the free liquid phase:

▲phenol ■ dopamine ● ibuprofen.[180]

Dopamine slightly increases the phase transition temperature (Fig.21a). The broadening of the phase transition peak becomes obvious only from 500 mM dopamine concentration. Although at 20 °C no macroscopic deswelling can be observed, the enthalpy of the transition drops sharply in the 1 M dopamine solution (Table 7). Ibuprofen has virtually no effect on T_{VPT} and its enthalpy increasing effect is very moderate (Fig.21b, Table 7). The effect of both dopamine and ibuprofen differs greatly from that of phenol, in which case a significant

reduction of the phase transition temperature and broadening of the response curve was observed already at lowest guest molecule concentrations.

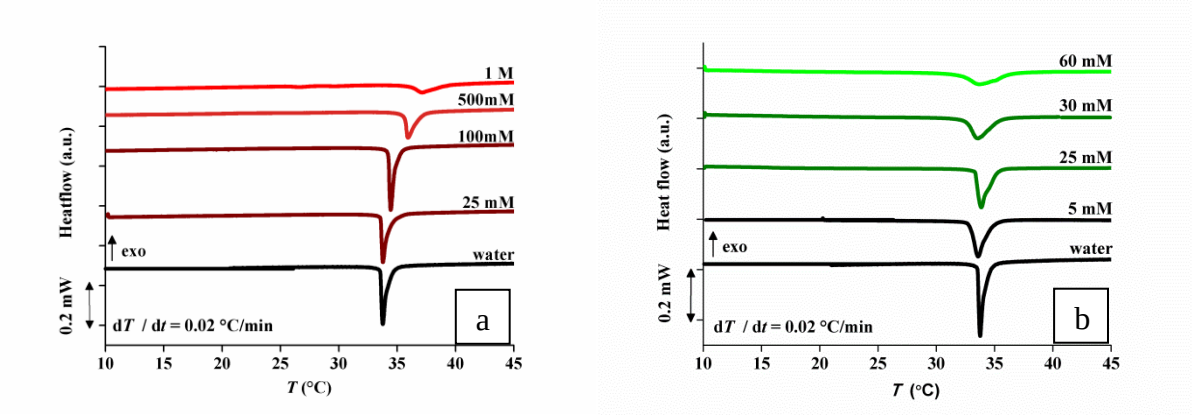

Figure 21. DSC response of powdered PNIPA gel in (a) dopamine and (b) ibuprofen solutions with different concentrations. Successive curves are shifted vertically.

Table 7. Δ*H* values of the phase transition of PNIPA hydrogel swollen in aqueous dopamine and ibuprofen solutions.

Dopamine		Ibuprofen	
c (mM)	Δ*H* (J/g)	*c* (mM)	Δ*H* (J/g)
0	57 ± 5	0	57 ± 5
25	55 ± 5	10	59 ± 5
100	60 ± 6	35	61 ± 5
500	50 ± 5	50	61 ± 5
1000	33 ± 3	100	61 ± 5

Unlike for phenols, interactions between dopamine and PNIPA molecules could not be detected by NMR investigations (Fig.22). However, a substantial part of the dopamine molecules showed only a very low mobility indicating oligomerization, or even polymerization of dopamine. The coexistence of the aromatic ring and amine group in the dopamine molecule were reported to be the driving force of self-polymerization, however the detailed mechanism is not revealed yet. Most probably the oxidation of catechol to a quinone is followed by a polymerization, in a like manner to melanin formation.[183,184]

Similarly to dopamine, in the CRAMPS spectra of the ibuprofen loaded gel intermolecular interactions between the drug and the polymer could not be clearly detected.

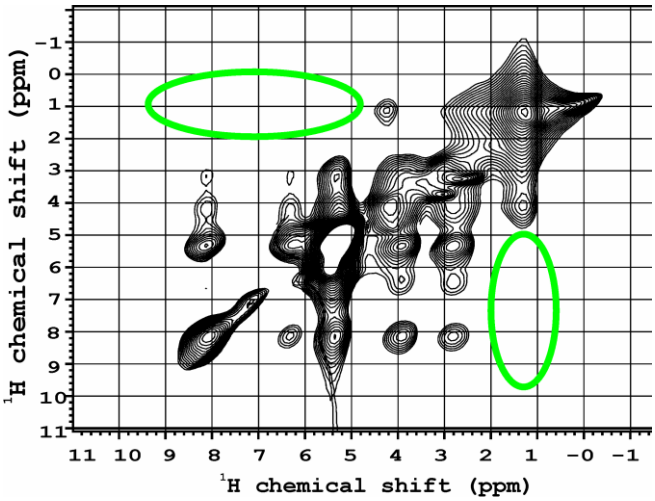

Figure 22. ^{1}H-^{1}H correlation CRAMPS spectra at 10 kHz spinning rate with 1000 μs of mixing time above VPT. The corresponding cross peaks are absent with dopamine (area inside ellipses) .[178]

It has been observed that the addition of small guest molecules, even at low concentration, influences noticeably the transition behaviour of the PNIPA hydrogel. Several additives, e.g. inorganic salts, phenols and benzene derivatives (salicylaldehyde, 3,4-dimethoxybenzaldehyde, hydroxy-benzaldehyde, ethylvanillin, benzoic acid, methyl-p-hydroxybenzoate), saccharide and organic solvents (methanol, ethanol, dimethyl sulfoxide) were found to reduce the T_{VPT} of PNIPA. The transition temperature can be increased by the addition of surfactants (e.g. sodium dodecyl sulphate) or organic quaternary ammonium salts.[50,51,52,53] The T_{VPT} shift depends on the structure and the concentration of the additive, but no correlation was found with hydrophobicity or solubility, suggesting that specific additive – polymer interactions may be the major factors in controlling the T_{VPT}.[50]

In investigations of phenol – PNIPA systems it was found that all phenols have a major impact on the phase transition of the PNIPA gel. In aqueous solution, they reduce the T_{VPT} proportionally to their concentration (Fig.23) and affect the rate of heat release. The extent depends both on the number and on the position of the hydroxyl groups. When the –OH groups are in meta position, increasing their number reduces the concentration required to initiate a phase transition already at 20 °C. Increasing the number of the –OH groups in adjacent position on the other hand shifts this concentration to higher values.

The effect of phenols was compared to that of two widely used aromatic drug molecules that are expected to behave differently: dopamine and ibuprofen. The aminoethyl phenol derivative, dopamine, has an opposite effect to phenols: it increases the phase transition

temperature, though its impact is much more limited compared to that of phenols. Contrary to all these, ibuprofen has no effect on T_{VPT} at all. As neither the solubility nor the acid/base properties (Table 2) provide an explanation for the different effect of phenols, dopamine and ibuprofen, an understanding of the intramolecular interactions is required.

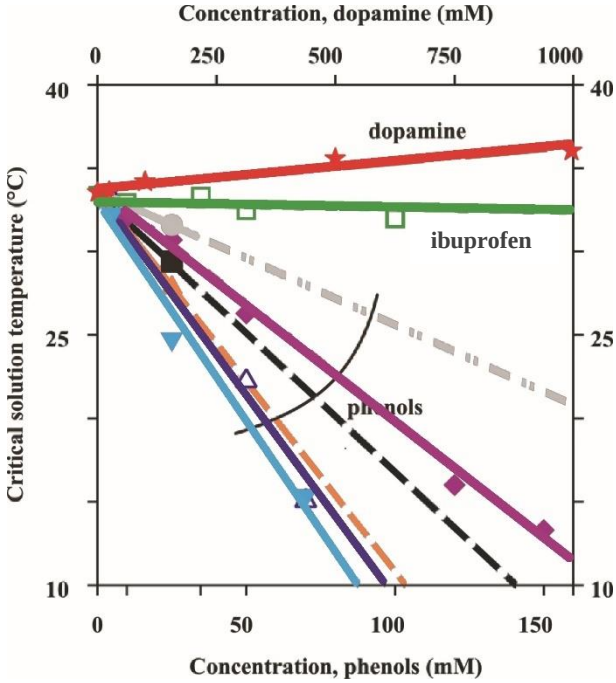

Figure 23. T_{VPT} of PNIPA gel in aqueous solutions from DSC measurements. For phenols and ibuprofen the lower, for dopamine the upper concentration scale applies. Δ phenol, ◆ 1,2-dihydroxybenzene (catechol), ▲1,3-dihydroxybenzene (resorcinol), ■ 1,4-dihydroxybenzene (hydroquinone), ● 1,2,3-trihydroxybenzene (pyrogallol), ▼ 1,3,5-trihydroxybenzene (phloroglucinol), □ ibuprofen ★4-(2-aminoethyl)benzene-1,2-diol (dopamine).[181]

4.2.3. Interactions between small aromatic molecules and the PNIPA hydrogel seen in dry state; implications for drug delivery

The disadvantage of drug transport systems based on the quick phase transition of swollen gels that they are not suitable for a retard drug release. A possible solution can be the application of dried drug loaded gels that provide prolonged release during the slow reswelling due to their shape memory. It is expected that interactions observed in swollen state are preserved during the drying process, and thus influence the thermal properties of the dry drug – polymer system. In order to obtain deeper insight into the interactions between the guest molecules and the polymer, dry PNIPA matrices loaded with three types of drugs affecting the swollen state in different ways – phenol, dopamine hydrochloride and ibuprofen sodium – were investigated by STA measurements.

Table 8. Selected properties of the guest molecules in simultaneous thermal analysis (STA) experiments.

	Phenol	Dopamine hydrochloride	Ibuprofen sodium	
Melting	Melting: T = 40.89 °C ΔH_{fus} = 11.51 kJ/mol[185] Sublimation: T = – 43-40 °C ΔH_{sub} = 65.3-69.7 kJ/mol[186]	T = 241 °C (decomposition)[187]	β	T = 190 °C[77,79,188]
			γ	T = 200 °C ΔH_{fus} = 10.8 kJ/mol[77,79,188]
Boiling	T = 181.87 °C ΔH_{vap} = 45.69 kJ/mol[185]			

The composition of the drug loaded dry PNIPA gel samples is summarized in Table 16. The significantly lower guest molecule uptake for phenol compared to both drug molecules is due to the collapsed state of hydrogel resulted by the phenolic concentration of the swelling medium.

Table 9. Composition of dry drug loaded PNIPA gels.[180]

Guest molecule	Uptake* $\frac{mmol_{guest}}{g_{dry\ gel}}$	Sample composition*		
		$\frac{Guest}{monomer}$ molar ratio	w/w%	
			Guest	Monomer
Phenol	2.2	0.25	17.1	82.9
Dopamine hydrochloride	15.1	1.71	74.1	25.9
Ibuprofen sodium	14.2	1.61	76.3	23.7

* based on uptake measurement (Eq.2)

The decomposition of PNIPA gel occurs in a single step and is preceded by 3.4% water loss around 100 °C, indicating that even after a week-long storage in a desiccator some water is still retained. The glass transition at ca 130 °C is not well-pronounced on the DTA curve (Fig.24). These observations are in a good agreement with the literature.[12,189] Degradation takes place from 330 to 430 °C resulting in 94.9% mass loss and 478.0 J/g_{sample} enthalpy change. The corresponding DTG and DTA peaks appear at 415.5 and 414.5 °C, respectively. Considering the water content, the decomposition enthalpy of the water-free PNIPA gel can be estimated as ΔH = 56.0 kJ/$mol_{monomer}$. Residual mass at 650 °C is 1.7%.

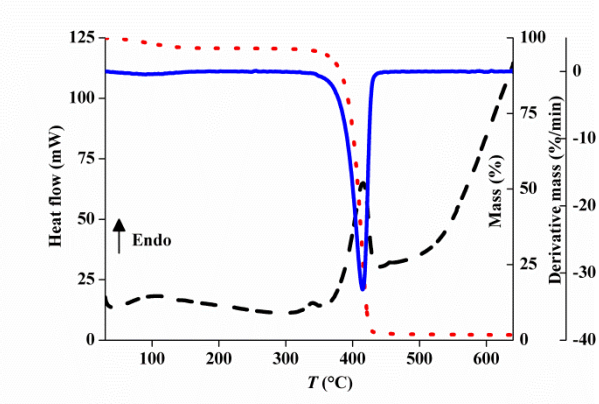

Figure 24. Thermogravimetric (TG), differential thermogravimetric (DTG) and differential thermal analysis (DTA) responses of pure PNIPA gel.
TG: dotted line, DTG: solid line, DTA: dashed line.

In the thermal response of pure phenol no separate water loss can be distinguished (Fig.25a). The melting peak appears at 43 °C on the DTA curve. The sharpness of the melting peak and the corresponding enthalpy (9.4 kJ/mol) indicates the lack of sublimation.[185] In the

50-140 °C range phenol completely evaporates into the nitrogen flow (100% mass loss). The corresponding DTA (137 °C) and DTG (136 °C) peaks are below the normal boiling point (182 °C)[185], that can be attributed to the dynamic conditions. The molar heat of the melting (54.9 kJ/mol) overestimates the heat of evaporation,[185] due to the highly volatile nature of phenol.

Since the PNIPA gel collapses in 500 mM phenol solution, this sample was prepared above LCST conditions, where the polymer forms ca. 10 nm thick hydrophobic walls instead of the freely moving organic chains. Phenol molecules are distributed in the hydrophobic walls as well as in the ca. 100 nm cavities.[60] The liquid phase retained is limited, although the swelling degree is still 8.2 (Fig.20). NMR investigations revealed that close to the phase transition state a direct interaction develops between the phenol and the polymer chains. The thermal response of the guest – PNIPA gel system (Fig.25b) cannot be derived as a simple proportional combination of the pure phenol (Fig.25a) and PNIPA gel (Fig.24) curves. The melting peak of phenol and the T_g of PNIPA are not recognizable. The mass loss belonging to the first step on the TG curve (60-280 °C) significantly exceeds the phenol content (Table 9). According to Figure 24 PNIPA gel starts to degrade only at higher temperature, and therefore it may not contribute to this effect. Since according to the mass balance the loaded sample contains 24% water even when dried until constant mass, this step can be attributed to the slow discharge of phenol and strongly bound water molecules, indicating phenol – water – PNIPA gel interaction. The high water content contributes to the elasticity observed on the macroscopic sample. Decomposition of the phenol loaded hydrogel occurs at 382 °C. The higher thermal sensitivity may be the result of the weakening polymer – polymer attraction and the less ordered structure as the loaded gel is drying, due to the phenol – PNIPA gel interaction. The high surface area of the remaining porous polymer may also contribute to the higher thermal sensitivity. This can be concluded from the comparison of the corresponding residues at 650 °C. Considering the PNIPA content of the sample (Table 9), the estimated degradation heat of PNIPA is 62 $kJ/mol_{monomer}$, which is in a relatively good agreement with the enthalpy obtained for pure PNIPA gel. It is very probable that no phenol remains in the gel at high temperatures.

On the TG curve of pure dopamine hydrochloride a wide and complex step can be observed in the 220-500 °C region with the total mass loss of 77.2% and 22.8% residue, in compliance with the reference data[183] (Fig.25c). The melting peak appears on the DTA curve at 244.7 °C with a corresponding enthalpy of 36.8 kJ/mol. According to the DTG response, the decomposition starts already at the melting point resulting in a peak maximum at 327 °C and heat effect of 85.5 kJ/mol. A well separable heat (66.9 kJ/mol) belongs to the tail of the DTG curve. The total heat of decomposition can be estimated as 155.4 kJ/mol.

Dopamine behaves as it is expected from the swollen state behaviour. Dopamine and PNIPA degrade practically independently based on the STA observations. On the thermal response curves of dopamine loaded PNIPA gel characteristic regions belonging to the drug and the gel can be identified and practically no changes in peak positions can be observed (Fig.25c and d). The residue at 650 °C (ca. 21%) and the clearly recognisable melting peak of dopamine (224.8°C) also confirms the independent decomposition of the components. The melting enthalpy 21 kJ/mol$_{dopamine}$ is about 60% of that obtained for pure dopamine. Possibly a part of the drug interacts preferentially with other dopamine molecules,[183,184] thus only a limited amount contributes to this peak. The DTG signals of the drug and the gel are very close to each other (Fig.26): the peak at 313.9 °C belongs to dopamine, and the DTG peak at 405.4 °C corresponds to the PNIPA gel. The estimated 81 kJ/mol$_{dopamine}$ decomposition enthalpy is in a good agreement with that obtained for pure the pure dopamine hydrochloride. The slight shifts in the DTG peak positions can be attributed to the modified signal shape rather than any interaction.

The TG curve of pure ibuprofen sodium racemate (Fig.25e) reveals an initial water loss of 2.8 % below 100 °C. The 198 °C peak in the DTA response is related to the melting of the gamma form of ibuprofen sodium,[77,188] however, the corresponding enthalpy (16.1 kJ/mol$_{dry\ ibuprofen}$) is significantly higher than the reference value (Table 9). Decomposition takes place at 465 °C (ΔH = 84.8 kJ/mol$_{dry\ ibuprofen}$), leaving 25.7% residue.

The PNIPA gel was highly swollen in 500 mM ibuprofen solution during the sample preparation. Ibuprofen, although its effect in swollen state is very moderate, modifies the PNIPA signal the most. In the ibuprofen loaded system a dehydration process with the mass loss of 9.0%, ending at ca. 145 °C was observed (Fig.25f). As the pure drug and the pure polymer retain only a limited amount of water, this increased attraction of water can be attributed to the composite system. The melting point of ibuprofen is hardly detectable and shifted to ca 184 °C. Instead of distinguishing responses in the mixed system around the temperatures characteristic to the individual components, the degradation DTG peaks of both the polymer and ibuprofen "disappear" and a single peak appears at a significantly lower temperature, above 300 °C with an elongated tail that ends around at 500 °C (total mass loss 81.1%, total heat 419.2 J/g$_{sample}$). This significant shift of decomposition can be attributed to the less ordered and more temperature sensitive gel structure in the presence of ibuprofen, and reveal that the degradation of ibuprofen is also promoted by the decomposition of the polymer. The total residual mass (8.3%) that is much less of that can be estimated from the pure signals,

confirms this synergetic effect and suggests that a part of ibuprofen is strongly attracted to the polymer chains.

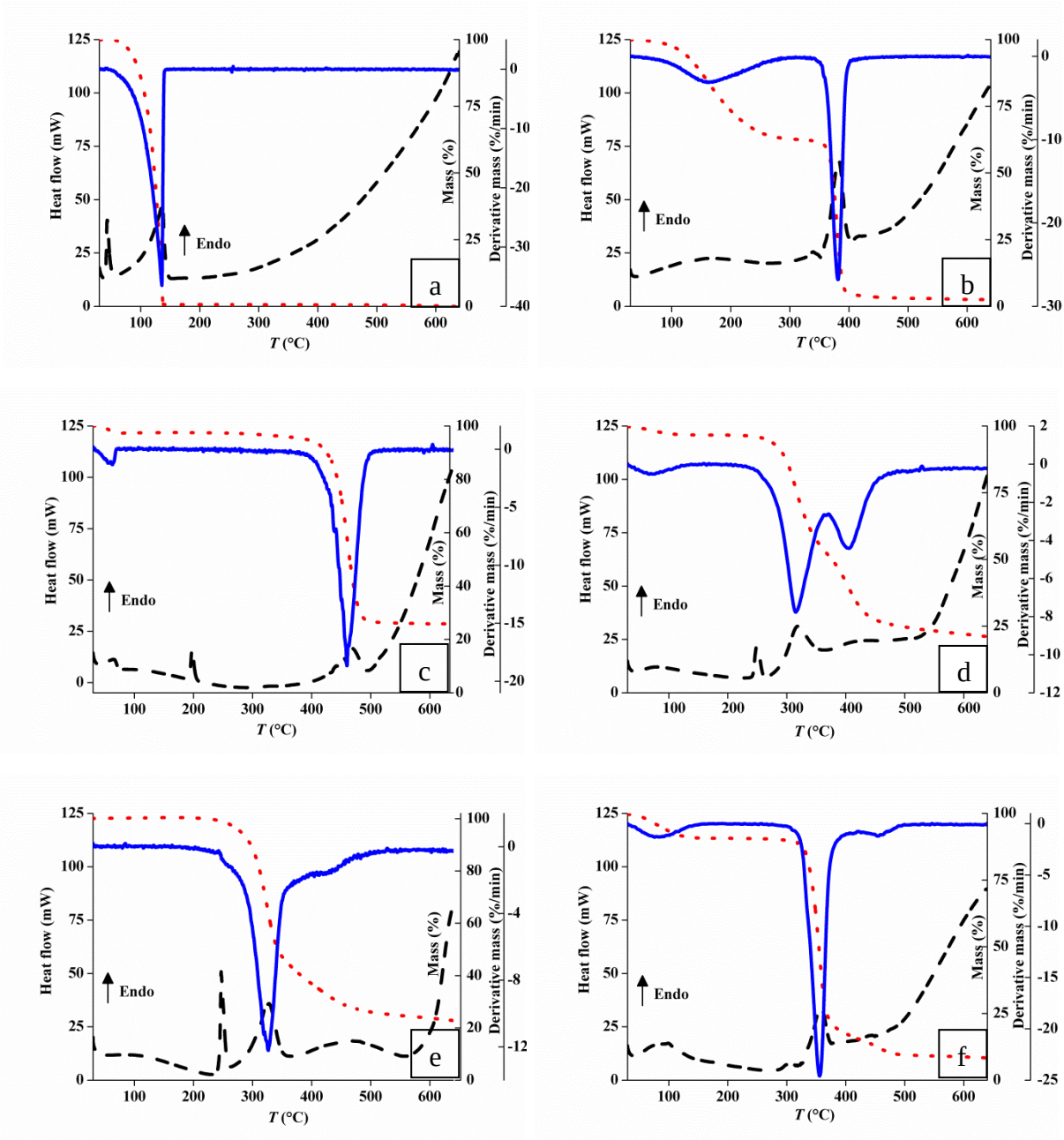

Figure 25. TG, DTG and DTA responses of (a) phenol (b) phenol loaded PNIPA gel (c) dopamine hydrochloride (d) dopamine hydrochloride loaded PNIPA gel (e) ibuprofen sodium and (f) ibuprofen sodium loaded PNIPA gel in N_2 flow. TG: dotted line, DTG: solid line, DTA: dashed line.[180]

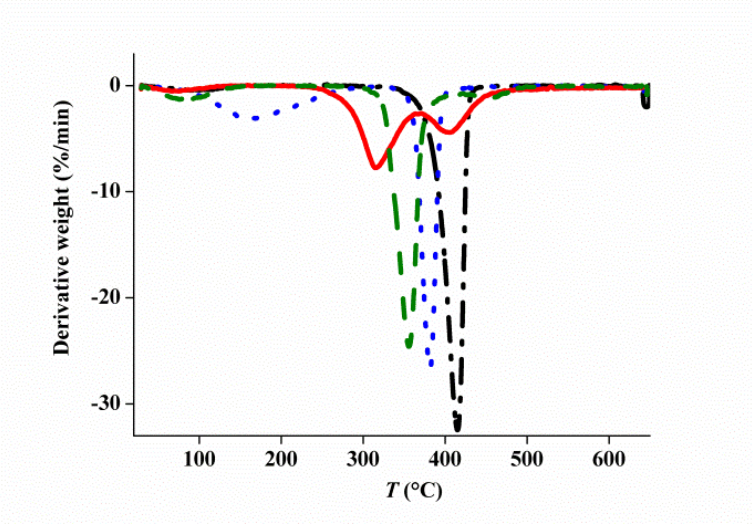

Figure 26. Comparison of the DTG response of PNIPA gel samples loaded with different drug molecules in N_2 flow. Pure PNIPA gel: dotted-dashed line, phenol loaded gel: dotted line, dopamine hydrochloride loaded gel: solid line, ibuprofen sodium loaded gel: dashed line.[180]

Direct interactions between the drug molecules and the PNIPA polymer chains are expected to significantly affect the drug release effectiveness of the dry guest loaded systems. These may not only influence the amount of drug that can be released but also its morphology. As water evaporates from the drug – PNIPA systems, host – guest interactions determine the final crystalline form of the loading drugs. By drying the loaded gel matrices amorphous or small crystalline particles can develop from the drug that may facilitate accurate dosage and dissolution. Crystallization of the three selected guest molecules – phenol, dopamine hydrochloride and ibuprofen sodium – within the PNIPA matrix was investigated by XRD method.

According to XRD spectra, all three drugs recrystallize when their 500 mM aqueous solutions are dried in free conditions (Fig.27a, c and e). The diffractogram obtained on PNIPA gel swollen in pure water showed that the dry gel is amorphous. The lack of crystalline peaks in the spectrum of the phenol loaded gel (Fig.27b) indicates that the crystallization of phenol confined in the gel is hindered, that can be attributed to the hydrogen bond formation between phenol and PNIPA, which was confirmed by NMR measurements.[74,75] This conclusion is consistent with the observations reported earlier, i.e. that hydrogen bonding between the drug molecule and polymer chains inhibits the mobility and thus the nucleation and crystallization of phenol.[55,74] The amorphous state of phenol in the dry gel is also confirmed by STA measurements, where the absence of the phenol melting peak was observed. Since it is accompanied by the strong bonding of water molecules – as it was also revealed by STA –, the

phenol – PNIPA gel interaction not only hinders crystallization of phenol, but results in a high residual water content and thus elasticity even in samples dried until mass stability.

By contrast, dopamine hydrochloride slowly crystallises during the drying process (Fig.27d). This can be attributed to the strong guest – guest interaction[183,184] that may prevent the dopamine – PNIPA gel interaction even in confined conditions, but fosters crystallization. These findings can be confirmed STA investigations. The independent decomposition of PNIPA gel and dopamine hydrochloride refers to the lack of interaction; while the reduced area of the clearly recognisable melting peak implies that part of the dopamine is in interaction with other dopamine molecules, thus only a limited amount can contribute to this peak.

In the ibuprofen sodium incorporated gel fast crystallization of the drug can be observed (Fig.27e). While hydrogen bonding between ibuprofen and PNIPA was reported in some studies,[190,191] no clear evidence of chemical interaction between the guest molecule and the hydrogel was found by NMR investigations. While the synergetic decomposition of the drug and the polymer in STA investigations implies interaction, the remaining degradation and melting peak of free ibuprofen sodium on STA curves and the observed crystallization of ibuprofen during the drying process suggest that even if there is any interaction, only a part of ibuprofen is bound.

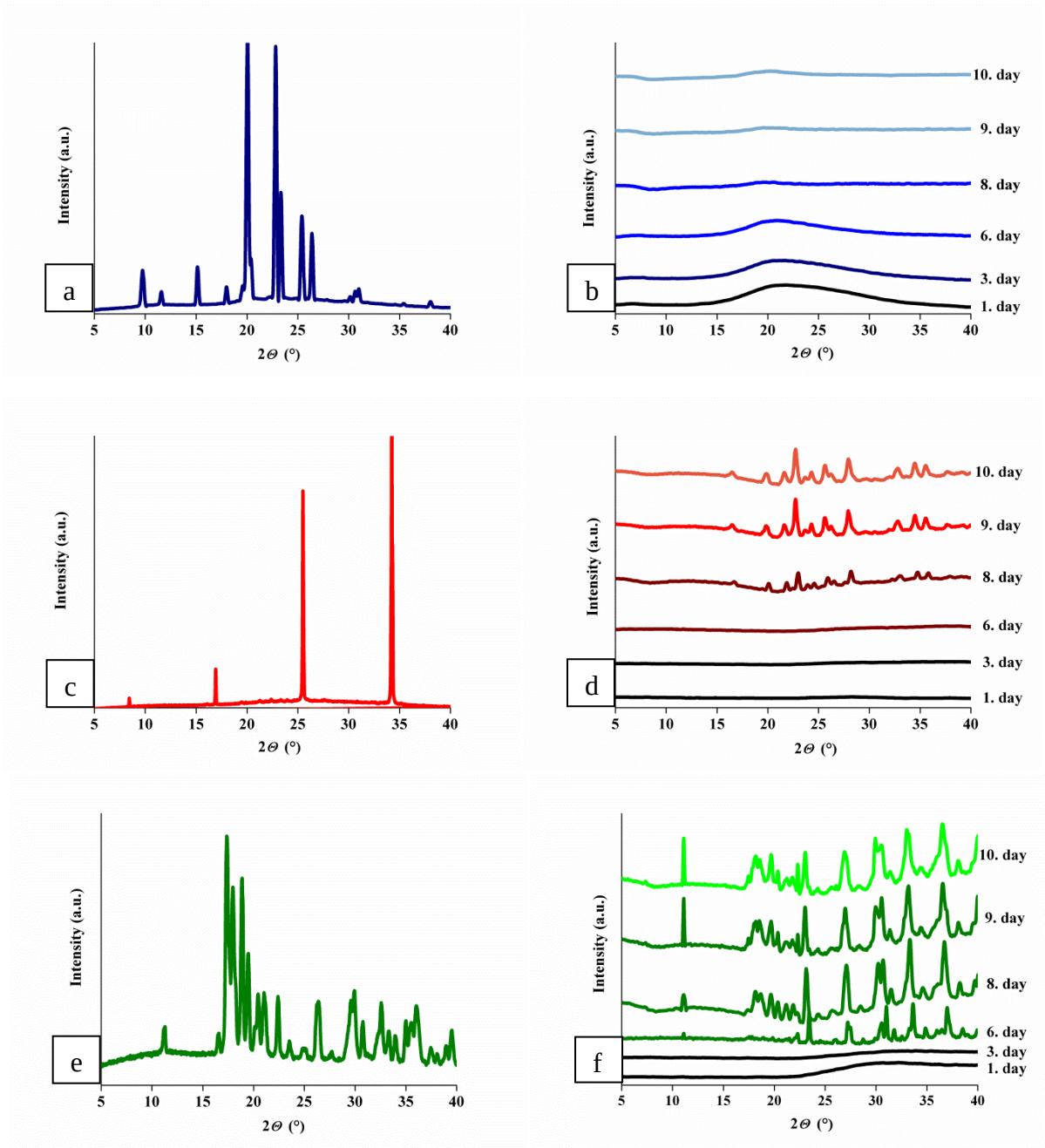

Figure 27. XRD spectra of the guest molecules and the guest-PNIPA gel systems during the drying process: (a) phenol (b) phenol loaded PNIPA gel (c) dopamine hydrochloride (d) dopamine hydrochloride loaded PNIPA gel (e) ibuprofen sodium (f) ibuprofen sodium loaded PNIPA gel. Successive curves are shifted vertically for clarity.[181]

Table 10. Drug crystallite sizes crystallized from solutions and confined in PNIPA gel.

Guest molecule	Estimated crystallite size (nm)	
	Crystallized from solution	Crystallized in PNIPA gel
Phenol	118 ± 47	no crystals
Dopamine hydrochloride	124 ± 19	37 ± 14
Ibuprofen sodium	95 ± 15	63 ± 20

In the dry polymer matrix phenol is preserved in amorphous state. When drying in free conditions, the crystallite size of phenol is 118 nm. For dopamine hydrochloride significant, while for ibuprofen sodium a slighter reduction in the crystallite size occurs when confined in the gel matrix. The size of dopamine crystallites reduces from 124 nm to 37 nm when dried within the gel network. In case of ibuprofen the crystallite sizes are 95 nm and 63 nm, in free and in confined states, respectively.

Drug – polymer interactions significantly affect the drying process of loaded gels. Observed variations in the thermal responses of the three drug loaded dry PNIPA gel samples can be interpreted in terms of the different molecular interactions in confined conditions. The elongated collective release of phenol and water suggests that the interaction between PNIPA gel and phenol is mediated by the retained water molecules (Fig.29b). The reduced area of the dopamine melting peak indicates that part of the dopamine forms dimers or oligomers, and this strong guest – guest relation may hinder the interaction with the polymer (Fig.29d). The disappearance of the individual ibuprofen and PNIPA degradation peaks and the presence of a single decomposition peak at a significantly lower temperature suggest that a part of ibuprofen molecules is in a strong interaction with PNIPA gel that survives even at elevated temperatures (Fig.29f).

According to XRD spectra the hydrogen bridges between phenol and PNIPA hinder the crystallization during the drying process, giving rise to amorphous phenol (Fig.31b). Unlike in the case of phenol, in the dopamine (Fig31d) and ibuprofen loaded (Fig31d) gels the lack of guest – polymer interactions result in the gradual crystallization of drug molecules. The size of the dopamine and the ibuprofen crystallites inside the gel matrix are significantly smaller compared to those developed in free state (Table 10). These observations reveal that host – guest interactions greatly influence the crystalline state as well as the crystallite size of the stored drug molecules, thus significantly determine their rate of release. Particle size reduction and/or the formation of amorphous state of the drugs can enhance dissolubility, while strong drug – polymer interactions may result in the reduction of the released amount of drug

molecules.[55,66,76] According to the above observations, the dry PNIPA based drug carrier systems may be suitable not only for retard release, but also for enhancing solubility and thus bioavailability of poorly water-soluble drugs.

5. PNIPA – carbon nanoparticle hybrid gels

Despite its various biomedical potentials, the poor mechanical properties of PNIPA hydrogel may limit its application as structural biomaterial.[80] Durability of PNIPA gel can be enhanced by incorporating carbon nanoparticles into the hydrogel. The presence of nanoparticles might also influence the kinetics of the temperature induced phase transition and result in infrared irradiation sensitivity.

The effect of carbon nanoparticles on the properties of PNIPA gel was examined on carbon nanotube (3, 6, 12 and 24 mg CNT/g_{NIPA}) and graphene oxide (2, 15, and 20 GO/g_{NIPA}) incorporated gels. The pH values of CNT and GO suspensions were 2.7 and 4.0, respectively.

5.1. Morphology of hybrid gels

Upon the incorporation of carbon nanoparticles into PNIPA the transparent gel became black (with CNT) or brown (with GO). In CNT-PNIPA samples macroscopic heterogeneity (Fig.28) can be observed by naked eye. On the contrary, in GO hybrid gels visibly no aggregation occurs even in the most concentrated samples.

Figure 28. Digital optical microscopic images of the cross section of the lyophilised gel films[159]

For both nanoparticle containing composite samples a “wall region” and an “inner region” are clearly distinguishable in images (not shown here). Typical SEM images of both regions are displayed in Figure 29. In pure PNIPA films these two regions are very similar: wide amorphous pores separated by thin polymer walls. In the composite samples the morphology depends on the type of nanoparticle. Both with CNT and GO the wall and inner

regions, respectively, are significantly different indicating that the orientation of the CNPs might be influenced by interaction with the wall. Nevertheless, the heat transfer during the freezing process may also lead to layer formation. Further morphological differences developed along the axis in the composite gel cylinders particularly with CNT due to sedimentation during gelation.

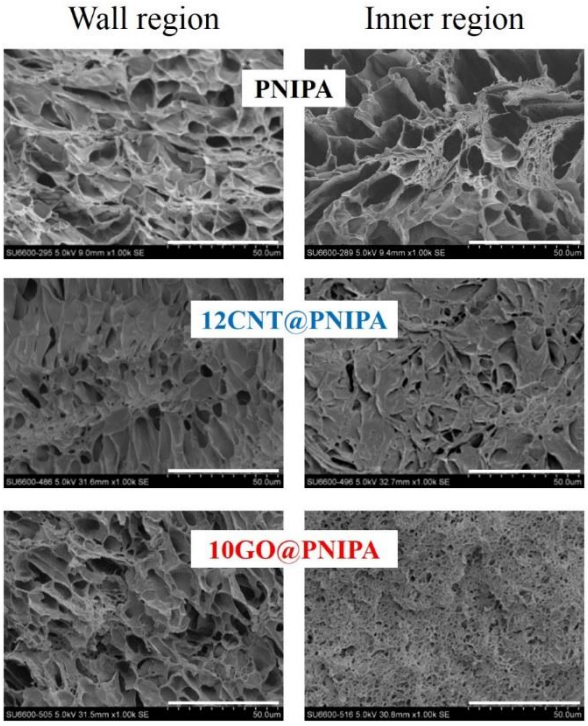

Figure 29. SEM images of PNIPA, 12 mg CNT/g_{NIPA} (12CNT@PNIPA) and 10 mg GO/g_{NIPA} (10GO@PNIPA) lyophilised hybrid gel films. The scale bar is 50 μm[159]

Pore size distributions of CNT containing composites (Fig.30b) are not very different from pure PNIPA (Fig.30a). On the other hand, the GO content unambiguously has a stronger influence on the pore structure (Fig.30c and 30d). Interestingly, the lower GO content has a more significant influence.

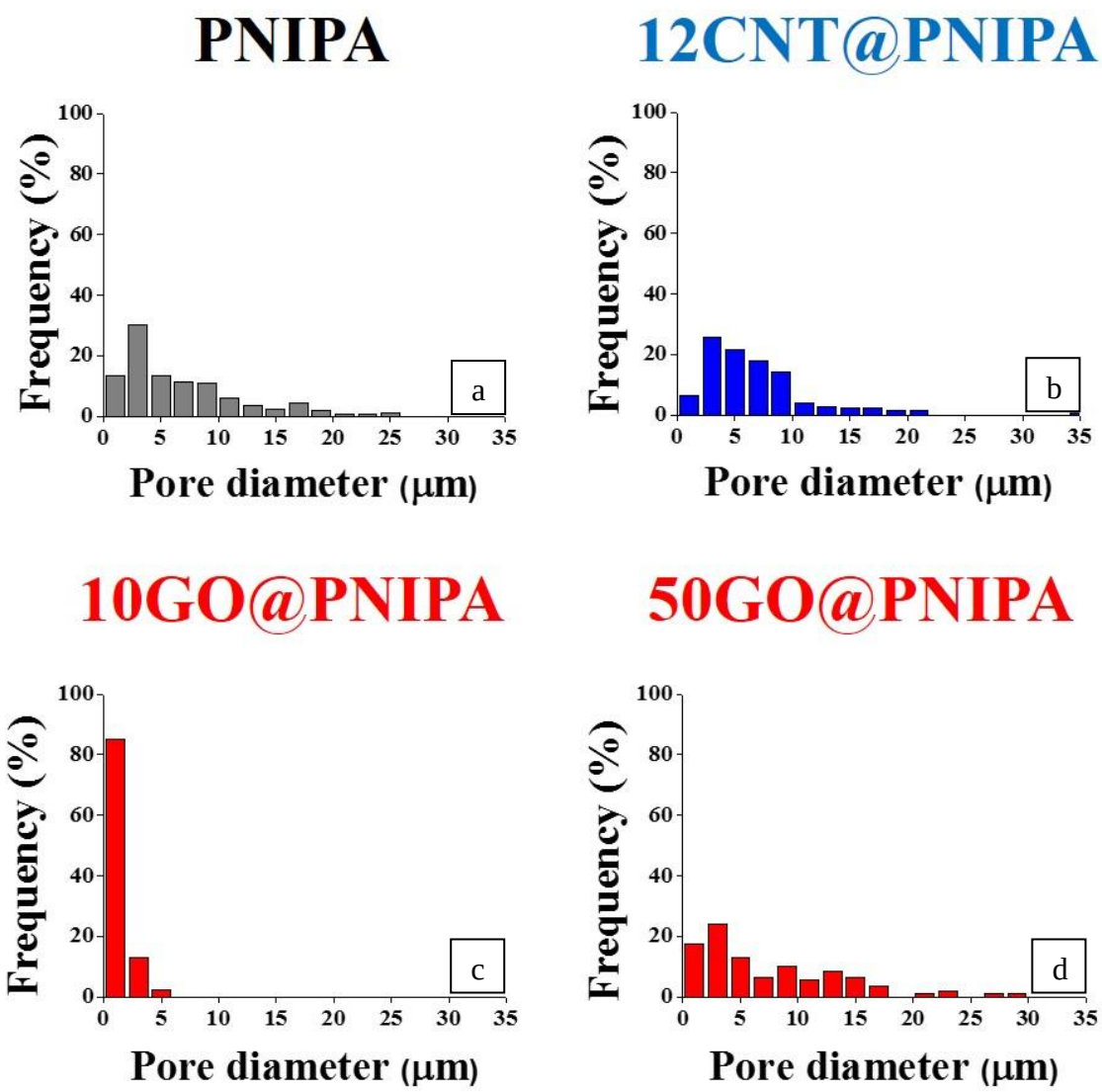

Figure 30. Pore size distribution (a) bulk of PNIPA, (b) 12 mg CNT/g_{NIPA}, (c) 10 mg GO/g_{NIPA} and (d) 50 mg GO/g_{NIPA} lyophilised gel.[159]

5.2. Swelling and mechanical properties

Comparing the swelling degree and the elastic modulus of the hydrogels significant differences were found between the two sets of composites (Fig.31a). CNT slightly but monotonically reduced the swelling degree, that can be due to (a) the reduction in volume from the presence of CNT (b) the increasing proportion of hydrophobic components in the hybrid gel;[192,193,194] (c) the polymer molecule movement inhibiting effect of nanotubes;[195] and (d) the solvent diffusion hindering property of the three-dimensional network formed by irregularly distributed nanotubes in case of high additive concentrations.[196] Practically no effect of CNTs on the elastic modulus was detected.

A more pronounced and non-linear effect of GO incorporation was observed in the composites. Even 15 mg GO/g_{NIPA} content led to an abrupt drop by ca. 33% in the swelling degree. Further increase of the GO content had no observable effect on the swelling (Fig.31a). The elastic modulus increased monotonically in the whole examined GO concentration range (Fig.31b). A similar observation on sodium alginate/polyacrylamide (PAM) hydrogels with comparable GO content (0.5-5 w/w%) was reported by of Fan et al.[120] PNIPA systems with significantly higher cross-link ratio and 1-10 w/w% GO content displayed a contrary trend.[115] Incorporation of CNPs significantly improved the fracture stress properties of PNIPA (Fig.31d). CNT containing gels tolerate greater deformation before they break, while GO incorporated gels bore higher stress at smaller deformation. The fraction points are compared in Figure e: in GO – PNIPA gels the fracture stress is independent on the nanoparticle content, while CNT-PNIPA gels exhibit a limited enhancement.

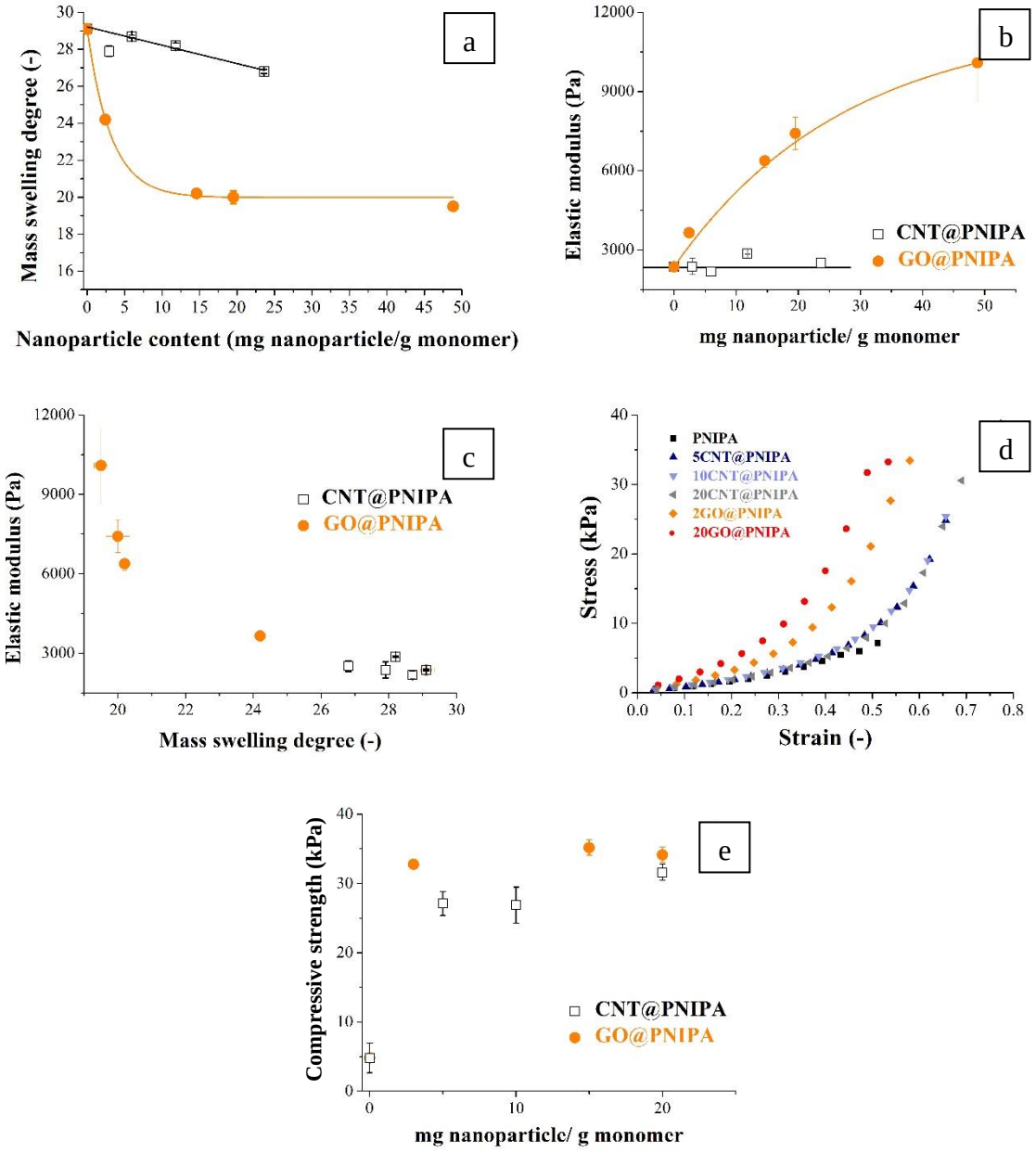

Figure 31. (a) Mass swelling degree in pure water at 20 °C (b) Elastic modulus of composite gels (solid lines are guides for the eye) (c) Correlation of modulus and swelling degree (d) Stress-strain curves (e) Compressive strength of composite gels.[159]

5.3. Response of hybrid gels to various stimuli

5.3.1. Temperature induced phase transition

Due to their influence on the PNIPA gel swelling features and heat absorbing capacity, carbon nanoparticles may also alter the kinetics of the VPT of the hydrogel. Upon immersion into warm water the disks of CNT – PNIPA and GO – PNIPA samples immediately turned opaque, similarly to pure PNIPA (Fig.32).

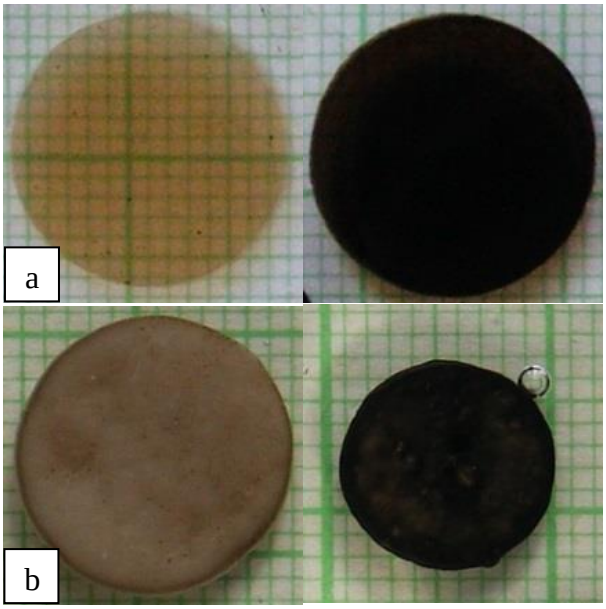

Figure 32. PNIPA composite gel disks with increasing GO content (a) before and (b) after the temperature induced phase transition.

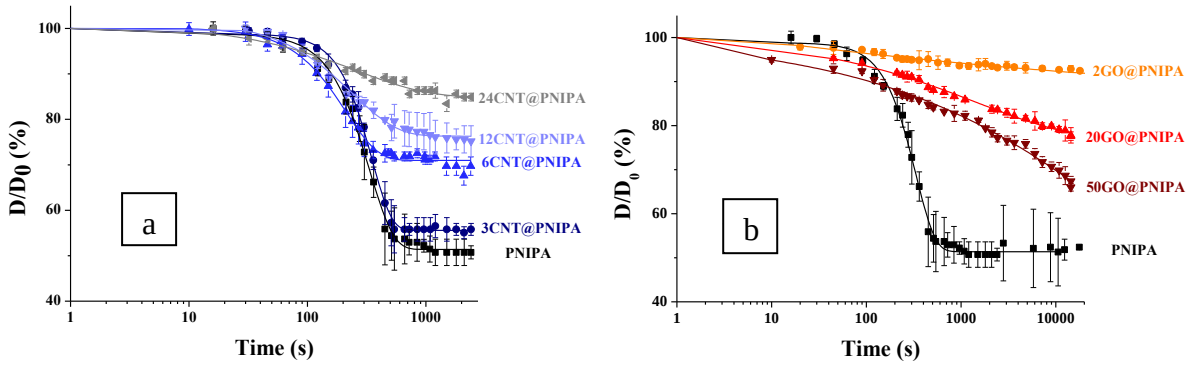

Figure 33. Deswelling kinetics of (a) CNT (3-24 mg CNT/g_{NIPA}) and (b) GO (2-50 mg CNT/g_{NIPA}) composite gels at 50 °C. Symbols are experimental values, continuous lines are fits to Equation 8. Note the order of magnitude difference in range of the *x* axis scales.[159]

Figure 33 shows that the presence of CNPs appreciably modified the kinetic response of the PNIPA gel. The behaviour of composite gels during the temperature-jump was strongly affected by both the quality and quantity of nanoparticles. To quantify the effects, experimental shrinkage-curves were fitted to a modified exponential decay function

$$\frac{D}{D_0} = \left(\frac{D}{D_0}\right)_{fin} + Ae^{-\left(\frac{t}{\tau}\right)^p}, \qquad \text{(Eq. 12)}$$

where $\left(\frac{D}{D_0}\right)_{fin}$ is the final relative diameter, *A* is a pre-exponential constant and τ is the time constant of the overall volumetric thermal response. The results are listed in Table 11. The shrinkage curve of the pure PNIPA could be fitted to a compressed exponential function ($p > 1$), indicating a possible jamming behaviour, with a time constant in good agreement with the value reported previously.[197] The time constants of the CNT containing systems were smaller, i.e. CNT slightly accelerated the response of the pure PNIPA gels.[197] $\left(\frac{D}{D_0}\right)_{fin}$ correlated with the CNT content: a higher loading resulted in a more limited shrinkage. Increasing CNT loading also significantly decreased the value of exponent *p*, indicating that the deswelling is becoming more complicated at higher CNT concentration (Table 11.). In the highest CNT content in the experiment (24 mg/g_{NIPA}) stretched exponential behaviour ($p < 1$) was found, suggesting multiple relaxation processes with different timescales.

Whereas 2000 s was largely sufficient for the relaxation of CNT – PNIPA gels (Figure 33a), a timeframe of even an order of magnitude longer was insufficient for the GO – PNIPA gels. For the GO incorporated samples values of the fitting parameters (Table 11) can be used only for qualitative comparisons, as the absence of measured swelling limit $\left(\frac{D}{D_0}\right)_{fin}$ makes the fitted parameters uncertain. Nevertheless, it can be concluded that, contrary to CNT, the lowest GO content has the strongest effect on the deswelling kinetics. A significant deceleration of the thermal response was observed at all the three concentrations (Figure 33b), which resembles the effect of the increased cross-linking density in pure PNIPA gels.[197] All curve fits yielded a stretching parameter $p < 1$, indicating multiple processes.

Table 11. Fitting parameters of the temperature induced phase transition from Equation 12.[159]

Sample	$\left(\frac{D}{D_0}\right)_{fin}$ (%)	A (%)	τ (s)	p	R^2
PNIPA	51.4	47.5	334	2.14	0.995
3CNT@PNIPA	55.6	43.2	348	2.58	0.997
6CNT@PNIPA	71.0	29.1	211	1.60	0.990
12CNT@PNIPA	76.3	25.4	241	1.15	0.987
24CNT@PNIPA	84.9	16.0	259	0.721	0.971
2GO@PNIPA	90.5	9.5	1437	0.266	0.932
20GO@PNIPA	76.5	23.7	1470	0.412	0.994
50GO@PNIPA	34.2	60.1	53762	0.286	0.992

$\left(\frac{D}{D_0}\right)_{fin}$: relative diameter, A: pre-exponential factor; τ: time constant of thermal response; p: exponent; R^2: coefficient of determination.

5.3.2. Infrared light sensitivity of PNIPA hybrid gels

Carbon materials including nanoparticles are known for their high IR absorption. Recent experimental and theoretical studies found that the presence of a carbon network structure increases thermal diffusivity in PNIPA gels compared to pure water. It was also observed that latent heat influences thermal diffusivity. As was expected,[127,128,198] addition of both CNT and GO resulted in improved IR sensitivity (Fig. 34a and 34b). The doped systems, however, displayed significant differences depending on the type and concentration of nanoparticle incorporated.

Fast shrinkage on exposure to IR laser irradiation, and quick recovery of the gels after the exposure was observed in all cases. After laser exposure, a quick recovery to the swollen and transparent state was observed. These observations are in a good agreement with those reported earlier.[127,198,199] The phenomenon can be explained by the photon absorption of carbon nanoparticles leading to the generation of excitons, which decay into heat and result in the local warming and thus phase transition of the gel.[127,198] During the exposition gel samples collapsed in a circular zone of 5 mm around the centre of the incident beam. The measured temperature fluctuations may be attributed to the low thermal conductivity of the gels, even in the presence of nanoparticles (Fig. 34c).

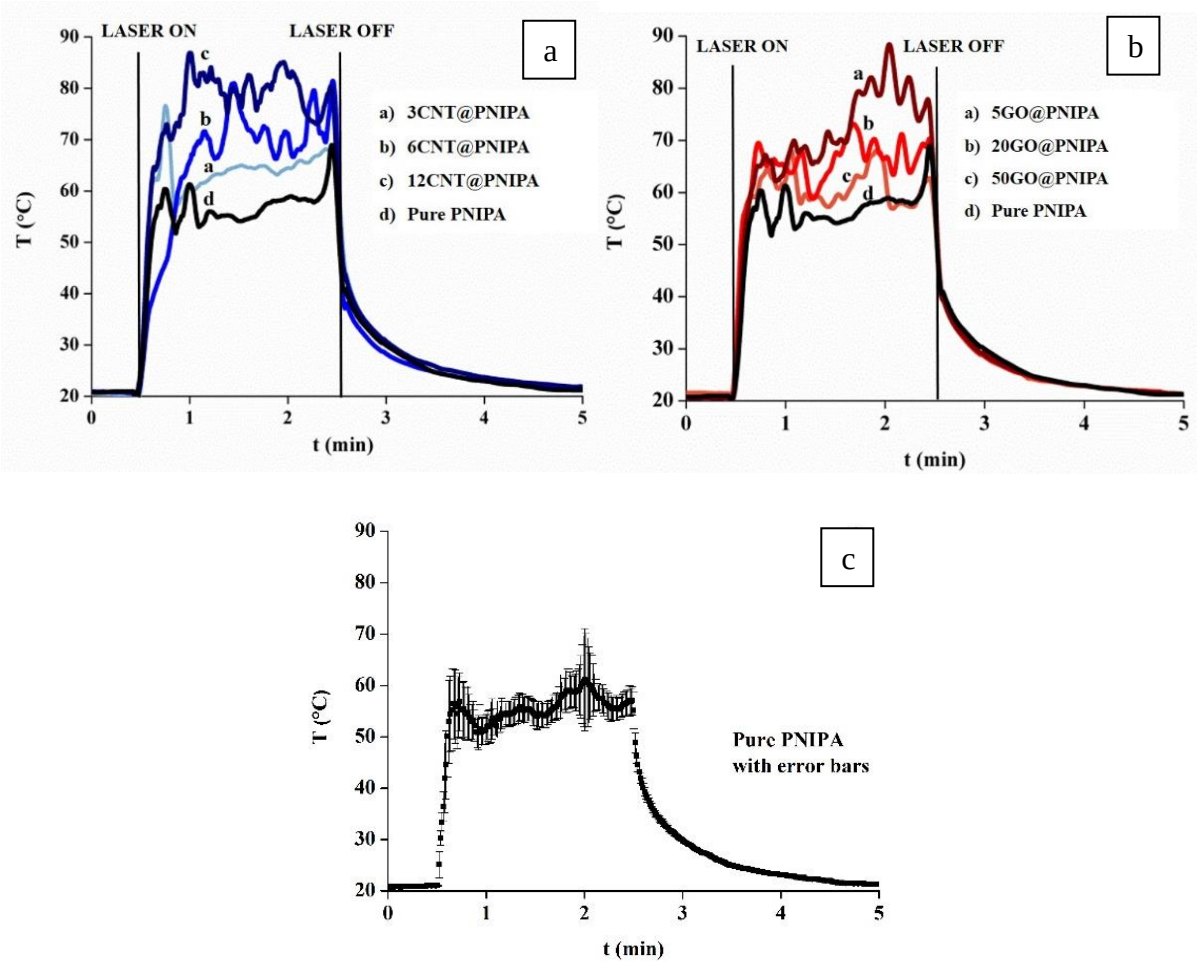

Figure 34. Temperature (*T*) profile of (a) CNT and (b) GO containing PNIPA gels upon IR laser exposure (t: observation time) at 20 °C (c) Temperature profile of pure PNIPA with error bars.[159]

In both sets of systems a monotonic correlation was found between the nanoparticle content and the temperature rise in the sample, but with different trend. In the CNT – PNIPA systems the gels reached proportionally higher temperature with increasing CNT concentration (Fig. 35). Incorporating a low amount of GO to PNIPA resulted in the same enhanced response that in CNT – PNIPA with similar CNT content, but adding more GO systematically reduced the effect.

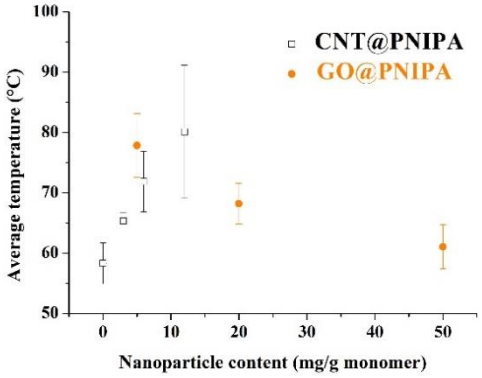

Figure 35. Average temperature values of PNIPA composites during IR laser exposure of the lyophilised gel films.[159]

5.3.3. Comparison of the effect of CNT and GO

The differences observed between CNT and GO might be attributed rather to their chemical behaviour than geometrical shape. The multiwall carbon nanotubes contain Russian doll-like concentric carbon tubes of graphite like array. The external cylinder is decorated by oxygen containing surface functional groups, but their concentration is relatively low and thus, they do not significantly modify the graphitic structure. That is, the reactivity of the CNTs in the radical polymerization is modest. However, their surface is more hydrophobic which leads to their aggregation. GO is made of a few strongly damaged graphene sheets richly decorated with oxygen. The hydrophilic surface allows good dispersibility. The delocalised electron system however, is severely damaged and most of the electrons are localised as double bonds reactive in radical reactions. Due to these chemical differences GO particles may act as hubs covalently linked to several polymer chains which is less typical with CNT. This behaviour influences the response of the two different nanoparticles during the swelling and stress-strain observations. While GO units act more or less independently from each other but strongly related to the polymer chains, CNT works as “free” agglomerates. Increasing the CNT content increases the number of agglomerates in the precursor solution. Hydrophilic GO tends to form bulky agglomerate of randomly oriented GO units only at the higher concentrations.

The modified distortion of electron structure also leads to different heat conductivity and IR absorption performance of the two nanoparticles. In low concentration CNT has only a limited influence of the deswelling kinetics. Although increasing the CNT content may lead to better heat conductivity, the higher amount of CNT filler delays relaxation and increases the

time constant. The chains have to relax around more and more aggregates. Also, with CNTs, the higher their amount in the gel the better is their IR absorption.

In GO – PNIPA systems, the complexity of the deswelling process is reflected by the $p < 1$ relation already at the lowest concentration. Several processes may superimpose: e.g. by increasing the number of GO units we elevate the number of potentially reactive double bonds without increasing the NIPA and BA concentration; at high GO concentration the randomly oriented self-assembly of the particles may occur; etc. The units participating the relaxation become overall heavier and heavier. The stronger IR absorption at low GO concentration seems to reveal that these complex processes suppress the IR responsivity of the hybrid.

Incorporation of CNT and GO results in different effects in the behaviour of the hybrids. Beside somewhat influencing the porous morphology of the hybrids, their effect on the swelling degree and the elastic modulus shows a different trend, but both of them significantly enhances the fracture stress tolerance of the PNIPA hydrogel itself. The mechanical properties of PNIPA gel were improved by incorporating GO, while the swelling degree of the GO – PNIPA systems significantly decreased. In contrast, CNT – PNIPA composites exhibited swelling and mechanical properties similar to those of pure PNIPA. Significant differences were observed in the thermal response of the different systems. The time constant and the swelling ratio of the temperature-induced shrinkage can thus be adjusted by selecting the type and amount of nanoparticle loading. This could provide a means for accurately controlling deswelling kinetics, e.g., in the drug release profile of PNIPA systems, as well as could be employed in sensor applications, where fast and excessive shrinkage can be a significant drawback. The above observations may open the route for the construction of novel drug transport and actuator systems, however, further and thorough experimentation is required.

6. Summary

Hydrogels are covalently-bound three-dimensional macromolecular networks that are able to absorb large quantities of water during their swelling. Smart hydrogels exhibit a reversible, abrupt volume phase transition (VPT) in response to external physical or chemical stimuli. In my PhD research, I investigated the most studied temperature responsive polymer, the poly(*N*-isopropylacrylamide) (PNIPA), which is a frequently proposed vehicle of controlled drug release. The goal of present work was to obtain profound insight to the interactions of the PNIPA hydrogel that may determine its potential for drug delivery applications.

Despite the large number of studies into the phase transition of PNIPA, up to this day there is no agreement on the ionic or non-ionic character of the hydrogel, which is due to that distinguishing the effects of intrinsic ionic groups of the polymer from those of attendant ions in solution is difficult. With the goal of looking for evidence of intrinsic ionic behaviour, I investigated the properties of the PNIPA homopolymer hydrogel over a wide range of pH and ionic strength values. According to observations of the swelling, osmotic, potentiometric titration and differential scanning calorimetric (DSC) behaviour, the intrinsic ion content of the hydrogel is lower than 1% and the osmotic response to added salt is also inconsistent with that of polyelectrolyte systems. This conclusion forecloses the idea that charged ionic groups acquired during the free radical synthesis of PNIPA play a significant role in the saga of past experimental inconsistencies. It was also found that the behaviour of the gel at the transition threshold is governed not by the ionic strength, but by the anion concentration of the surrounding solution. At high pH the network chains become increasingly hydrolysed, and ultimately collapse, in response to the elevated anion concentration.

Small aromatic molecules are known to influence the swelling behaviour of the PNIPA hydrogel. Despite that the nature and strength of these interactions are crucially important in terms of controlled delivery, these phenomena are poorly understood. For this reason, our research group previously studied the effect of meta substituted phenols (phenol; 1,2-dihydroxybenzene and 1,3,5-trihydroxybenze) on PNIPA and found that the swelling properties of the gel correlate with the substitution pattern of the guest molecules. My aim was to continue these investigations by carrying out swelling and DSC measurements on the effect of various phenol substitution arrangements on the hydrogel. I also extended my experiments to two drug molecules widely used in practice: dopamine (4-(2-aminoethyl) benzene-1,2-diol) and ibuprofen (2-(4-isobutylphenyl)-propionic acid).

Phenols have a reducing effect on the T_{VPT} of PNIPA, which is proportional to their concentration. At fixed temperature, all phenols induce a rapid gel collapse at a "critical" concentration (c_{crit}) that was characteristic of the guest molecule chemical structure. It was concluded that relative to phenol, ortho hydroxyl substitutions increase, while meta positions decrease c_{crit} at 20 °C. According to X-ray powder diffraction (XRD) investigations, crystallisation of phenol confined in the polymer matrix is hindered during the drying process, which results in the formation of amorphous phenol. This phenomenon can be attributed to the strong chemical bonding between phenol and PNIPA, which was confirmed by NMR studies.

Dopamine has a fundamentally different effect to phenols: it slightly increases the T_{VPT} and does not induce VPT even at a very high concentration. In NMR and simultaneous thermal analytical (STA) experiments no interaction was observed between the drug and PNIPA, which allows the crystallisation of the guest molecules within the dry polymer matrix. Based on XRD spectra, significantly smaller dopamine crystallites develop when drying in the gel compared to that in free conditions.

Similarly to phenols ibuprofen reduces the swelling degree of the gel, but only to a slight extent and does not induce phase transition at 20°C. In NMR investigations no clear evidence was found of chemical interaction between ibuprofen and PNIPA. XRD studies revealed the fast crystallisation of ibuprofen within the polymer matrix during the drying process, however, contrary to dopamine, only a minor crystallite size reduction occurred.

Investigations on carbon nanoparticle incorporated composite gels were motivated by two main reasons. Albeit the PNIPA gel has various biomedical benefits, its poor mechanical strength due to high water content restricts its drug delivery applications involving repetitive loading. This problem can be overcome by producing composite hydrogels by incorporating nanocarbons into the gel matrix. On the other hand, the strong light absorption of carbon nanoparticles may offer new functional sensitivity for PNIPA. My aim was to obtain a comparable evaluation of the impact of carbon nanotubes (CNT) and graphene oxide (GO) nanoparticles on the hydrogel, by investigating composite systems synthesised under identical conditions. It was observed that nanocarbons can be added to the polymer only in limited amounts, however, both CNT and GO exert a reinforcing effect at the applied low concentrations by enhancing the fracture stress tolerance of the hydrogel. The elastic modulus and swelling degree of the CNT containing composite are similar to those of pure PNIPA gel. By contrast, GO enhances the elastic modulus and significantly decreases the swelling degree of polymer. I also found that both nanocarbons improve the infrared sensitivity of the hydrogel and that the kinetics of the temperature induced VPT can be controlled by carefully selecting the type and the concentration of the nanoparticle.

7. New scientific results

1. I have demonstrated that the intrinsic ionic content of the poly(*N*-isopropylacrylamide) (PNIPA) hydrogel is vanishingly small. I found that the composition (i.e. the pH, but even more, the ionic composition) of the swelling buffer solution influences the equilibrium swelling degree of the PNIPA gel. [ME1]

2. I have concluded that the studied phenols have significant phase transition temperature (T_{VPT}) reducing impact on the PNIPA hydrogel, which is proportional to their concentration. Dopamine increases the T_{VPT}, though its effect is limited. Ibuprofen has no influence on the temperature of the volume phase transition in the wide concentration range examined. [ME3] [ME4] [ME5] [ME6]

3. I found that in the presence of phenols, the phase transition of the PNIPA hydrogel takes place even at temperatures significantly lower than 34 °C. I determined the critical concentrations required to induce the transition already at 20 °C, which depend both on the number and on the position of the OH groups of the guest molecule. Raising the number of OH groups in meta positions decreases, while in orto positions elevates the critical concentration compared to phenol. Increasing the number of OH groups also results in the widening of the transition [ME4] [ME5]

4. Different interactions were observed in PNIPA gels swollen in aqueous solutions of phenol, dopamine and ibuprofen. Phenol, which forms strong interaction with the hydrogel, is preserved in its amorphous state upon solvent removal. Dopamine and ibuprofen, which show only weak interaction, crystallize during the drying process. Crystallites confined in the gel matrix are significantly smaller than those developed in free conditions. [ME4]

5. Both carbon nanotubes (CNT) and graphene oxide (GO) increase the compressive strength of the PNIPA hydrogel even at low concentrations. The kinetics of the temperature-induced phase transition can be controlled by selecting the type and the concentration of the loading nanoparticles. I have demonstrated that the infrared (IR) sensitivity of the hydrogel can enhanced by both CNT and GO, and that the effect depends on the dispersibility of the nanoparticles. [ME2]

8. References

(1) Lin, C. C.; Metters, A. T. Hydrogels in Controlled Release Formulations: Network Design and Mathematical Modeling. *Adv. Drug Deliv. Rev.* **2006**, *58* (12–13), 1379–1408.

(2) Qiu, Y.; Park, K. Environment-Sensitive Hydrogels for Drug Delivery. *Adv. Drug Deliv. Rev.* **2012**, *64*, 49–60.

(3) Makino, K.; Hiyoshi, J.; Ohshima, H. Effects of Thermosensitivity of Poly (N-Isopropylacrylamide) Hydrogel upon the Duration of a Lag Phase at the Beginning of Drug Release from the Hydrogel. *Colloids Surfaces B Biointerfaces* **2001**, *20* (4), 341–346.

(4) Schmaljohann, D. Thermo- and pH-Responsive Polymers in Drug Delivery. *Adv. Drug Deliv. Rev.* **2006**, *58* (15), 1655–1670.

(5) Cuggino, J. C.; Contreras, C. B.; Jimenez-Kairuz, A.; Maletto, B. A.; Alvarez Igarzabal, C. I. Novel poly(NIPA-Co-AAc) Functional Hydrogels with Potential Application in Drug Controlled Release. *Mol. Pharm.* **2014**, *11* (7), 2239–2249.

(6) Bawa, P.; Pillay, V.; Choonara, Y.; du Toit, L. Stimuli-Responsive Polymers and Their Applications in Drug Delivery. *Biomed. Mater.* **2009**, *4*, 022001–022016.

(7) Hoffman, A. S. Hydrogels for Biomedical Applications. *Adv. Drug Deliv. Rev.* **2012**, *64*, 18–23.

(8) Peppas, N.; Bures, P.; Leobandung, W.; Ichikawa, H. Hydrogels in Pharmaceutical Formulations. *Eur. J. Pharm. Biopharm.* **2000**, *50* (1), 27–46.

(9) Galperin, A.; Long, T. J.; Ratner, B. D. A Degradable, Thermo-Sensitive Poly(N-Isopropyl Acrylamide)- Based Scaffold with Controlled Porosity for Tissue Engineering Applications. *Biomacromolecules* **2011**, *11* (10), 2583–2592.

(10) Zhang, X. Z.; Lewis, P.; Chu, C. C. Fabrication and Characterization of a Smart Drug Delivery System: Microsphere in Hydrogel. *Biomaterials* **2005**, *26* (16), 3299–3309.

(11) Ahmed, E. M. Hydrogel: Preparation, Characterization, and Applications. *J. Adv. Res.* **2013**, *6* (2), 105–121.

(12) Biswas, C. S.; Patel, V. K.; Vishwakarma, N. K.; Tiwari, V. K.; Maiti, B.; Maiti, P.; Kamigaito, M.; Okamoto, Y.; Ray, B. Effects of Tacticity and Molecular Weight of Poly(N -Isopropylacrylamide) on Its Glass Transition Temperature. *Macromolecules* **2011**, *44*, 5822–5824.

(13) Zhu, S.; Zhou, Z.; Zhang, D.; Jin, C.; Li, Z. Design and Synthesis of Delivery System Based on SBA-15 with Magnetic Particles Formed in Situ and Thermo-Sensitive PNIPA as Controlled Switch. *Microporous Mesoporous Mater.* **2007**, *106* (1–3), 56–61.

(14) Cabane, E.; Zhang, X.; Langowska, K.; Palivan, C. G.; Meier, W. Stimuli-Responsive Polymers and Their Applications in Nanomedicine. *Biointerphases* **2012**, *7* (1–4), 1–27.

(15) Cameronde Las Heras Alarcon, C.; Pennadam, S.; Alexander. Stimuli Responsive Polymers for Biomedical Applications. *Chem. Soc. Rev.* **2005**, *34* (3), 276–285.

(16) Kobiki, Y.; Suzuki, a. Characteristic Lenght of Polymer Gel Surfaces. *Int. J. Adhes. Adhes.* **1999**, *19* (July 1998), 411–416.

(17) Yoshida, R.; Kiyotaka, S.; Okana, T.; Sakurai, Y. Pulsatile Drug Delivery Systems Using Hydrogels Ryo Yoshida A, Kiyotaka Sakai A, Teruo Okano B and Yasuhisa Sakurai B. *Advanved Drug Deliv. Revieuws* **1993**, *11*, 85–108.

(18) Halperin, A.; Kröger, M.; Winnik, F. M. Poly(N-Isopropylacrylamide) Phase Diagrams: Fifty Years of Research. Invited Review. *Angew. Chemie Int. Ed.* **2015**.

(19) Heskins, M.; Guilleta, J. E. Solution Properties of Poly(N-Isopropylacrylamide). *J. Macromol. Sci. A* **1968**, *2* (8), 1441–1455.

(20) Shibayama, M.; Tanaka, T. Small Angle Neutron Scattering Study on poly(N-Isopropyl Acrylamide) Gels near Their Volume Phase Transition Temperature. *J. Chem. Phys.* **1992**, *97*, 6829–6841.

(21) Nagahama, K.; Inomata, H.; Saito, S. Measurement of Osmotic Pressure in Aqueous Solutions of Poly(ethylene Glycol) and poly(N-Isopropylacrylamide). *Fluid Phase Equilib.* **1994**, *96*, 203–214.

(22) Ray, B.; Okamoto, Y.; Kamigaito, M.; Sawamoto, M.; Seno, K.; Kanaoka, S. .; Aoshima, S. Effect of Tacticity of poly(N-Isopropylacrylamide) on the Phase Separation Temperature of Its Aqueous Solutions. *Polym. J.* **2005**, *37*, 234−237.

(23) Hirano, T.; Okumura, Y.; Kitajima, H.; Seno, M.; Sato, T. Dual Roles of Alkyl Alcohols as Syndiotactic-Specificity Inducers and Accelerators in the Radical Polymerization of N-Isopropylacrylamide and Some Properties of Syndiotactic poly(N-Isopropylacrylamide). *J. Polym. Sci. Part A Polym. Chem.* **2006**, *44* (15), 4450−4460.

(24) Pelton, R. H.; Pelton, H. M.; Morphesis, A.; Rowells, R. L. Particle Sizes and Electrophoretic Mobilities of poly(N-Isopropylacrylamide) Latex. *Langmuir* **1989**, *5*, 816–818.

(25) Bischofberger, I.; Trappe, V. New Aspects in the Phase Behaviour of Poly-N-Isopropyl Acrylamide: Systematic Temperature Dependent Shrinking of PNiPAM Assemblies Well beyond the LCST. *Sci. Rep.* **2015**, *5*, 15520.

(26) Clara-Rahola, J.; Fernandez-Nieves, A.; Sierra-Martin, B.; South, A. B.; Lyon, L. A.; Kohlbrecher, J.; Barbero, A. F. Structural Properties of Thermoresponsive poly(N-Isopropylacrylamide)-Poly(ethyleneglycol) Microgels. *J. Chem. Phys.* **2012**, *136*, 214903.

(27) Virtanen, O. L. J.; Richtering, W. Kinetics and Particle Size Control in Non-Stirred Precipitation Polymerization of N-Isopropylacrylamide. *Colloid Polym. Sci.* **2014**, *292* (8), 1743–1756.

(28) Schild, H. G.; Tirrel, D. A. Microcalorimetric Detection of Lower Critical Solution Temperatures in Aqueous Polymer Solutions. *J. Phys. Chem.* **1994**, *94*, 4352–4356.

(29) Hirotsu, S.; Hirokawa, Y. Volume-Phase Transitions of Ionized N-Isopropylacrylamide Gels. *J. Chem. Phys.* **1987**, *87*, 1392–1395.

(30) Karg, M.; Pastoriza-Santos, I.; Rodriguez-González, B.; von Klitzing, R.; Wellert, S.; Hellweg, T. Temperature, pH, and Ionic Strength Induced Changes of the Swelling Behavior of PNIPAM-Poly(allylacetic Acid) Copolymer Microgels. *Langmuir* **2008**, *24* (12), 6300–6306 DOI: 10.1021/la702996p.

(31) Pelton, R. H.; Pelton, H. M.; Morphesis, A. Particle Sizes and Electrophoretic Mobilities of poly(N-Isopropylacrylamide) Latex. *Langmuir* **1989**, *5*, 816–818.

(32) Bischofberger, I.; Trappe, V. New Aspects in the Phase Behaviour of Poly-N-Isopropyl Acrylamide: Systematic Temperature Dependent Shrinking of PNiPAM Assemblies Well beyond the LCST. *Sci. Rep.* **2015**, *5*, 15520.

(33) Zhang, J.; Chu, L. Y.; Li, Y. K.; Lee, Y. M. Dual Thermo- and pH-Sensitive poly(N-Isopropylacrylamide-Co-Acrylic Acid) Hydrogels with Rapid Response Behaviors. *Polymer (Guildf).* **2007**, *48* (6), 1718–1728 DOI: 10.1016/j.polymer.2007.01.055.

(34) Jones, M. S. Effect of pH on the Lower Critical Solution Temperatures of Random Copolymers of N-Isopropylacrylamide and Acrylic Acid. *Eur. Polym. J.* **1999**, *35* (5), 795–801.

(35) Cai, H.; Zhang, Z. P.; Ping, C. S.; Bing, L. H.; Xiao, X. Z. Synthesis and Characterization of Thermo- and pH- Sensitive Hydrogels Based on Chitosan-Grafted N-Isopropylacrylamide via γ-Radiation. *Radiat. Phys. Chem.* **2005**, *74* (1), 26–30.

(36) Beltran, S.; Baker, J. P.; Hooper, H. H.; Blanch, H. W.; Prausnitz, J. M. Swelling Equilibria for Weakly Ionizable, Temperature-Sensitive Hydrogels. *Macromolecules* **1991**, *24*, 549–551.

(37) Brazel, C. S.; Peppas, N. a. Synthesis and Characterization of Thermo- and Chemomechanically Responsive Poly(N-Isopropylacrylamide-Co-Methacrylic Acid) Hydrogels. *Macromolecules* **1995**, *28* (24), 8016–8020.

(38) Krušić, M. K.; Filipović, J. Copolymer Hydrogels Based on N-Isopropylacrylamide and Itaconic Acid. *Polymer (Guildf).* **2006**, *47* (1), 148–155.

(39) Suzuki, A.; Suzuki, H. Hysteretic Behavior and Irreversibility of Polymer Gels by pH Change. *Chem. Phys.* **1995**, *103*, 4706–4710.

(40) Sörensen, S. P. L. Enzymstudien. II. Mitteilung Ijber Die Messung Und Die Hedeutung Der wasserstofHonenkonzentration Hei Enzymatischen Prozessen. *Biotech. Zeitschrift* **1909**, *21*, 131–304.

(41) Geever, L. M.; Nugent, M. J. D.; Higginbotham, C. L. The Effect of Salts and pH Buffered Solutions on the Phase Transition Temperature and Swelling of Thermoresponsive Pseudogels Based on N-Isopropylacrylamide. *J. Mater. Sci.* **2007**, *42* (23), 9845–9854.

(42) Hofmeister, F. On the Understanding of the Effects of Salts. *Arch. Exp. Pathol. und Pharmakologie* **1888**, 247–260.

(43) Inomata, H.; Goto, S.; Otake, K.; Saito, S. Effect of Additives on Phase Transition of N-Isopropylacrylamide Gels. *Langmuir* **1992**, *8* (2), 687–690.

(44) Zhang, Y.; Cremer, P. S. Interactions between Macromolecules and Ions: The Hofmeister Series. *Curr. Opin. Chem. Biol.* **2006**, *10* (6), 658–663.

(45) Zhang, Y. J.; Furyk, S.; Bergbreiter, D. E.; Cremer, P. S. Specific Ion Effects on the Water Solubility of Macromolecules: PNIPAM and the Hofmeister Series. *J. Am. Chem. Soc.* **2005**, *127* (23), 14505–14510.

(46) Panayiotou, M.; Freitag, R. Influence of the Synthesis Conditions and Ionic Additives on the Swelling Behaviour of Thermo-Responsive Polyalkylacrylamide Hydrogels. *Polymer (Guildf).* **2005**, *46* (18), 6777–6785.

(47) Eeckman, F.; Amighi, K.; Moës, A. J. Effect of Some Physiological and Non-Physiological Compounds on the Phase Transition Temperature of Thermoresponsive Polymers Intended for Oral Controlled-Drug Delivery. *Int. J. Pharm.* **2001**, *222* (2), 259–270.

(48) Subbarao, C. V.; Chakravarthy, I. P. K.; Sai Bharadwaj, a. V. S. L.; Prasad, K. M. M. Functions of Hydrotropes in Solutions. *Chem. Eng. Technol.* **2012**, *35* (2), 225–237.

(49) Hopkins Hatzopoulos, M.; Eastoe, J.; Dowding, P. J.; Rogers, S. E.; Heenan, R.; Dyer, R. Are Hydrotropes Distinct from Surfactants? *Langmuir* **2011**, *27* (20), 12346–12353.

(50) Bianco-Peled, H.; Gryc, S. Binding of Amino Acids to "Smart" Sorbents: Where Does Hydrophobicity Come into Play? *Langmuir* **2004**, *20* (1), 169–174.

(51) Koga, S.; Sasaki, S.; Maeda, H. Effect of Hydrophobic Substances on the Volume-Phase Transition of N-Isopropylacrylamide Gels. *J. Phys. Chem. B* **2001**, *105* (19), 4105–4110.

(52) Koga, S.; Kawashima, T.; Sasaki, S. Elastic Relaxation of Collapsed Poly(alkylacrylamide) Gels and Their Complexes with Phenol. *J. Phys. Chem. B* **2004**, *108* (30), 10838–10844.

(53) Kawashima, T.; Koga, S.; Annaka, M.; Sasaki, S. Roles of Hydrophobic Interaction in a Volume Phase Transition of Alkylacrylamide Gel Induced by the Hydrogen-Bond-Driving Alkylphenol Binding. *J. Phys. Chem. B* **2006**, *109*, 1055–1062.

(54) Dhara, D.; Chatterji, P. R. Effect of Hydrotropes on the Volume Phase Transition in Poly(N-Isopropylacrylamide) Hydrogel. *Langmuir* **1999**, No. 23, 930–935.

(55) Coughlan, D. C.; Corrigan, O. I. Drug-Polymer Interactions and Their Effect on Thermoresponsive poly(N-Isopropylacrylamide) Drug Delivery Systems. *Int. J. Pharm.* **2006**, *313* (1–2), 163–174.

(56) Coughlan, D. C.; Quilty, F. P.; Corrigan, O. I. Effect of Drug Physicochemical Properties on Swelling/deswelling Kinetics and Pulsatile Drug Release from Thermoresponsive poly(N-Isopropylacrylamide) Hydrogels. *J. Control. Release* **2004**, *98* (1), 97–114.

(57) Suzuki, Y.; Tomonaga, K.; Kumazaki, M.; Nishio, I. Change in Phase Transition Behavior of an NIPA Gel Induced by Solvent Composition: Hydrophobic Effect. *Polym. Gels Networks* **1996**, *4* (2), 129–142.

(58) Kosik, K.; Wilk, E.; Geissler, E.; László, K. Distribution of Phenols in Thermoresponsive Hydrogels. *Macromolecules* **2007**, *40*, 2141–2147.

(59) Kosik, K.; Rochas, C.; Geissler, E. Phase Transition in Poly(N-Isopropylacrylamide) Hydrogels Induced by Phenols. *Macromolecules* **2003**, No. 2, 7771–7776.

(60) László, K.; Kosik, K.; Geissler, E. High-Sensitivity Isothermal and Scanning Microcalorimetry in PNIPA Hydrogels around the Volume Phase Transition. *Macromolecules* **2004**, *37* (26), 10067–10072.

(61) László, K.; Kosik, K.; Rochas, C.; Geissler, E. Phase Transition in Poly(N-Isopropylacrylamide) Hydrogels Induced by Phenols. **2003**, *36*, 7771–7776.

(62) Hofmann, C. H.; Schönhoff, M. Dynamics and Distribution of Aromatic Model Drugs in the Phase Transition of Thermoreversible poly(N-Isopropylacrylamide) in Solution. *Colloid Polym. Sci.* **2012**, *290* (8), 689–698.

(63) Sousa, R. G.; Prior-Cabanillas, A.; Quijada-Garrido, I.; Barrales-Rienda, J. M. Dependence of Copolymer Composition, Swelling History, and Drug Concentration on the Loading of Diltiazem Hydrochloride (DIL.HCl) into poly[(N-Isopropylacrylamide)-Co-(Methacrylic Acid)] Hydrogels and Its Release Behaviour from Hydrogel Slabs. *J. Control. Release* **2005**, *102* (3), 595–606.

(64) Fu, G.; Soboyejo, W. O. Investigation of Swellable Poly (N-Isopropylacrylamide) Based Hydrogels for Drug Delivery. *Mater. Sci. Eng. C* **2011**, *31* (5), 1084–1090.

(65) Abu Samah, N. H.; Heard, C. M. Enhanced in Vitro Transdermal Delivery of Caffeine Using a Temperature- and pH-Sensitive Nanogel, poly(NIPAM-Co-AAc). *Int. J. Pharm.* **2013**, *453* (2), 630–640.

(66) Zhang, J. T.; Huang, S. W.; Liu, J.; Zhuo, R. X. Temperature Sensitive poly[N-Isopropylacrylamide-Co-(Acryloyl Beta-Cyclodextrin)] for Improved Drug Release. *Macromol. Biosci.* **2005**, *5* (3), 192–196.

(67) Yoshida, R.; Sakai, K.; Okano, T.; Sakurai, Y. Drug Release Profiles in the Shrinking Process of Thermoresponsive poly(N-Isopropylacrylamide-Co-Alkyl Methacrylate) Gels. *Ind. Eng. Chem. Res.* **1992**, *31* (10), 2339–2345.

(68) Jeon, G.; Yanga, S. Y.; Kim, J. K. Functional Nanoporous Membranes for Drug Delivery. *J. Mater. Chem* **2012**, *22*, 14814–14834.

(69) Lee, P. I. Kinetics of Drug Release from Hydrogel Matrices. *J. Control. Release* **1985**, *2*, 277–288.

(70) Gupta, P.; Vermani, K.; Garg, S. Hydrogels: From Controlled Release to pH-Responsive Drug Delivery. *Drug Discov. Today* **2002**, *7* (10), 569–579.

(71) Robert, C. C. R.; Buri, P. A.; Peppas, N. Influence of the drug solubility and dissolution medium on the release from poly(Z-hydroxyethyl methacrylate) microspheres. *J. Control. Release* **1987**, *5*, 151–157.

(72) Huang, X.; Brazel, C. S. On the Importance and Mechanisms of Burst Release in Matrix-Controlled Drug Delivery Systems. *J. Control. Release* **2001**, *73* (2–3), 121–136.

(73) Lee, P. I.; Kim, C. J. Probing the Mechanisms of Drug Release from Hydrogels. *J. Control. Release* **1991**, *16* (1–2), 229–236.

(74) Zahedi, P.; Lee, P. I. Solid Molecular Dispersions of Poorly Water-Soluble Drugs in poly(2-Hydroxyethyl Methacrylate) Hydrogels. *Eur. J. Pharm. Biopharm.* **2007**, *65* (3), 320–328.

(75) Grassi, M.; Colombo, I.; Lapasin, R. Drug Release from an Ensemble of Swellable Crosslinked Polymer Particles. *J. Control. Release* **2000**, *68* (1), 97–113.

(76) Lu, S.; Anseth, K. S. Photopolymerization of Multilaminated Poly (HEMA) Hydrogels for Controlled Release. *J. Control. Release* **1999**, *57* (3), 291–300.

(77) Martín, Á.; Scholle, K.; Mattea, F.; Meterc, D.; Cocero, M. J. Production of Polymorphs of Ibuprofen Sodium by Supercritical Antisolvent (SAS) Precipitation. *Cryst. Growth Des.* **2009**, *9* (5), 2504–2511.

(78) Bakhbakhi, Y.; Alfadul, S.; Ajbar, A. Precipitation of Ibuprofen Sodium Using Compressed Carbon Dioxide as Antisolvent. *Eur. J. Pharm. Sci.* **2013**, *48* (1–2), 30–39.

(79) Lee, T.; Zhang, C. Dissolution Enhancement by Bio-Inspired Mesocrystals: The Study of Racemic (R,S)-(±)-Sodium Ibuprofen Dihydrate. **2008**, *25* (7), 1563–1571.

(80) Tong, X.; Zheng, J.; Lu, Y.; Zhang, Z.; Cheng, H. Swelling and Mechanical Behaviors of Carbon Nanotube/poly(vinyl Alcohol) Hybrid Hydrogels. *Mater. Lett.* **2007**, *61* (8–9), 1704–1706.

(81) Perez, E. M.; Martin, N. Π-Π Interactions in Carbon Nanostructures. *Chem. Soc. Rev.* **2015** DOI: 10.1039/c5cs00578g.

(82) Hu, K.; Kulkarni, D. D.; Choi, I. Graphene-Polymer Nanocomposites for Structural and Functional Applications. *Prog. Polym. Sci.* **2014**, *39* (11), 1934–1972.

(83) Gaharwar, A. K.; Peppas, N. A.; Khademhosseini, A. Nanocomposite Hydrogels for Biomedical Applications. *Biotechnol. Bioeng.* **2014**, 441–453.

(84) Schexnailder, P.; Schmidt, G. Nanocomposite Polymer Hydrogels. *Colloid Polym. Sci.* **2009**, *287*, 1–11.

(85) Giuseppe Hampel, C.; Spizzirri, S.; Parisi, U. G.; Picci, O. I.; Iemma, N. Carbon Nanotubes Hybrid Hydrogels in Drug Delivery: A Perspective Review. *Biomed Res. Int.* **2014**, 825017/1–825017/17.

(86) Sahoo, N. S.; Rana, W.; Cho, J. L.; Li, H.; Chan, S. Polymer Nanocomposites Based on Functionalized Carbon Nanotubes (2010). *Prog. Polym. Sci.* **2010**, *35*, 837–867.

(87) Pandey, G.; Wolters, M.; Thostenson, T.; Heider, D. Localized Functionally Modified Glass Fibers with Carbon Nanotube Networks for Crack Sensing in Composites Using Time Domain Reflectometry. *Carbon N. Y.* **2012**, *50*, 3816– 3825.

(88) C. Tsonos, C. Pandis, N. Soin, D. Sakellari, E. Myrovali, S. Kripotou, A. Kanapitsas, E. Siores. Multifunctional Nanocomposites of Poly(vinylidene Fluoride) Reinforced by Carbon Nanotubes and Magnetite Nanoparticles. *Express Polym. Lett.* **2015**, 1104–1118.

(89) K., Voitko, A., Tóth, E., Demianenko, G., Dobos, B., Berke, O., Bakalinska, Grebenyuk, E., Tombácz, V., Kuts, Y., Tarasenko, M., Kartel, K., László. Catalytic Performance of Carbon Nanotubes in H2O2 Decomposition: Experimental, and Quantum Chemical Study. *J. Colloid Interface Sci.* **2015**, *437*, 283–290.

(90) Tóth A., Törőcsik A., Tombácz E., Oláh E., Li C., Klumpp E., Geissler E., Laszlo K. Interaction of Phenol and Dopamine with Commercial MWCNTs. *J. Colloid Interface Sci.* **2011**, *364*, 469–475.

(91) Yun J., Im J. S., Lee Y-S. Electro-Responsive Transdermal Drug Delivery Behavior of PVA/PAA/ MWCNT Nanofibers. *Eur. Polym. J.* **2011**, *47*, 1893–1902.

(92) Kim H., Abdala A. Graphene/polymer Nanocomposites. *Macromolecules* **2010**, *43*, 6515–6530.

(93) Kuila T., Bose S., Mishra A. K., Khanra P. Chemical Functionalization of Graphene and Its Applications. *Prog. Mater. Sci.* **2012**, *57*, 1061– 1105.

(94) Wu X., Lin T. F., Tang Z. H., Guo B. Natural Rubber/graphene Oxide Composites: Effect of Sheet Size on Mechanical Properties and Straininduced Crystallization Behavior. *Express Polym. Lett.* **2015**, *9*, 672–685.

(95) Pedrazzoli D., Dorigato A., Conti T., Vanzetti L., B.; M., P. A. Liquid Crystalline Polymer Nanocomposites Reinforced with in-Situ Reduced Graphene Oxide. *Express Polym. Lett.* **2015**, *9*, 709–720.

(96) Liu, J.; Cui, L.; Losic, D. Graphene and Graphene Oxide as New Nanocarriers for Drug Delivery Applications. *Acta Biomater.* **2013**, *9* (12), 9243–9257.

(97) Lee, Y. H. Carbon Nanotubes and Graphene for Soft Electronics. In *Carbon Nanotubes and Graphene: Some Recent Developments*; Seoul, 2014.

(98) O. BREUER, U. S. Big Returns From Small Fibers: A Review of Polymer/Carbon Nanotube Composites. *Polym. Compos.* **2004**, *25* (630–645).

(99) Jonathan N. Coleman, Umar Khan, Werner J. Blau, Y. K. G. Small but Strong: A Review of the Mechanical Properties of Carbon Nanotube–polymer Composites. *Carbon N. Y.* **2006**, *44*, 1624–1652.

(100) Cirillo, G.; Hampel, S.; Spizzirri, U. G.; Parisi, O. I.; Picci, N.; Iemma, F. Carbon Nanotubes Hybrid Hydrogels in Drug Delivery: A Perspective Review. *Biomed Res. Int.* **2014**.

(101) Owen C. Compton, S. T. N. Graphene Oxide, Highly Reduced Graphene Oxide, and Graphene: Versatile Building Blocks for Carbon-Based Materials. *Small* **2010**, *6* (6), 711–723.

(102) C. Kostagiannakopoulou, E. Fiamegkou, G. Sotiriadis, V. K. Thermal Conductivity of Carbon Nanoreinforced Epoxy Composites. *J. Nanomater.* **2016**, *2016*.

(103) Shunsuke Sakurai, Fuminori Kamada, Don N Futaba, Motoo Yumura, K. H. Influence of Lengths of Millimeter-Scale Single-Walled Carbon Nanotube on Electrical and Mechanical Properties of Buckypaper. *Nanoscale Res. Lett.* **2013**, *8*, 546–553.

(104) Frans H. J., Maurer, C. R. A. Dispersion and Interaction of Graphene Oxide in Amorphous and Semi-Crystalline Nano-Composites: A PALS Study. *J. Phys. Conf. Ser.* **2010**, *618*, 12020.

(105) Jian Xie. Fabrication of High-Surface-Area Graphene Nanocomposites via a Facile Chemical Route. In *Graphene Science Handbook: Fabrication Methods*; Mahmood Aliofkhazraei, Nasar Ali, William I. Milne, Cengiz S. Ozkan, Stanislaw Mitura, J. L. G., Ed.; Google Commerce Ltd, 2016.

(106) Xiao-Lin Xiea, Yiu-Wing Maia. Dispersion and Alignment of Carbon Nanotubes in Polymer Matrix: A Review. *Mater. Sci. Eng. R* **2005**, *49*, 89–112.

(107) Robert J. Young, Ian A. Kinloch, Lei Gong. The Mechanics of Graphene Nanocomposites: A Review. *Compos. Sci. Technol.* **2012**, *72*, 1459–1476.

(108) Lurayni Diaz-Chacon, Renaud Metz, Philippe Dieudonné, Said Tahir, Mehrdad Hassanzadeh, Eleida Sosa. Graphite Nanoplatelets Composite Materials: Role of the Epoxy-System in the Thermal Conductivity. *J. Mater. Sci. Chem. Eng.* **2015**, *3*, 5–87.

(109) Balandin, A. A. Thermal Properties of Graphene and Nanostructured Carbon Materials. *Nat. Mater.* **2011**, *10*, 569–581.

(110) Chen, Y. S.; Tsou, P. C.; Lo, J. M.; Tsai, H. C.; Wang, Y. Z.; Hsiue, G. H. Poly(N-Isopropylacrylamide) Hydrogels with Interpenetrating Multiwalled Carbon Nanotubes for Cell Sheet Engineering. *Biomaterials* **2013**, *34* (30), 7328–7334.

(111) Islam M. F., Alsayed A. M., Dogic Z., Zhang J. Nematic Nanotube Gels. *Phys. Rev. Lett.* **2004**, *92*, 088303/1–088303/4.

(112) Yang Z., Cao Z., Sun H., L. Y. Composite Films Based on Aligned Carbon Nanotube Arrays and a poly(N-Isopropyl Acrylamide) Hydrogel (). *Adv. Mater.* **2008**, *20*, 2201–2205.

(113) Li Z., Shen J., Ma H., Lu X., Shi M., Li N. Preparation and Characterization of pH- and Temperature- Responsive Hydrogels with Surface-Functionalized Graphene Oxide as the Crosslinker. *Soft Matter* **2012**, *8*, 3139– 3145.

(114) Lo, C.-W.; Zhu, D.; Jiang, H. An Infrared-Light Responsive Graphene-Oxide Incorporated poly(N-Isopropylacrylamide) Hydrogel Nanocomposite. *Soft Matter* **2011**, *7* (12), 5604.

(115) X, Ma; Y., Li; W., Wang; Q., Ji; Y, Xia. Temperature-Sensitive poly(N-Isopropylacrylamide)/graphene Oxide Nanocomposite Hydrogels by in Situ Polymerization with Improved Swelling Capability and Mechanical Behavior. *Eur. Polym. J.* **2013**, *49* (2), 389–396.

(116) Mingchao Wang, Cheng Yan, L. M. Graphene Nanocomposites. In *Composites and Their Properties*; Hu, N., Ed.; INTECH Open Access Publisher, 2012.

(117) Hui, Z.; Zhang, X.; Yu, J. Carbon Nanotube-Hybridized Supramolecular Hydrogel Based on PEO-B-PPO-B-PEO/ß- Cyclodextrin as a Potential Biomaterial. *J. Appl. Polym. Sci.* **2010**, *116* (4), 1894–1901.

(118) Sang Won Kim, Taehoon Kim, Yern Seung Kim, Hong Soo Choi, H. J. L.; Seung Jae Yang, C. R. P. Surface Modifications for the Effective Dispersion of Carbon Nanotubes in Solvents and Polymers. *Carbon N. Y.* **2012**, *50*, 3–33.

(119) Goenka, S.; Sant, V.; Sant, S. Graphene-Based Nanomaterials for Drug Delivery and Tissue Engineering. *J. Control. Release* **2014**, *173* (1), 75–88.

(120) Fan, J.; Shi, Z.; Lian, M.; Li, H.; Yin, J. Mechanically Strong Graphene Oxide/sodium Alginate/polyacrylamide Nanocomposite Hydrogel with Improved Dye Adsorption Capacity. *J. Mater. Chem. A* **2013**, *1* (25), 7433.

(121) Liu, J.; Cui, L.; Kong, N.; Barrow, C. J.; Yang, W. RAFT Controlled Synthesis of Graphene/polymer Hydrogel with Enhanced Mechanical Property for pH-Controlled Drug Release. *Eur. Polym. J.* **2014**, *50* (1), 9–17.

(122) Hou, C.; Zhang, Q.; Wang, H.; Li, Y. Functionalization of PNIPAAm Microgels Using Magnetic Graphene and Their Application in Microreactors as Switch Materials. *J. Mater. Chem.* **2011**, *21* (28), 10512.

(123) Andras Tél, Rita A. Bauer, Zsófia Varga. Heat Conduction in poly(N-Isopropylacrylamide) Hydrogels. *Int. J. Therm. Sci.* **2014**, *85*, 47–53.

(124) Quanwen Liao, Zhichun Liu, Wei Liu, Chengcheng Deng, N. Y. Extremely High Thermal Conductivity of Aligned Carbon Nanotube-Polyethylene Composites. *Sci. Rep.* **2015**, *5*, 16543–15549.

(125) Campbell, S. B.; Hoare, T. Externally Addressable Hydrogel Nanocomposites for Biomedical Applications. *Curr. Opin. Chem. Eng.* **2014**, *4*, 1–10 .

(126) Cirillo, G.; Hampel, S.; Spizzirri, U. G.; Parisi, O. I.; Picci, N.; Iemma, F. Carbon Nanotubes Hybrid Hydrogels in Drug Delivery: A Perspective Review. *Biomed Res. Int.* **2014**, *2014*, ID 825017.

(127) Zhu, C. H.; Lu, Y.; Peng, J.; Chen, J. F.; Yu, S. H. Photothermally Sensitive poly(N-Isopropylacrylamide)/graphene Oxide Nanocomposite Hydrogels as Remote Light-Controlled Liquid Microvalves. *Adv. Funct. Mater.* **2012**, *22* (19), 4017–4022.

(128) Miyako, E.; Nagata, H.; Hirano, K.; Hirotsu, T. Photodynamic Thermoresponsive Nanocarbon–Polymer Gel Hybrids. *Small* **2008**, *4* (10), 1711–1715.

(129) Zhang X, Pint CL, Lee MH, Schubert BE, Jamshidi A, Takei K, Ko H, Gillies A, Bardhan R, Urban JJ, Wu M, Fearing R, Javey A. Optically- and Thermally-Responsive Programmable Materials Based on Carbon Nanotube-Hydrogel Polymer Composites. *Nano Lett.* **2011**, *11* (8), 3239–3244.

(130) Guo, F.; Kim, F.; Han, T. H.; Shenoy, V. B.; Huang, J.; Hurt, R. H. Hydration-Responsive Folding and Unfolding in Graphene Oxide Liquid Crystal Phases. *ACS Nano* **2011**, *5* (10), 8019–8025.

(131) W. Jing; Yin-song, W.; Xiao-ying, Y.; Yuan-yuan, L.; Jin-rong, Y.; Rui, Y.; Ning, Z. Graphene Oxide Used as a Carrier for Adriamycin Can Reverse Drug Resistance in Breast Cancer Cells. *Nanotechnology* **2012**, *23*, 355101.

(132) Pan, Y.; Bao, H.; Sahoo, N. G.; Wu, T.; Li, L. Water-Soluble poly(N-Isopropylacrylamide)– Graphene Sheets Synthesized via Click Chemistry for Drug Delivery. *Adv. Funct. Mater.* **2011**, *21*, 2754–2763.

(133) Nicolas, S.; Julien, M.; Patrick, C. Stimuli-Responsive Nanocarriers for Drug Delivery. *Nat. Mater.* **2013**, *12*, 991–1003.

(134) Molinspiration Cheminformatics. Molecular Properties and Bioactivity Score Calculating Software. Molinspiration Cheminformatics 2015.

(135) ChemAxon Ltd. Properties Viewer Molecular Modelling Software. 2015.

(136) CRC Press. *CRC Handbook of Chemistry and Physics*, 95th ed.; Raton, Ed.; 2014.

(137) Merck Millipore. *Material Safety Data Sheets 15.15*; 2014.

(138) Royal Society of Chemistry. Chemical Structure Database http://www.chemspider.com/Chemical-Structure.971.html?rid=86771d76-5f58-4e51-adce-eb11e88f415f (accessed Jan 1, 2015).

(139) R. H. Perry, C. H. Chilton, S. D. K. *Chemical Engineers' Handbook 4th Edition*.

(140) Royal Society of Chemistry. Chemical Structure Database http://www.chemspider.com/Chemical-Structure.13837760.html?rid=dbcd0a47-e289-4fd1-a99b-399b73f958ec (accessed Jan 1, 2015).

(141) Fisher Scientific. *Material Safety Data Sheets No. 11230*; 2009.

(142) Royal Society of Chemistry. Chemical Structure Database http://www.chemspider.com/Chemical-Structure.764.html?rid=02c79508-eb05-48e0-9c45-cc3d564eb41c (accessed Jan 1, 2015).

(143) Merck Millipore. *Material Safety Data Sheets 13.2*; 2014.

(144) Royal Society of Chemistry. Chemical Structure Database http://www.chemspider.com/Chemical-Structure.4878.html?rid=8792be92-c83b-41e2-8d49-696831a4fdb3 (accessed Jan 1, 2015).

(145) Santa Cruz Biotechnology. Pyrogallol Datasheet http://www.scbt.com/datasheet-203368-pyrogallol.html (accessed May 7, 2015).

(146) J.M. Loveridge Ltd. *Material Safety Data Sheets No. 395*; 2002.

(147) Royal Society of Chemistry. Chemical Structure Database http://www.chemspider.com/Chemical-Structure.13835557.html?rid=0373d953-ee7c-44d5-b267-a106ca9e121c (accessed Jan 1, 2015).

(148) Merck Millipore. *Material Safety Data Sheets 8.2*; 2013.

(149) Royal Society of Chemistry. Chemical Structure Database http://www.chemspider.com/Chemical-Structure.352.html?rid=f15e2415-1c4e-48df-9fb2-9aea58d7bc5c (accessed Jan 1, 2015).

(150) Services, P. P. Dopamine Datasheet http://www.druginfosys.com/Drug.aspx?query=40+mg/ml&form=Inj&drugCode=261&drugName=Dopamine+%28HCl%29&type=8&Ing=%3D1 (accessed May 7, 2015).

(151) Council of Europe. *European Pharmacopoeia 5th Edition, ISBN 139789287152817*; 2004.

(152) Royal Society of Chemistry. Chemical Structure Database http://www.chemspider.com/Chemical-Structure.661.html?rid=229b3028-7ede-4c8e-bb96-60bfde941e15 (accessed Jan 1, 2015).

(153) Terebetski, J. L. Influence of Polymers on Supersaturation of Ibuprofen Sodium in Vitro and in Vivo: A Mchanistic Evaluation, PhD Thesis, 2014.

(154) Royal Society of Chemistry. Chemical Structure Database http://www.chemspider.com/Chemical-Structure.3544.html?rid=438138ab-9add-4305-bdf7-f4d222dc9e57&page_num=0 (accessed Jan 1, 2015).

(155) Ertl, P.; Rohde, B.; Selzer, P. Fast Calculation of Molecular Polar Surface Area as a Sum of Fragment Based Contributions and Its Application to the Prediction of Drug Transport Properties. *J. Med. Chem.* **2000**, *43*, 3714–3717.

(156) Wang, J.; Xie, X. Q.; Hou, T.; Xu, X. Fast Approaches for Molecular Polarizability Calculations. *J. Phys. Chem. A* **2007**, *111* (20), 4443–4448.

(157) Meylan, W. M.; Howard, P. H. Atom/fragment Contribution Method for Estimating Octanol–water Partition Coefficients. *J. Pharm. Sci.* **1995**, *84* (1), 83–92.

(158) Marcano, D. C.; Kosynkin, D. V.; Berlin, J. M.; Sinitskii, A.; Sun, Z.; Slesarev, A.; Alemany, L. B.; Lu, W.; Tour, J. M. Improved Synthesis of Graphene Oxide. *ACS Nano* **2010**, *4* (8), 4806–4814.

(159) Manek, E.; Berke, B.; Miklósi, N.; Sajbán, M.; Domán, A.; Fukuda, T.; Czakkel, O.; László, K. Thermal Sensitivity of Carbon Nanotube and Graphene Oxide Containing Responsive Hydrogels. *Express Polym. Lett.* **2016**, *10* (8), 710–720.

(160) Madarász, J.; Székely, E.; Halász, J.; Bánsághi, G.; Varga, D.; Simándi, B.; Pokol, G. Ammonium Carbamate Type Self-Derivative Salts of (R-)- and Racemic α-Methylbenzylamine: Composition and Thermal Stability by Evolved Gas Analyses (TG-FTIR and TG/DTA-MS). *J. Therm. Anal. Calorim.* **2013**, *111* (1), 567–574

(161) Snowden, M. J.; Thomas, D.; Vincent, B. Use of Colloidal Microgels for the Absorption of Heavy Metal and Other Ions from Aqueous Solution. *Analyst* **1993**, *118*.

(162) Horkayt, F.; Zrínyi, M. Studies on the Mechanical and Swelling Behavior of Polymer Networks Based on the Scaling Concept. 4. Extension of the Scaling Approach to Gels Swollen to Equilibrium in a Diluent of Arbitrary Activity. *Macromolecules* **1982**, *15*, 1306–1310.

(163) Geissler, E.; Hecht, A.M.; Horkay, F.; Zrinyi, M. Compressional Modulus of Swollen Polyacrylamide Networks. *Macromolecules* **1988**, *21*, 2594–2599.

(164) Treloar, L. R. G. *The Physics of Rubber Elasticity*, 3rd ed.; Clarendon: Oxford, 1975.

(165) de Gennes, P.-G. *Scaling Concepts in Polymer Physics*; Cornell University Press: Ithaca, NY, 1979.

(166) László, K.; Kosik, K.; Rochas, C.; Geissler, E. Phase Transition in poly(N-Isopropylacrylamide) Hydrogels Induced by Phenols. *Macromolecules* **2003**, *36*, 7771–7776.

(167) E.Geissler, F.Horkay, A. M. H. Osmotic and Scattering Properties of Chemically Cross-Linked poly(viny1 Alcohol) Hydrogels. *Macromolecules* **1991**, *24*, 6006–6011.

(168) A-M Hecht, A. Guillermo, F. Horkay, S. Mallam, J. F. Legrand, E. G. Structure and Dynamics of a Poly(dimethylsiloxane) Network: A Comparative Investigation of Gel and Solution. *Macromolecules* **1992**, *25*, 3677–3684.

(169) Horkay, F., Basser, P. J., Londono, D.J., Hecht, A.M., Geissler, E. Ions in Hyaluronic Acid Solutions. *J. Chem. Phys.* **2001**, *131*, 184902.

(170) Horkay, F., Basser, P. J., Hecht, A.M., Geissler, E. Chondroitin Sulfate in Solution: Effects of Mono- and Divalent Salts. *Macromolecules* **2012**, *45*, 2882−2890.

(171) László, K.; Tombácz, E.; Novák, C. pH-Dependent Adsorption and Desorption of Phenol and Aniline on Basic Activated Carbon. *Colloids Surfaces A Physicochem. Eng. Asp.* **2007**, *306* (1–3 SPEC. ISS.), 95–101.

(172) Smith, R. M. The pH-Rate Profile for the Hydrolysis of a Peptide Bond. *J. Am. Chem. Soc.* **1998**, *120* (35), 8910–8913.

(173) Benrebouh, A.; Avoce, D.; Zhu, X. X. Thermo- and pH-Sensitive Polymers Containing Cholic Acid Derivatives. *Polymer (Guildf).* **2001**, *42* (9), 4031–4038

(174) Kosik, K.; Wilk, E.; Geissler, E.; László, K. Interaction of Phenols with Thermo-Responsive Hydrogels. *Colloids Surfaces A Physicochem. Eng. Asp.* **2008**, *319* (1–3), 159–164.

(175) Dobrynin, A. V.; Rubinstein, M. Theory of Polyelectrolytes in Solutions and at Surfaces. *Prog. Polym. Sci.* **2005**, *30*, 1049−1118.

(176) Horkay, F., Basser, P. J., Hecht, A. M., Geissler, E. Osmotic and SANS Observations on Sodium Polyacrylate Hydrogels in Physiological Salt Solutions. *Macromolecules* **2000**, *33*, 8329–8333.

(177) Nagahama, K.; Inomata, H.; Saito, S. Measurement of Osmotic Pressure in Aqueous Solutions of Poly-(Ethylene Glycol) and poly(N-Isopropylacrylamide). *Fluid Phase Equilib.* **1994**, *96*, 203–214.

(178) László, K.; Manek, E.; Vavra, S.; Geissler, E.; Domján, A. Host-Guest Interactions in Poly(N-Isopropylacrylamide) Hydrogels. *Chem. Lett.* **2012**, *41* (10).

(179) Domjan, A.; Manek, E.; Geissler, E.; László, K. Host-Guest Interactions in poly(N-Isopropylacrylamide) Hydrogel Seen by One- and Two-Dimensional 1H CRAMPS Solid-State NMR Spectroscopy. *Macromolecules* **2013**, *46* (8), 3118–3124.

(180) Manek, E.; Domján, A.; Menyhárd, A.; László, K. Host-Guest Interactions in poly(N-Isopropylacrylamide) Gel: A Thermoanalytical Approach. *J. Therm. Anal. Calorim.* **2015**, *120* (2), 1273–1281.

(181) Manek, E.; Domján, A.; Madarász, J.; László, K. Interactions in Aromatic Probe Molecule Loaded poly(N-Isopropylacrylamide) Hydrogels and Implications for Drug Delivery. *Eur. Polym. J. Spec. Issue SI BiPoCo 2014* **2014**, *68*, 657–664.

(182) a) Domján, A.; Manek, E.; Geissler, E.; László, K. Host-Guest Interactions in poly(N-Isopropylacrylamide) Hydrogel Seen by One- and Two-Dimensional 1H CRAMPS Solid-State NMR Spectroscopy. *Macromolecules* **2013**, *46* (8), 3118–3124.

(183) Xiong, S.; Wang, Y.; Yu, J.; Chen, L.; Zhu, J.; Hu, Z. Polydopamine Particles for next-Generation Multifunctional Biocomposites. *J. Mater. Chem. A* **2014**.

(184) Zhang, Y.; Panneerselvam, K.; Ogaki, R.; Hosta-Rigau, L.; Van Der Westen, R.; Jensen, B. E. B.; Teo, B. M.; Zhu, M.; Städler, B. Assembly of poly(dopamine)/poly(N -Isopropylacrylamide) Mixed Films and Their Temperature-Dependent Interaction with Proteins, Liposomes, and Cells. *Langmuir* **2013**, *29* (32), 10213–10222

(185) National Institute of Standards and Technology, Phenol http://webbook.nist.gov/cgi/cbook.cgi?ID=C108952&Mask=4#Thermo-Phase (accessed May 8, 2015).

(186) Enthalpy of vaporization www.phs.d211.org/science/smithcw/AP Chemistry (accessed May 8, 2015).

(187) Rahway, N. *The Merck Index, 12nd Edition*; 1996.

(188) Zhang, G.; Paspal, S.; Suryanarayanan, R.; Grant, D. Racemic Species of Sodium Ibuprofen: Characterization and Polymorphic Relationships. *J. Pharm. Sci.* **2003**, *92* (7), 1356–1366.

(189) Sousa, R.; Magalhaes, W.; Freitas, R. Glass Transition and Thermal Stability of poly(N-Isopropylacrylamide) Gels and Some of Their Copolymers with Acrylamide. *Polym Degrad. Stabil ity* **1998**, *61*, 275–281.

(190) Jiang, H.; Wang, L. Ibuprofen Induced Drug Loaded Polymeric Micelles. *Chinese Chem. Lett.* **2011**, *22*, 1123–1126.

(191) Zhou, Z.; Zhu, S.; Zhang, D. Grafting of Thermo-Responsive Polymer inside Mesoporous Silica with Large Pore Size Using ATRP and Investigation of Its Use in Drug Release. *J. Mater. Chem.* **2007**, *17* (23), 2428.

(192) Li, H.; Wang, D. Q.; Liu, B. L.; Gao, L. Z. Synthesis of a Novel Gelatin-Carbon Nanotubes Hybrid Hydrogel. *Colloids Surfaces B Biointerfaces* **2004**, *33* (2), 85–88

(193) Satarkar, N. S.; Johnson, D.; Marrs, B. Hydrogel-MWCNT Nanocomposites: Synthesis, Characterization, and Heating with Radiofrequency Fields. *J. Appl. Polym. Sci. 117* (3), 2010.

(194) Haider, S.; Park, S.-Y.; Saeed, K.; Farmer, B. L. Swelling and Electroresponsive Characteristics of Gelatin Immobilized onto Multi-Walled Carbon Nanotubes. *Sensors Actuators B* **2007**, *124* (2), 517–528.

(195) Song, Y. S. A Passive Microfluidic Valve Fabricated from a Hydrogel Filled with Carbon Nanotubes. *Carbon N. Y.* **2012**, *50* (3), 1417–1421.

(196) Li, H.; Wang, D. Q.; Liu, B. L.; Gao, L. Z. Synthesis of a Novel Gelatin-Carbon Nanotubes Hybrid Hydrogel. *Colloids Surfaces B Biointerfaces* **2004**, *33* (2), 85–88.

(197) Krisztina László, Andrei Fluerasu, Abdellatif Moussaïd, Erik Geissler. Deswelling Kinetics of PNIPA Gels. *Soft Matter* **2010**, *6*, 4335–4338.

(198) Zhang, X.; Pint, C. L.; Lee, M. H.; Schubert, B. E.; Jamshidi, A.; Takei, K.; Ko, H.; Gillies, A.; Bardhan, R.; Urban, J. J.; Wu, M.; Fearing, R.; Javey, A. Optically- and Thermally-Responsive Programmable Materials Based on Carbon Nanotube-Hydrogel Polymer Composites. *Nano Lett.* **2011**, *11* (8), 3239–3244

(199) Fujigaya, T.; Nakashima, N. Single-Walled Carbon Nanotubes as a Molecular Heater for Thermoresponsive Polymer Gel Composite. In *Carbon Nanotubes - Polymer Nanocomposites*; INTECH Open Access Publisher: Department of Applied Chemistry, Graduate School of Engineering, Kyushu University, Japan, 2011; pp 379–396.

(200) Mongay, C.; Cerda, V. A Britton-Robinson Buffer of Known Ionic Strength. *Ann. Chim.* **1974**, *64*, 409–412.

9. Publications related to the PhD thesis

Articles

1. **E. Manek**, E. Tombácz, E. Geissler, K. László. Search for origin of discrepancies among osmotic measurements in the PNIPAM - water system. *Periodica Polytechnica Chemical Engineering* 2017; 61 (1): 39-50.
   IF 0.557

2. **Manek**, B. Berke, N. Miklósi, M. Sajbán, A. Domán, T. Fukuda, O. Czakkel, K. László. Thermal sensitivity of carbon nanotube and graphene oxide containing responsive hydrogels. *Express Polymer Letters* 2016; 10 (8):710-720.
   IF 2.761

3. **E. Manek**, A. Domján, A. Menyhárd, K. László. Host-guest interactions in poly(*N*-isopropylacrylamide) gel: a thermoanalytical approach. *Journal of Thermal Analysis and Calorimetry* 2015; 120 (2):1273-1281.
   IF 2.042

4. **E. Manek**, A. Domján, J. Madarász, K. László. Interactions in aromatic probe molecule loaded poly(*N*-isopropylacrylamide) hydrogels and implications for drug delivery. *European Polymer Journal Special Issue: SI BiPoCo* 2014, 2015; 68:657-664.
   IF 3.370

5. A. Domján, **E. Manek**, E. Geissler, K. László. Host-guest interactions in poly(*N*-isopropylacrylamide) hydrogel seen by one- and two-dimensional ^{1}H CRAMPS solid-state NMR Spectroscopy. *Macromolecules* 2013; 46 (8):3118-3124.
   IF 6.560

6. K. László, **E. Manek**, Sz. Vavra, E. Geissler, A. Domján. Host-guest interactions in poly(*N*-isopropylacrylamide) hydrogels. *Chemistry Letters* 2012; 41 (10):1055-1056.
   IF 1.200

Conferences

Oral presentations

1. Krisztina László, **E. Manek**. Interactions in poly(*N*-isopropylacrylamide) hydrogels and their hybrids with carbon nanoparticles. Implications for drug delivery, ENSOR seminar, 03.03.2015, University of Brighton, Brigthon, United Kingdom

2. **E. Manek**, A. Menyhárd, A. Domján, K. László. Simultaneous thermal analysis in the research of drug release (Szimultán termikus analízis a hatóanyagleadás kutatásának szolgálatában). Annual Meeting of the Thermoanalytical Working Committee, Hungarian Academy of Sciences (MTA Termoanalitikai Munkabizottságának Ülése), 10.12.2014, Budapest, Hungary

3. **E. Manek**, A. Domján, A. Menyhárd, J. Madarász, K. László. Host-guest interactions in poly(*N*-isopropylacrylamide) gel seen by thermal simultaneous thermal analysis and powder X-ray diffraction method. 12th International Symposium on Bioscience and Nanotechnology, 14-15.11.2014, Toyo University, Kawagoe, Japan

4. **E. Manek**, A. Domján, A. Menyhárd, K. László. Thermal methods in the research of drug delivery (Termikus módszerek a hatóanyagleadás-kutatás szolgálatában). Cosmetical Symposium 2014, Organised by the Division of Cosmetical and Household Chemistry, Hungarian Chemical Society (MKE Kozmetikai és Háztartásvegyipari Társasága, Kozmetikai Szimpózium 2014), 13.11.2014, Budapest, Hungary
   Book of abstracts (Program és Előadás Összefoglalók) p.12, ISBN 978-963-9970-51-9

5. **E. Manek**, A. Domján, J. Madarász, K. László. Role of the interactions between hydrogels and drug molecules in drug delivery (Hidrogélek és hatóanyagmolekulák kölcsönhatásának szerepe a tervezett hatóanyagleadásban). Cosmetical Symposium 2014, Organised by the Division of Cosmetical and Household Chemistry, Hungarian Chemical Society (MKE Kozmetikai és Háztartásvegyipari Társasága, Kozmetikai Szimpózium 2014), 13.11.2014, Budapest
   Book of abstracts (Program és Előadás Összefoglalók) p.13, ISBN 978-963-9970-51-9

6. **E. Manek**, A. Domján, J. Madarász, T. Sovány, K. László. Interactions of poly(*N*-isopropylacrylamide) hydrogels with small aromatic molecules of environmentally and biomedically relevance. 2nd International Conference on Bio-based Polymers and Composites (BiPoCo 2014), 24-28.08.2014, Visegrád, Hungary

7. **E. Manek**, A. Domján, J. Madarász, K. László. Interactions of poly(*N*-isopropylacrylamide) hydrogel with small aromatic molecules of environmental and biomedical relevance (Poli(*N*-izopropilakrilamid) hidrogélek kölcsönhatásai környezetileg és orvosbiológiailag releváns kis aromás molekulákkal). XI. Conference of György Oláh Doctoral School of BME (Oláh György Doktori Iskola XI. Konferenciája), 06.02.2014, Budapest, Hungary

8. K. László, **E. Manek**, Sz. Vavra, E. Geissler, A. Domján. Host-guest interactions in poly(*N*-isopropylacrylamide) hydrogels. Conference of the International Association of Colloid and Interface Scientists 2012 (IACIS 2012), 13-18.05.2012, Sendai, Japan

Poster presentations

1. **E. Manek**, B. Berke, N. Miklósi, M. Sajbán, K. László. Improvement of hydrogel biomedical potentials by the incorporation of carbon nanoparticles. International Symposium on Amphiphilic Polymers, Networks, Gels and Membranes (APNGM15), 30.08-02.09.2015, Budapest, Hungary

2. **E. Manek**, A. Domján, A. Menyhárd, J. Madarász, K. László. Host-guest interactions of poly(*N*-isopropylacrylamide) hydrogel with small aromatic probe molecules. Conference of the International Association of Colloid and Interface Scientists 2015 (IACIS 2015), 24-29.05.2015, Mainz, Germany

3. **E. Manek**, B. Berke, N. Miklósi, M. Sajbán, T. Fukuda, M. Trenikhin, T. Maekawa, Y. G. Kryazhev, K. László. Nanoparticle containing soft hybrid materials. Fourth Symposium on Future Challenges for Carbon-based Nanoporous Materials (4th CBNM 2015), 15-18.03.2015, Nagano, Japan

4. **E. Manek**, T. Mukhametzyanov, A. E. Klimovitskii, M. A. Varfolomeev, K. László. Poly(*N*-isopropylacrylamide) (PNIPA) hydrogel-aromatic model molecule systems for drug delivery applications. ENSOR seminar, 03.03.2015, University of Brighton, Brighton, United Kingdom

5. **E. Manek**, B. Berke, N. Miklósi, M. Sajbán, T. Fukuda, M. Trenikhin, T. Maekawa, Y. G. Kryazhev, K. László. Kinetics of the temperature induced phase transition of poly(*N*-isopropylacrylamide)-carbon nanoparticle hybrid hydrogels. ENSOR seminar, 03.03.2015, University of Brighton, Brighton, United Kingdom

6. **E. Manek**, K. László. Differential scanning calorimetric studies on carbon nanoparticle-polymer composite materials. Summer school of calorimetry: "Calorimetry and thermal methods in catalysis", 22-27.06.2013, Lyon, France

7. Domján, **E. Manek** , E. Geissler, K. László. Influence of phenols on the phase transition of poly(*N*-isopropyl acrylamide) hydrogels. 12th Annual UNESCO/IUPAC Workshop and Conference on Macromolecules & Materials, 25-28.03.2013, Stellenbosch, South Africa

8. **E. Manek**, K. László. Influence of pH and ionic strength on the phase transition of monolithic PNIPA hydrogels. 12th Annual UNESCO/IUPAC Workshop and Conference on Macromolecules & Materials, 25-28.03.2013, Stellenbosch, South Africa

9. **E. Manek**, K. László. Multiwall carbon nanotube-soft hydrogel hybrid materials. X. Conference of the György Oláh Doctoral School of BME, 07.02.2013, Budapest, Hungary

10. **E. Manek**, Sz. Vavra, G. Filipcsei, E. Tombácz, K. László. Acid/base behaviour of monolithic PNIPA hydrogels. 10th Conference on Colloid Chemistry, 27-29.08.2012, Budapest, Hungary

11. Sz. Vavra, **E. Manek**, K. László. Comparison of poly(*N*-isopropylacrylamide) hydrogels and cryogels. Innovative systems for sustainable 10th Conference on Colloid Chemistry, 27-29.08.2012, Budapest, Hungary

12. Sz. Vavra, **E. Manek**, A. Domján, E. Geissler, K. László. Influence of tyrosine derivatives on the phase transition of poly(*N*-isopropylacrylamide) hydrogels. Advanced Macromolecular Systems Across the Length Scales (AMSALS), 03-06.06.2012, Siófok, Hungary

10. Appendix

A1. Materials

Table A1. Aromatic molecules.

Guest molecule	Distributor	Purity
Phenol	Merck	99.5%
Cathecol (benzene-1,2-diol)	Merck	99%
Resorcinol (benzene-1,3-diol)	Merck	99%
Hydroquinone (benzene-1,4-diol)	Merck	99%
Pyrogallol (1,2,3-benzenetriol)	Merck	99%
Phloroglucinol (1,3,5-benzenetriol)	Merck	99%
Dopamine hydrochloride (4-(2-Aminoethyl)-1,2-benzenediol) hydrochloride)	Sigma-Aldrich	98%
Ibuprofen sodium (sodium 2-(4-isobutylphenyl) propanoate)	Sigma-Aldrich	99%

Table A2. Materials for PNIPA gel synthesis.

Component	Chemical formula	Distributor	Purity	Abbreviation
N-isopropylacrylamide	$C_6H_{11}NO$	Acros Organics	99%	NIPA
N,N'-methylenebisacrylamide	$C_7H_{10}N_2O_2$	Sigma-Aldrich	99%	BA
N,N,N',N'-tetramethylethylenediamine	$C_6H_{16}N_2$	Fluka	99%	TEMED
Ammonium persulphate	$(NH_4)_2S_2O_8$	Sigma-Aldrich	99%	APS

Table A3. Materials for the preparation of acid, base, salt and buffer solutions.

Component	Chemical formula	Distributor	Purity
Potassium hydroxide	KOH	Merck	AR*
Sodium hydroxide	NaOH	Merck	AR
Potassium chloride	KCl	Reanal	AR
Calcium chloride	$CaCl_2$	Merck	AR
Acetic acid	$C_2H_4O_2$	Reanal	AR
2-hydroxypropane-1,2,3-trioic acid	$C_6H_8O_7$	Reanal	99%
Boric acid	H_3BO_3	Reanal	AR
Phosphoric acid	$H3PO_4$	Reanal	AR
Sodium hydrogen phosphate	Na_2HPO_4	Reanal	AR
Disodium hydrogen phosphate dihydrate	$Na_2HPO_4 \cdot 2\ H_2O$	Reanal	AR
Disodium hydrogen phosphate dodecahydrate	$Na_2HPO_4 \cdot 12\ H_2O$	Reanal	AR
1H-Imidazole	$C_3H_4N_2$	Sigma-Aldrich	AR

*Analytical Reagent grade

A2. Buffers

Phosphate buffers listed in Table A4 were used. pH was adjusted with NaOH or KOH. For Britton-Robinson buffers an acid solution containing 0.4 M acetic acid, 0.4 M boric acid and 0.4 M phosphoric acid was mixed with 0.2 M NaOH solution according to Table A5.[200] Britton-Robinson buffers with constant ionic strength of 0.15 M were made of citric acid (from pH 3 to 5.5), imidazole (pH 6.5) and sodium tetraborate (pH 9) solutions. The pH values were adjusted by adding 1 M HCl or 1 M NaOH. The ionic strength was set to 0.15 M by KCl (Table A6).

Table A4. Composition of phosphate buffers.

pH	Materials in *V*=1L	pH adjusting component
3	0.7 mL H_3PO_4 (85%)	NaOH
4.5	6.80 g KH_2PO_4	-
5.5	13.12 g KH_2PO_4 + 1.39 g $Na_2HPO_4 \cdot 12\ H_2O$	-
6.5	13.80 g NaH_2PO_4	NaOH
9	17.40 g KH_2PO_4	KOH

Table A5. Composition of Britton-Robinson buffers.

pH	$V_{\text{acid mixture}}$ (mL)	V_{NaOH} (mL)
3	100	17.5
4.5	100	29.3
5.5	100	38.6
6.5	100	47.5
9	100	68.0

Table A6. Composition of Britton-Robinson buffers of constant ionic strength (0.15 M).

Citric acid buffers (V=1 L)			
pH	$m_{\text{anhidrous citric acid}}$ (g)	m_{KCl} (g)	m_{NaOH} (g)
3	6.3400	9.7100	18.9000
4.5	6.3400	6.5600	49.4000
5.5	6.3400	3.3800	83.7000
Imidazole buffers (V=1 L)			
	$V_{\text{1M HCl}}$ (mL)	m_{KCl} (g)	$m_{\text{imidazole}}$ (g)
6.5	79.1800	5.2820	6.8080
Sodium tetraborate buffers (V=1 L)			
	$V_{\text{1M HCl}}$ (mL)	m_{KCl} (g)	m_{borax} (g)
9	10.2000	7.4570	9.5343

A3. Potentiometric titration

The acid-base properties of PNIPA hydrogel were studied at 20ºC by continuous potentiometric titration in the pH range of 3 to 10 in CO_2-free media on a laboratory-developed system. The NaCl background electrolyte concentrations were 0.01, 0.1 and 1 M, respectively. The initial pH was measured before titration. At each titration point the equilibrium of acid – base consumption was defined by the criterion for pH settling (≤0.0005 pH/s). Surface excess amounts of H^+ (n^{σ}_{H+}) and OH^- (n^{σ}_{OH-}) were calculated from the electrode output signal. The specific net proton surface excess amount ($n^{\sigma} = n^{\sigma}_{H+} - n^{\sigma}_{OH-}$) for dilute solution adsorption[60] was derived directly from the initial and equilibrium concentrations of the solute at each point of the titration and plotted as a function of the equilibrium pH. The reversibility of the titration

was tested in a cycle of forward and backward titrations from the immersion pH 5.5, increasing to pH 10, then descending to pH 3, and finally returning to pH.

A4. DSC response of the PNIPA hydrogel in buffers and in KCl solutions

Figure 14 of the main text shows that with phosphate and Britton-Robinson buffers of different pH, a correlation exists between swelling degree and solution pH**,** but there is no systematic variation with *I*. At constant pH = 4.5 the swelling degree depends strongly on the ionic strength. By contrast, for buffers with constant ionic strength the swelling degree is practically independent of the pH of the solution.

The DSC response of PNIPA gels was also investigated in phosphate buffers (Figure A1a) at fixed pH = 4.5 and at various ionic strengths (Figure A1b), as well as in buffers of constant ionic strength (Figure A1c). In phosphate buffers a systematic downward shift of the onset temperature and broadening of the phase transition is observed with increasing pH, but there is no correlation between T_{onset} and I (Fig. 14). In Britton-Robinson buffers at fixed I = 0.15 M, T_{onset} shifts only slightly to lower temperatures with increasing pH, with no visible change either in the shape of the endothermic transition peak or in the correlation between T_{onset} and pH or I (Fig.14). T_{onset} displays the same I dependence for Britton-Robinson buffers with fixed pH. It can be concluded that the swelling properties are affected not only by the pH set by a buffer but also by the composition of the buffer. Setting the pH, however, also changes the ionic strength of the solvent. These findings highlight the importance of the background electrolyte.

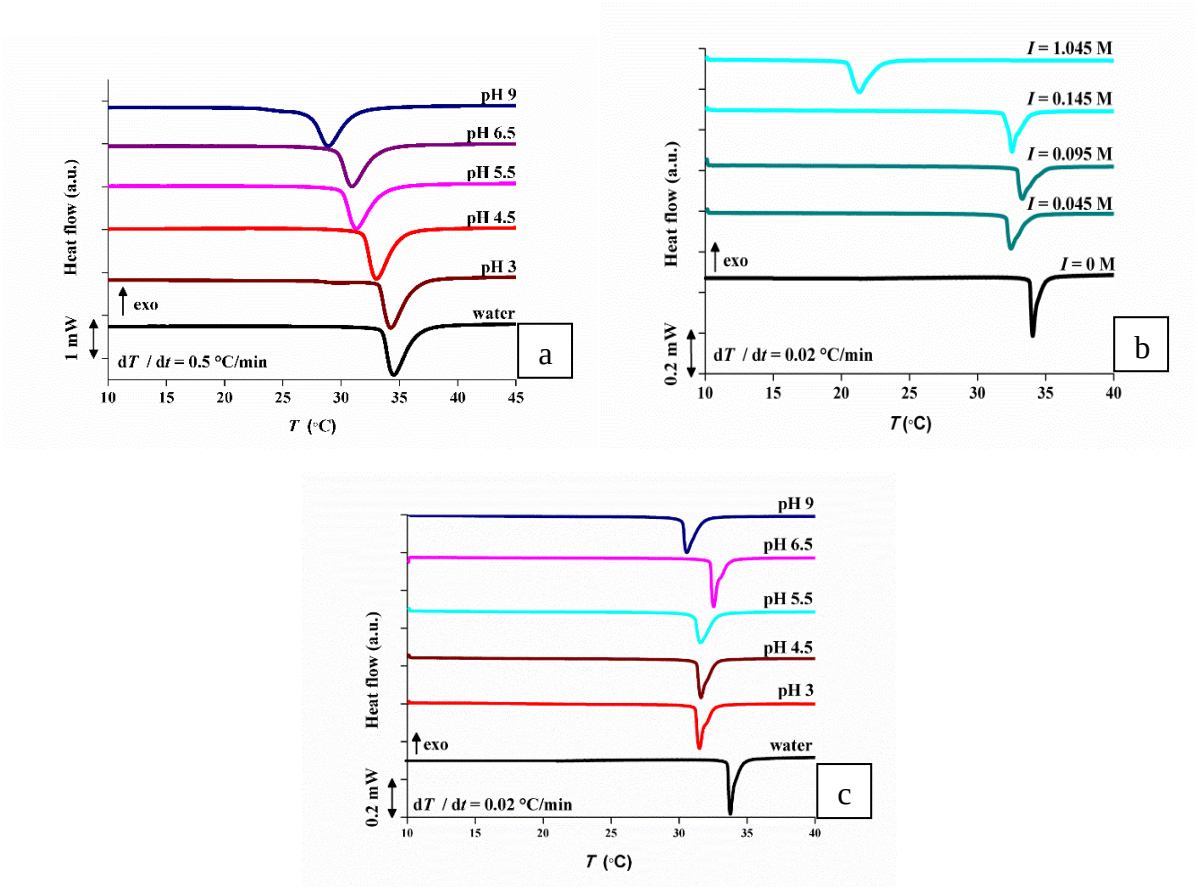

Figure A1. DSC response of PNIPA swollen in (a) phosphate buffer solutions of different pH, (b) in Britton-Robinson buffers pH 4.5 of various ionic strengths and (c) in various buffers with constant ionic strength 0.15 M

Table A7. Enthalpy and entropy of the VTP in buffer solutions

	ΔH (J/g_{drygel})	ΔS (J/g K)
Phosphate buffers	63.8 ± 3.1	0.21 ± 0.01
Britton-Robinson buffers pH = 4.5, various *I*	66.6 ± 2.7	0.22 ± 0.01
I = 0.15 M, various pH	76.8 ± 6.0	0.25 ± 0.02

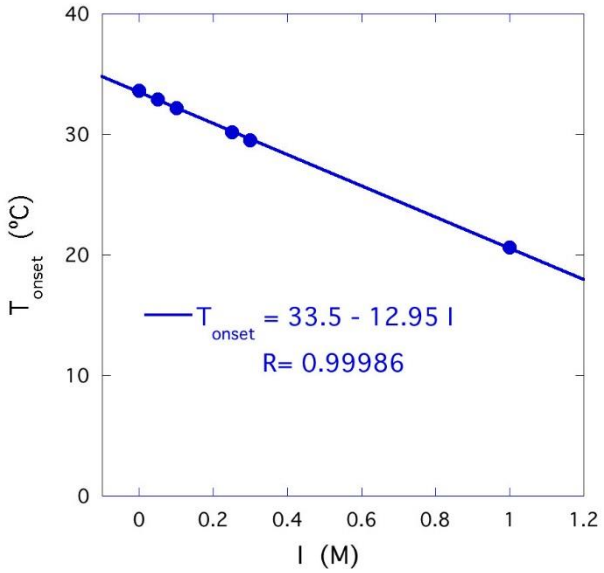

Figure A2. Dependence of the onset temperature T_{onset} on the ionic strength of KCl

A5. Solid state ^{1}H NMR spectroscopy

NMR measurements were carried out by the NMR Research Group of the Research Centre for Natural Sciences of the Hungarian Academy of Sciences. Dry gel disks were equilibrated in solutions of phenol (60 mM), cathecol (120 mM) and dopamine (1 M) in deuterated water for one week at 6 °C. After reaching the equilibrium swelling degree samples were incubated above LCST (25 °C for phenol and cathecol, 42 °C for dopamine) and were regularly removed and placed into the NMR rotor to check the stability of tuning and matching conditions. NMR spectra were recorded on a Varian NMR system operating at ^{1}H at 600 MHz with a Chemagnetics 3.2 mm narrow bore triple-resonance T3 probe in double-resonance mode. Single pulse NMR measurements were carried out with 2.5 μs long π/2 pulse and with 10 s repetition delay. For the combined rotation and multiple-pulse spectroscopy (CRAMPS) experiments wPMLG-5 sequences were used with the same pulse length and delay as for the single pulse spectra. The on-resonance position of the RF field lays outside the spectral response (–5 kHz from the centre of the proton spectra). The proton chemical shift resonances were referenced with a single pulse spectrum of a H_2O sample (4.8 ppm). Spinning speed was 10 kHz for both techniques. Hydrogels were studied above LCST conditions, where the otherwise freely moving organic chains form thick hydrophobic walls that still confine the swelling liquid. Single pulse spectra provide information about the mobile species, while the signals of the less mobile ones are broadened by dipolar interactions. The CRAMPS method suppresses this broadening effect of dipole-dipole interactions so the signals of the less mobile components are better resolved, but that of the mobile components are distorted.

DECLARATION

I, Enikő Rita Manek hereby declare that this PhD dissertation is the result of my own work. All content that was taken from other sources – either literally or reworded – is clearly indicated and its source is presented in the reference list.

Budapest, 25 February 2018 …….

Enikő Rita Manek

NYILATKOZAT

Alulírott Manek Enikő Rita kijelentem, hogy ezt a doktori értekezést magam készítettem, és abban csak a megadott forrásokat használtam fel. Minden olyan részt, amelyet szó szerint, vagy azonos tartalomban, de átfogalmazva más forrásból átvettem, egyértelműen, a forrás megadásával megjelöltem.

Budapest, 2018. február 25. …….

Manek Enikő Rita

Köszönetnyilvánítás

Ezúton szeretném kifejezni mély tiszteletemet témavezetőmnek, László Krisztinának, akinek szorgalma és fáradhatatlan elhivatottsága példaértékű számomra. Külön szeretném megköszönni neki, hogy a hagyományoktól eltérően külső egyetem végzőseként is feltétlen bizalommal és szeretettel fogadott csoportjába.

Szeretném megköszönni Bosznai Gyurinak kedvességét és ötletes megoldásait.

Társszerzőimnek, Berke Barbarának, Czakkel Orsolyának, Domján Attilának, Takahiro Fukudának, Erik Geisslernek, Madarász Jánosnak, Menyhárd Alfrédnak, Tombácz Etelkának és Vavra Szilviának a gyümölcsöző együttműködést.

Hallgatóimnak, Miklósi Nikolettának, Sajbán Mónikának és Vincze Istvánnak a tanulságos és jó hangulatú közös munkát.

Az OTKA K75182, OTKA K101861 és az FP7-PEOPLE-2010-IRSES-269267 pályázatoknak, valamint a Pungor Ernő, Campus France és Campus Hungary ösztöndíjaknak az anyagi támogatást.

Szeretném köszönetemet kifejezni a Lágy Anyagok Kutatócsoport és a BME Fizikai Kémia és Anyagtudományi Tanszék valamennyi dolgozójának, különösen pedig Szilágyi Andrásnak és Gyarmati Benjáminnak, akiknek segítőkészségére és tanácsaira bármikor számíthattam.

Mindenekfelett hálával tartozom rendkívüli szüleimnek és fogadott nagyszüleimnek feltétel nélküli szeretetükért és támogatásukért. Hálás vagyok, hogy mellettem lehetnek életem ezen fontos pillanatában, és szívből remélem, hogy sikereim rengeteg örömmel és büszkeséggel töltik el őket.

Köszönöm szépen drága kishúgomnak, Fanninak, hogy nem csak testvérként, hanem lelki társként is kíséri utamat.

Végül szeretném megköszönni kedves barátaimnak, Hégely Lászlónak, Fehér Anikónak, Sofia de Leónnak, Józó Murielnek és Ganyecz Leventének, hogy hűségesen kitartanak mellettem.